Distribution Agreement

In presenting this thesis or dissertation as a partial fulfillment of the requirements for an advanced degree from Emory University, I hereby grant to Emory University and its agents the non-exclusive license to archive, make accessible, and display my thesis or dissertation in whole or in part in all forms of media, now or hereafter known, including display on the world wide web. I understand that I may select some access restrictions as part of the online submission of this thesis or dissertation. I retain all ownership rights to the copyright of the thesis or dissertation. I also retain the right to use in future works (such as articles or books) all or part of this thesis or dissertation.

Signature:

_____ _____

Maria Christine White Date

Effects of Packaging Signal Divergence on Influenza A Virus Reassortment

By

Maria Christine White
Doctor of Philosophy

Graduate Division of Biological and Biomedical Sciences
Immunology and Molecular Pathogenesis

_____
Anice C. Lowen, Ph.D.
Advisor

_____
Richard W. Compans, Ph.D.
Committee Member

_____
Jacob Kohlmeier, Ph.D.
Committee Member

_____
David A. Steinhauer, Ph.D.
Committee Member

_____
Sean Stowell, M.D., Ph.D.
Committee Member

Accepted:

_____
Lisa A. Tedesco, Ph.D.
Dean of the James T. Laney School of Graduate Studies

_____
Date

Effects of Packaging Signal Divergence on Influenza A Virus Reassortment

By

Maria Christine White
M.S., University of North Carolina Wilmington, 2014

Advisor: Anice C. Lowen, Ph.D.

An abstract of
A dissertation submitted to the Faculty of the
James T. Laney School of Graduate Studies of Emory University
in partial fulfillment of the requirements for the degree of
Doctor of Philosophy
in the Graduate Division of Biological and Biomedical Sciences
in Immunology and Molecular Pathogenesis
2019

Abstract

Effects of Packaging Signal Divergence on Influenza A Virus Reassortment

By Maria Christine White

Influenza A virus (IAV) is an RNA virus with a segmented genome. Since the IAV genome comprises eight different segments, IAVs can exchange genetic material in a process called reassortment. Reassortment occurs when two different IAVs co-infect the same cell and mixing of the two viral genomes takes place within the cell. Reassortment therefore allows the production of new viruses that are different from both parental viruses. Regions of the IAV genome called packaging signals serve to direct incorporation of the eight segments during virus assembly, and these packaging signals are found on both termini of each of the eight IAV segments. Since these packaging signals are specific to each segment and to each strain of IAV, we hypothesized that nucleotide differences within the packaging signal regions could limit reassortment efficiency. To test this hypothesis, we used two viruses representative of the two seasonal IAV lineages currently circulating in the human population (H3N2 and H1N1), and made virus pairs that encoded the same proteins but different packaging signals on a single segment. We then evaluated how frequently segments carrying matched vs mismatched packaging signals were incorporated into reassortant progeny. We found that matched packaging signals were preferred on the HA segment, but not on the NA or NS segments. These data suggest that the movement of NA and NS segments between seasonal IAVs is unlikely to be restricted at the level of packaging, while movement of the HA segment would be more constrained. Therefore, our results indicate that the importance of packaging signal differences in IAV reassortment is segment dependent. Furthermore, our data suggest that the packaging signals of the HA segment could be an important factor in determining the likelihood that two IAV strains of public health interest will undergo reassortment.

Not only can reassortment increase the diversity of viruses circulating within a given host species, but it can also facilitate transfer of novel IAVs to a new host species. IAV pandemic strains are formed in part by the introduction of an HA segment from a nonhuman virus, such as an avian virus, into a human virus. Since the mixing of avian and human IAVs can result in the formation of a pandemic strain, we next addressed how likely it would be for an HA segment from an avian IAV to reassort with a human IAV. We tested the compatibility of HA packaging signals from two avian viruses that pose a threat to human health (H5N8 and H7N9) with a human seasonal H3N2 strain. We showed that sequence differences in the packaging signals between these avian and human IAV HA segments limited the potential for reassortment to occur. We did find, however, that human viruses still incorporated the avian virus HA segments at a low level in animals that were co-infected with both IAVs. This observed low level of avian virus HA segment incorporation into human viruses could be significant if the reassortant virus had a fitness advantage in the human population, such as escape from pre-existing immunity. Overall, these findings offer important insight into the mechanisms that underlie the emergence of new IAVs and highlight the continued need for IAV surveillance, especially in areas where avian and human IAVs are in close contact.

Effects of Packaging Signal Divergence on Influenza A Virus Reassortment

By

Maria Christine White
M.S., University of North Carolina Wilmington, 2014

Advisor: Anice C. Lowen, Ph.D.

A dissertation submitted to the Faculty of the
James T. Laney School of Graduate Studies of Emory University
in partial fulfillment of the requirements for the degree of
Doctor of Philosophy
in the Graduate Division of Biological and Biomedical Sciences
in Immunology and Molecular Pathogenesis
2019

Acknowledgements

I would first and foremost like to thank my advisor, Anice Lowen, whose mentorship and guidance I will value for the remainder of my scientific career. I am grateful for her strong support and the many opportunities she provided me during my time in her lab. I would like to thank my committee members, Richard Compans, David Steinhauer, Jacob Kohlmeier, and Sean Stowell, for productive and enjoyable committee meetings, from which many good ideas and experiments arose. Their wisdom, advice, and encouragement throughout my Ph.D. are deeply appreciated. I would also like to thank my parents, who have been unwavering in their support of me since I discovered my passion for research over ten years ago.

Table of Contents

Chapter I: Introduction

Implications of Segment Mismatch for Influenza A Virus Evolution

Maria C. White[1] and Anice C. Lowen[1]

[1]Department of Microbiology and Immunology, Emory University School of Medicine, Atlanta, GA, USA

Published in *Journal of General Virology*, 2018, 99(1):3-16, PMID: 29244017

[a]The "dissertation aims" section of this chapter was not included in the above publication; it remains unpublished

All figures were generated by MCW with input from ACL

Abstract

Influenza A virus (IAV) is an RNA virus with a segmented genome. These viral properties allow for the rapid evolution of IAV under selective pressure, due to mutation occurring from error-prone replication and the exchange of gene segments within a co-infected cell, termed reassortment. Both mutation and reassortment give rise to genetic diversity, but constraints shape their impact on viral evolution: just as most mutations are deleterious, most reassortment events result in genetic incompatibilities. The phenomenon of segment mismatch encompasses both RNA- and protein-based incompatibilities between co-infecting viruses and results in the production of progeny viruses with fitness defects. Segment mismatch is an important determining factor of the outcomes of mixed IAV infections and has been addressed in multiple risk assessment studies undertaken to date. However, due to the complexity of genetic interactions among the eight viral gene segments, our understanding of segment mismatch and its underlying mechanisms remain incomplete. Here, we summarize current knowledge regarding segment mismatch and discuss the implications of this phenomenon for IAV reassortment and diversity.

Abbreviations

CPSF30, cleavage and polyadenylation specificity factor 30; DI, defective interfering; HA, hemagglutinin; HRM, high resolution melt; IAV, influenza A virus; NA, neuraminidase; NEP, nuclear export protein; NP, nucleoprotein; NS1; non-structural protein 1; NS2, non-structural protein 2; pH1N1, 2009 H1N1 pandemic strain; UTR, untranslated region; VAR, variant; vRNAs, viral RNAs; vRNPs, viral ribonucleoprotein complexes; WT, wild-type.

Introduction

Influenza A virus (IAV) is an enveloped, negative sense, single stranded RNA virus with eight gene segments (1). The segmented nature of the IAV genome allows the exchange of gene segments between viruses that co-infect the same cell, which can result in the formation of progeny viruses that are genetically distinct from both parental viruses. This process of genetic exchange is termed reassortment. Reassortment has a major impact on IAV evolution and therefore plays a substantial role in the ecology and epidemiology of IAV.

The principle reservoir of IAV resides in aquatic birds, although IAV can infect a diverse range of hosts, including humans, poultry, swine, horses, and other mammals. IAV is grouped into distinct subtypes according to the antigenicity of two of its surface glycoproteins, hemagglutinin (HA) and neuraminidase (NA), of which there are currently 18 known HA subtypes and 11 known NA subtypes. Viruses of the H17N10 and H18N11 subtypes are confined to bats, while viruses of the remaining HA and NA subtypes circulate in wild birds (2-5).

In humans, IAV causes both epidemics and pandemics. IAV epidemics occur yearly during the winter months in both the Northern and Southern hemispheres. Reassortment among co-circulating seasonal IAV strains has been detected repeatedly and found to give rise to epidemiologically important strains (6-10). Despite the evolutionary success of certain reassortant genotypes, however, comprehensive investigation of the fate of intra-subtype reassortants derived from the human H3N2 lineage revealed that reassortment is usually deleterious, resulting in negative selection of reassortant progeny (11). This finding highlights the importance of segment mismatch in the evolution of seasonal IAV and indicates that inter-segment epistasis often functionally constrains reassortment even when co-infecting viruses are closely related.

Pandemics arise when an IAV strain acquires both antigenic novelty and the ability to spread efficiently through a human population. In the past century, there have been four IAV pandemics

(12-15). The origins of the 1918 H1N1 pandemic strain and the contribution of reassortment to its emergence remain under debate (16-18). In 1957, the PB1, HA, and NA genes from an avian H2N2 virus entered the human H1N1 background to form the H2N2 pandemic strain of that year. In 1968, the PB1 and HA genes from an avian H3 virus entered the human H2N2 background to form the 1968 H3N2 subtype pandemic strain (19). A notable feature of both the 1957 and the 1968 pandemic strains is the transmission of an avian PB1 gene to humans, accompanying its cognate HA (20). Lastly, extensive reassortment in swine brought together genes from avian, swine, and human IAV lineages to produce the 2009 pandemic strain (21-23).

In addition to epidemics and pandemics, over the past twenty years, multiple zoonotic IAV outbreaks have occurred when viruses capable of causing severe disease in humans emerged from birds (24-29). According to the World Health Organization (WHO), from 2003 to September 2017 there have been 860 human cases of H5N1 virus infection reported from 16 countries, with 454 of these cases resulting in death (30). Furthermore, as of September 2017, 1,564 laboratory-confirmed human cases of H7N9 virus infection have been reported in China, including at least 612 deaths (31). The H5N1 and H7N9 subtype viruses causing these zoonotic outbreaks arose through reassortment of multiple avian-adapted IAVs, including strains circulating in both wild and domestic birds (32-34). Interestingly, both the H5N1 and H7N9 zoonotic lineages derive their six "internal gene" (non-HA, non-NA) segments from an H9N2 subtype lineage that circulates widely in the poultry of Southeast Asia. This internal gene cassette appears to be conducive to reassortment that pairs it with multiple different HA/NA subtypes (32, 33, 35-37). In addition to the ongoing H5N1 and H7N9 IAV outbreaks, avian influenza viruses of other subtypes, such as H5N6, H9N2, H10N8, and H6N1 have sporadically caused disease in humans in China and Taiwan (37-40).

There is concern regarding the potential for viruses of these zoonotic subtypes to cause the next influenza pandemic. While the human population has little immunity against these avian IAVs, these viruses to date have not acquired effective human-to-human transmission, a key feature of a pandemic strain. Reassortment of zoonotic and human seasonal IAVs can facilitate the formation of a virus with both antigenic novelty and the ability to successfully transmit in humans. However, the fitness of reassortant progeny derived from divergent IAV strains is often limited by incompatibilities occurring at the RNA or protein levels (41, 42). Indeed, segment mismatch may be a major underlying reason that reassortment events involving H5N1 or H7N9 IAVs and seasonal human strains have not been detected to date.

As summarized above, IAVs are genetically diverse and circulate within a diverse range of host species. Under these conditions, reassortment can result in rapid viral evolution, potentially contributing to epidemics, pandemics, and cross-species transfers of the virus. In this review, we will explore reassortment, the constraints imposed on reassortment by segment mismatch, and the implications of segment mismatch for IAV evolution.

Mutation and reassortment in IAV evolution

Fixation of changes in the viral genome requires that a virus population is genetically diverse and that it is subject to either a stochastic bottleneck or a selective pressure. For IAV, two distinct mechanisms give rise to genetic variation: mutation and reassortment. The diversity of genotypes generated through these two processes is the raw material on which selection acts. IAV evolution in humans is driven in large part by antibody-mediated selection and takes two forms: i) antigenic drift, which is characterized by small changes and is a major feature of seasonal IAV, and ii) antigenic shift, which is characterized by large changes and is a major feature of pandemic IAV.

Drivers of IAV evolution in non-human hosts are less well-characterized than in humans and pressures unrelated to immunity, as well as stochastic processes, may play a larger role in these contexts.

Antigenic drift

Like all RNA viruses, IAVs are constantly mutating. These mutations are the result of the absence of proofreading capability of the viral RNA-dependent RNA polymerase. IAV polymerase error translates into approximately two mutations per replicated genome (43). The fixation of mutations that change the antigenicity of IAVs encompasses antigenic drift. Antibodies directed against the HA glycoprotein can neutralize the virus by blocking viral attachment to and/or fusion with the host cell (44-47). These anti-HA antibodies therefore drive antigenic drift of the virus towards antibody escape. Antigenic drift, in turn, has a major impact on the efficacy of vaccination; the mutations that the virus acquires over time lead to vaccine escape, therefore necessitating periodic reformulation of the vaccine in order to match the currently circulating strains (48-50).

In addition to mutation, reassortment can also contribute to antigenic drift (9). Since multiple sub-clades of seasonal H3N2 or H1N1 viruses co-circulate, there is the potential for reassortment between viruses of closely related lineages. Such intra-subtype reassortment events increase genomic diversity and contribute to the evolution and epidemiology of seasonal influenza (6, 7, 51, 52). Most notably, reassortment within H1N1 or H3N2 subtypes can place a drifted HA onto a more fit background, which can give rise to unusually severe epidemics, as seen in 1946-1947 and 2003-2004 (6, 51). Reassortment within IAV subtypes can also affect sensitivity to antiviral drugs. The global spread of adamantane-resistant IAVs was mapped to an H3N2 lineage that arose from an intra-subtype reassortment event (53, 54).

IAVs of the H1N1 and H3N2 subtypes have been co-circulating in humans since 1977 (55). Their reassortment is detected only sporadically, however, and sustained transmission of a human H1N1/H3N2 reassortant virus has occurred only in one instance. Namely, in 2001, reassortant H1N2 viruses were detected in humans in the United Kingdom (56). During the 2001-2002 season, H1N2 viruses were identified in 41 countries on four continents, causing various outbreaks across the globe and predominating over H3N2 and H1N1 viruses in several countries (56-59). However, in subsequent seasons, these reassortant H1N2 viruses failed to predominate. In addition to this outbreak, co-infection and reassortment between human H1N1 and H3N2 lineages was occasionally detected in humans prior to 2009 and, since the 2009 H1N1 pandemic strain (pH1N1) replaced the H1N1 seasonal lineage, a handful of additional co-infection and reassortment events between these two subtypes have been reported (60-68). Despite apparently ample opportunity for inter-subtype reassortment among human IAV lineages, the relatively low frequency with which reassortant viruses achieve sustained circulation suggests that evolutionary constraints lead to their negative selection. Indeed, analysis of reassortment between seasonal H3N2 and pH1N1 viruses in the laboratory supports this conclusion (69, 70).

Antigenic shift

Antigenic shift involves a large change in the antigenicity of influenza viruses circulating in the human population, and can result from introduction into humans of an IAV that circulates in non-human hosts, or introduction of the HA segment of a non-human IAV into a seasonal IAV background through reassortment (4, 5). As noted above, reassortment between human and avian IAVs led to the formation of the 1957 and 1968 pandemic strains (20). Reassortment was also critical in the emergence of the 2009 pandemic strain. In contrast to the 1957 and 1968 pandemics, however, this reassortment did not directly involve currently circulating human IAVs. In the years

prior to 2009, reassortment brought together gene segments from two distinct swine IAV gene pools, that of the Eurasian avian-like and the North American triple reassortant swine lineages. The triple reassortant lineage, in turn, incorporated viral genes of human, avian, and classical swine IAV origin. Thus, although the 2009 pandemic was caused by an intact swine IAV, the emergence of this swine virus resulted from extensive reassortment in pigs (21, 22, 71). Owing to a lack of IAV isolates in the years prior to 1918, the origins of the 1918 pandemic strain remain relatively unclear. Following sequencing of the reconstructed genome of the 1918 virus, it was suggested to have been introduced into humans *in toto* from an avian reservoir (17). A more recent analysis suggests, however, that reassortment between a previously circulating human IAV of the H1 subtype and an avian IAV may have placed the human H1 HA into a novel background and given rise to the 1918 pandemic (16).

Although reassortment is often associated with the emergence of IAV pandemic strains, it is likely not sufficient to give rise to highly fit, antigenically shifted variants. Indeed, experimental co-infection of pigs with swine IAVs of the precursor lineages to the 2009 pandemic strain did not yield a pandemic-like genotype at detectable levels (72). In other experimental settings, mutations selected following reassortment have been shown to compensate for genetic incompatibilities and thereby increase fitness of reassortant viruses. For example, amino acid substitutions in HA were found to reduce HA-NA mismatch in human-avian reassortant viruses (73, 74). Evidence of this phenomenon occurring in nature has also been reported in the context of intrasubtype reassortment of seasonal IAV (75). Owing to the difficulty of detecting low fitness precursors, and of differentiating adaptation to a new genetic context from adaptation to a new host, it is more challenging to demonstrate this phenomenon for pandemic IAV. Nevertheless, for a shifted virus

to be evolutionarily successful, mutations are likely needed to ease segment mismatch that arises from the reassortment event.

Before discussing segment mismatch and its causes in more detail, we will briefly consider other factors that impact the frequency of reassortment. In addition to viral genetic compatibility, virus extrinsic factors, such as the timing and dose of infection, have been shown to impact reassortment outcomes by altering the likelihood of co-infection.

Reassortment efficiency in the absence of segment mismatch

Although multiple methods exist by which to evaluate IAV reassortment in the laboratory (reviewed in (76)), studies regarding the circumstances that allow for robust reassortment are often confounded by segment mismatch. In order to examine the conditions that favor IAV reassortment and to determine a baseline frequency for this process, we developed a system that allowed IAV reassortment in the absence of segment mismatch. This system employed two influenza A/Panama/2007/99 (H3N2) [Pan/99] viruses that were phenotypically similar but genotypically distinct (77). Up to six silent mutations were introduced into the open reading frames (ORF) of each of the eight Pan/99 segments of one virus and it was designated as variant, or VAR. These mutations did not alter the fitness of the virus detectably but allowed for differentiation of the VAR virus from the wild-type (WT) Pan/99 virus using the post-PCR method high resolution melt (HRM) analysis (78). In this way, progeny viruses produced from WT/VAR co-infected cells could be genotyped in a streamlined fashion using HRM analysis, without the need for partial or full sequencing of virus isolates. Two different epitope tags were also introduced into the HA proteins of these viruses, to allow enumeration of infected and co-infected cells by flow cytometry. Because these two viruses were of the same strain background, the virus pairing was devoid of segment

mismatch. Using this system, we showed that reassortment was highly efficient in cell culture under high multiplicity conditions, with an average of 88% of the analyzed virus isolates containing a reassortant genome (77). Additionally, we found that the frequency of reassortment was dose-dependent, with higher levels of co-infection *in vitro* and higher inoculum dose *in vivo* resulting in increased reassortment. The observed dose dependency of reassortment was partly explained by Poisson statistics dictating the levels of co-infection; however, comparison to a computational simulation of co-infection and reassortment in cell culture indicated that reassortment was markedly more efficient than predicted based on random distribution of eight-segmented viruses into cells (79). A combination of further modeling and experimentation revealed that the abundant reassortment observed could be explained by high levels of incomplete viral genomes within singly-infected cells. In particular, the occurrence of incomplete genomes is thought to increase the proportion of productively infected cells that are co-infected (79). With sequential infection, rather than co-infection, a delay of up to 8 h between the WT/VAR virus inoculations allowed for robust reassortment *in vitro*, while a delay of up to 12 h allowed for robust reassortment *in vivo*. However, further time delay between the WT/VAR virus inoculations led to markedly reduced levels of co-infected cells in cell culture, which prevented reassortment. In vivo, a delay of 24 h or more blocked productive infection by the second virus. Stripping of sialic acid receptors from infected cells by NA may contribute to the reduction in superinfection over time (80). By excluding the limitations imposed by segment mismatch, this study demonstrated for the first time that reassortment is efficient both *in vitro* and *in vivo*, and that the timing and dose of infection strongly impact the likelihood of reassortment (77, 79, 81, 82). Taken together, the above studies suggest that i) virus extrinsic factors do not limit reassortment appreciably within a co-

infected cell, and ii) virus extrinsic factors such as timing and dose do, however, play a major role in determining the likelihood of co-infection at the levels of both the host and the individual cell.

Segment mismatch

As described above, reassortment occurs frequently in the absence of RNA or protein mismatch. Additionally, numerous studies to date have demonstrated that reassortment is prevalent in nature, in both avian and swine hosts (83-88). However, early evidence suggested that reassortment of IAV genes was not random. In 1979, Lubeck *et al.* demonstrated that reassortment between influenza A/Puerto Rico/8/34 (H1N1) [PR8] and influenza A/Hong Kong/8/68 (H3N2) viruses resulted in some segments being randomly distributed, as expected, while other segments appeared to be linked, occurring together with a higher frequency than expected (41). In particular, linkages between the polymerase gene segments PB2-PB1 and PB1-PA derived from the same parental virus were observed, suggesting that either i) these genes interacted with each other during IAV packaging, or ii) optimal protein-protein interactions occurred when these genes originated from the same parental strain, increasing the likelihood of detecting progeny viruses with these gene combinations (41). Later, using statistical approaches, the nonrandom association of IAV genes during reassortment was confirmed (42, 89). Similarly, multiple studies undertaken for risk assessment purposes have demonstrated that certain reassortants derived from i) swine IAVs and human IAVs and ii) avian IAVs and human IAVs have fitness defects when compared to the parental strains, suggesting incompatibilities between specific heterologous viral components (72, 90-96). These incompatibilities underlie segment mismatch and can be categorized as either RNA mismatch or protein mismatch.

RNA mismatch

RNA mismatch comprises incompatibilities between the viral RNAs (vRNAs) of two different IAV strains, and manifests at the packaging signal regions of IAV segments. Packaging signals direct the incorporation of the eight vRNAs into new virus particles. During reassortment, mixing of gene segments occurs, thus juxtaposing heterologous viral packaging signals.

IAV packaging. An IAV particle is only fully infectious if it contains one copy of each of the eight viral segments, as shown in Fig. 1. For many years, the mechanism by which packaging of eight distinct segments was achieved remained under debate. It was thought that either i) the packaging of the IAV genome was random, or ii) the packaging of the IAV genome was a selective process. Random assembly would require a full infectious genome to be generated purely by chance and, with eight segments, the probability of this occurring is 1/416 (97). A major argument in favor of a random packaging model was that observed PFU per particle ratios of IAV were low, in the range of 1/10 to 1/100 (98-100). Furthermore, if virus particles are able to package nine or more segments, this would bring the probability of packaging the eight distinct segments needed to make an infectious virus into the range of observed PFU/particle values (97). Some studies offered support for packaging of greater than eight segments per virion. Results of one such study showed that 3-5% of analyzed virions incorporated two different reporter versions of the same vRNA segment, and the authors estimated that IAVs must package 9 to 11 segments for this to occur by chance (101). In another study, reverse genetics techniques were used to produce an IAV that required delivery of nine segments to a cell to initiate productive infection (97). For these reasons, a model in which IAV randomly incorporated 9 to 11 vRNPs per particle was plausible.

However, strong evidence now suggests that a selective IAV packaging mechanism is at work. This evidence has been reviewed recently (102). Briefly, studies in the 1970s revealed that the eight IAV gene segments were present in equimolar ratios in a virus population (103) and that

most IAV plaque-forming units contained a single full set of segments (41, 104). In addition, virus populations released from cells that contained unequal copy numbers of the eight segments were nevertheless found to carry equal copy numbers of the vRNAs (105, 106). In subsequent years, fluorescence *in situ* hybridization analysis of vRNA composition in individual virions revealed that a majority of IAV particles contained eight distinct segments and packaged a single copy of any given gene (107). In addition, two virus-like RNAs developed from the same vRNA species were shown to compete for packaging (108), in agreement with previous studies demonstrating that defective interfering (DI) and standard segments of the same vRNA species compete for packaging (109-112). Taken together, these studies offered substantial support for a selective packaging mechanism and the existence of elements present in IAV viral ribonucleoprotein complexes (vRNPs) that allow for segment differentiation during packaging.

Packaging signals and segment interactions. IAV packaging signals direct the incorporation of each IAV segment into assembling virus particles. These packaging signals have been found to be segment and strain specific and comprised of both untranslated region (UTR) and coding sequence at the 3' and 5' end of each segment. A study reported in 2003 represented the first description of a defined segment specific packaging signal for IAV (113). An influenza A/WSN/33 (H1N1) [WSN] NA construct was designed that contained GFP inserted in place of the NA coding region, flanked by 202 nt of the wild-type NA 3' end (UTR + 183 nt coding region) and 185 nt of the wild-type NA 5' end (UTR + 157 nt coding region). After serially passaging a virus containing this NA construct, it was demonstrated that this model NA segment was efficiently incorporated into virus particles over time. Subsequently, another construct identical to the first was designed except with the coding regions removed. In the absence of these coding nucleotides, the NA segment was no longer efficiently packaged, although it was still replicated (113). Packaging signals have since

been defined for the remaining seven WSN IAV segments and found to comprise similarly broad regions of the 3' and 5' termini (114-118). A handful of studies also suggest that internal nucleotides outside the mapped termini may also contribute to packaging (119-121). Additionally, the amino acid sequence of the viral nucleoprotein (NP) might play an important role in directing packaging of the IAV segments (122). This NP amino acid code does not alter the role of packaging signals as previously described; rather, it may act in concert with the RNA-based packaging signals to instruct IAV segment bundling.

Elegant transmission electron microscopy studies have helped to visualize how the eight segments are arranged within a virus particle. By transversely sectioning viruses as they were budding off host cell membranes, Kawaoka and colleagues showed that IAV gene segments were arranged in a distinct "7+1" pattern, with seven segments in a circle surrounding one central segment as shown in Fig. 1 (123, 124). An array of IAVs were tested in this manner, including human, swine, and avian strains, and the same arrangement was observed for all strains tested. IAVs with spherical particles as well as filamentous particles were subsequently examined, with the same result (123). Therefore, it is likely that this arrangement is consistent across all budding IAVs. To date, the identity of the segments in this "7+1" pattern remains unknown; however, using electron tomography and characterizing the segments based on length, it was shown via sectioning of IAV particles that the identity of the central segment was likely PB2, PB1, PA, or HA (125).

The observation that the location (but not necessarily segment order or identity) of vRNAs within a virion is consistent, at least during budding, raises the question: how are the segments being held in this position? The presence of electron density between vRNPs suggested the existence of direct contacts, both between segments in the outer "7+1" circle and between the central segment and outer segments (125). Fournier *et al.* confirmed the presence of interactions between the segments

via electron tomography, and also showed that these interactions are likely occurring between the packaging signal regions of the IAV segments as previously mapped, as the locations of the interactions overlapped with the earlier described terminal packaging signal locations for each segment (126).

Packaging signal mismatch. Based on the majority of evidence gathered to date, a leading model of IAV genome packaging is that the vRNAs are arranged in a particular pattern during virion assembly and interact with each other via base-pairing interactions between adjacent packaging signal sequences. If sequence specific RNA-RNA interactions mediate selective genome assembly as this model suggests, it follows that segment mismatch at the RNA level would result from nucleotide differences among IAV strains. During IAV evolution, the RNAs of a given virus strain evolve coordinately, leading to optimal interactions among segments (Fig. 2a-b). When two divergent IAV strains undergo reassortment, the interactions between heterologous segments are expected to be less efficient since the precise sequences mediating these interactions might not be conserved (Fig. 2c). These inefficient interactions between vRNAs could, in turn, disfavor the production of certain reassortant genotypes. Indeed, packaging signal mismatch has been shown to dictate reassortment outcomes (127-129).

In an elegant series of experiments, Essere *et al.* showed that reassortment between influenza A/Moscow/10/99 (H3N2) and influenza A/Finch/England/2051/91 (H5N2) viruses resulted in strongly biased reassortment, with the H5 HA segment being unable to enter a H3N2 background (129). However, when packaging signals from the H3 HA segment were grafted onto the H5 HA segment, this allowed for efficient incorporation of the H5 HA segment into a H3N2 background, demonstrating that packaging signal mismatch was inhibiting the formation of these reassortant progeny. Additionally, the incorporation of the H5 HA segment (with H5 packaging signals) could

be achieved if accompanied by the H5N2 M segment, suggesting that the HA and M segments of this IAV strain interact at the level of genome assembly (129).

Influenza A and B viruses co-circulate in humans but never undergo reassortment. The reason for this could be multifactorial, but Baker *et al.* showed that by grafting IAV packaging signals onto full-length influenza B virus HA or NA glycoproteins, reassortant viruses could be rescued that contained either the influenza B virus HA, NA, or both in an IAV background (128). Their study demonstrated that packaging signal divergence between influenza A and B viruses is at least partly responsible for the lack of intertypic reassortment in nature. Interestingly, this study also serves as an example of RNA incompatibility with protein compatibility, as full-length influenza B virus HA protein was able to functionally complement an HA-deficient IAV (128).

Using a co-infection system based on Pan/99 WT and VAR viruses (described above), we recently examined the potential for packaging signal differences between seasonal H3N2 and pH1N1 viruses to shape reassortment outcomes. The advantage of this approach is that the co-infecting WT and VAR viruses are identical at the protein level, ensuring that biases in reassortment can be fully attributed to RNA sequence. Our data revealed that the presence of pH1N1 virus-derived packaging signals on the WT HA segment led to it being significantly under-represented in reassortant progeny viruses compared to a control virus that carried homologous Pan/99 packaging signals. These results confirmed the findings of Essere *et al*. that heterologous packaging signals on the HA segment can restrict reassortment and extended their observation to an H3N2 / H1N1 virus pairing. However, when the NA and NS segments were analyzed in a similar manner, the presence of homologous vs. heterologous packaging signals had no significant effect on packaging efficiency (127). Thus, this study suggests that the sensitivity to changes in packaging signal sequence may vary with segment.

Additionally, Gao and Palese successfully prevented IAV reassortment by rewiring the packaging signals of the HA and NS segments. Using the PR8 (H1N1) strain background, they grafted HA-specific packaging signals onto the NS segment and grafted NS-specific packaging signals onto the HA segment (130). This first-generation chimeric virus was able to undergo reassortment with the wild-type virus. However, after the original packaging signal sequences in terminal regions of the ORFs were disrupted via silent mutation, the chimeric virus lost its ability to reassort with the wild-type virus. This study provides further evidence for the role of packaging signals in IAV reassortment.

Protein mismatch

Similar to vRNAs, the proteins of the same virus strain co-evolve, so that the interactions between them are optimal (Fig. 2a-b). During reassortment, progeny viruses can form that are not severely affected by packaging signal mismatch, but encode proteins that are not compatible (Fig. 2c). While RNA mismatch can limit the diversity of IAVs formed after a co-infection event, protein mismatch manifests only after the formation of progeny viruses, when the newly-formed reassortants spread to new host cells (Fig. 3).

PB2-PB1-PA-NP mismatch. Mismatch among the polymerase components is a common form of protein mismatch. Reassortment between influenza A/equine/Prague/1/56 (H7N7) [Prague] and influenza A/Yokohama/2017/03 (H3N2) [Yokohama] viruses was shown to be restricted by incompatibilities between the subunits comprising the vRNP complex (PB2, PB1, PA, and NP) (131). The combination of Prague PB2, Prague PB1, and Yokohama PA resulted in the inability of the three subunits to form the heterotrimer necessary for IAV transcription and replication. Compensatory mutations in PB2 and/or PA allowed for increased replicative activity, suggesting that low activity of chimeric RNP complexes can be a limiting factor in IAV reassortment. Hatta

et al. made a similar observation using influenza A/Memphis/8/88 (H3N2) [Mem/88] and influenza A/Mallard/New York/6750/78 (H2N2) [Mal/NY] viruses. They were able to generate reassortant viruses containing either PB2/PB1/PA or PB2/PB1/PA/NP from Mem/88 in a Mal/NY background but were unable to generate viruses containing only the PB1 and PA genes of Mem/88 in a Mal/NY background, demonstrating the incompatibility of polymerase subunits between these two virus strains (132).

Similar studies have been undertaken utilizing viruses of the pH1N1 lineage in combination with heterologous IAV strains. In two such studies, reassortant viral polymerase complexes were generated and polymerase activity was compared to that of the wild-type polymerase complex (133, 134). Resulting data independently showed that i) the combination of pH1N1 PB2 and seasonal H1N1 (sH1N1) PB1 significantly reduced polymerase activity, and that a compensatory mutation in the sH1N1 PB1 could help alleviate this mismatch, and ii) replacing the pH1N1 PB2 or PB1 was less detrimental to polymerase activity than replacing the pH1N1 PA. Our own data on reassortment between pH1N1 and seasonal H3N2 viruses similarly revealed that replacement of the pH1N1 PA with that of the H3N2 virus was strongly disfavored. In particular, minireplicon studies and reassortment patterns indicated the pH1N1 PB2 required the cognate PA to support high polymerase activity and virus viability (69). Co-assortment of PB2 and PA of pH1N1 was also noted by Schrauwen et al. (70). Finally, an in-depth analysis of the heterologous $PB2_{pH1N1}$:PA_{H3N2} pairing revealed that the defect lied in impaired replication-initiation relative to the full pH1N1 polymerase complex, and that this phenotype mapped largely to PA_{H3N2} residues 184N and 383N (135). Overall, these data suggest that reassortment between various IAV lineages is limited by polymerase subunit mismatch.

HA-NA mismatch. Another common example of protein incompatibility is between the functions of the HA (receptor-binding) and NA (receptor-destroying) IAV glycoproteins. The function of these proteins must be balanced in order for incoming virus to attach to host cells and be successfully released at the end of the viral life cycle (136). A substantial body of literature indicates that, when these proteins are in imbalance, viruses exhibit fitness defects. Some examples of this literature follow. Studies performed with influenza A/USSR/90/77 (H1N1) [USSR] showed that reassortant viruses containing the USSR NA gene and HA genes of H3, H4, H10, or H13 subtypes exhibited extensive virion aggregation, and that treatment with a bacterial neuraminidase was able to irreversibly dissociate these virion clumps (137, 138). A subsequent study suggested that the USSR NA gene was essentially non-functional in both the reassortant and parental strains and, in the reassortant viruses, this functional defect could be compensated for by mutations in the HA segment which led to decreased sialic acid affinity (73). In the same study discussed above in the context of polymerase mismatch, Hatta *et al.* were able to generate viruses containing the HA and NA genes from Mem/88 (H3N2) in a Mal/NY (H2N2) background, but were unable to generate viruses containing only the HA or the NA gene from Mem/88, demonstrating the importance of having a functional balance between HA and NA genes for successful IAV replication (132). Castrucci and Kawaoka generated a mutant WSN (H1N1) virus that had a 24 amino acid deletion in the NA stalk, which rendered the virus unable to replicate in embryonated chicken eggs due to defective NA function (139). However, passage of this mutant virus in eggs resulted in egg-adapted viruses which were able to replicate efficiently. Half of these adapted viruses displayed reduced affinity for sialic acid residues when compared to the parental virus, and analysis of the HA gene sequence of one of these viruses revealed mutations near the receptor binding site (140). Thus, reduction in HA affinity was found to compensate for low NA activity.

These findings underscore the importance of balanced HA-NA function for viral fitness and highlight the role of mutation in correcting functional imbalances.

NS-vRNP mismatch. A third example of protein mismatch involves gene products of the IAV NS segment in combination with the vRNP components. The NS segment encodes two proteins: the non-structural protein 1 (NS1) and the non-structural protein 2 (NS2). NS1 allows IAV to evade the host antiviral response by delaying the onset of interferon production (141). NS2, also referred to as the nuclear export protein (NEP), interacts with nucleoporins in the host cell nuclear membrane, enabling IAV vRNPs to exit the nucleus (142). In addition to these classical roles, it has also been shown that both NS proteins influence viral transcription and replication. For example, the addition of NS2 to vRNP reconstitution assays alters the relative accumulation of mRNA, cRNA, and vRNA, resulting in a shift towards replication products (vRNA and cRNA) and away from transcription products (mRNA) (143). Additionally, co-immunoprecipitation assays have revealed that NS1 interacts physically with vRNPs (144, 145), while genetic approaches suggest a role in the regulation of vRNA production (146). NS1 also contributes to control of viral gene expression by enhancing the translation of viral proteins (147-149).

Using highly pathogenic avian influenza viruses, Wang *et al.* introduced NS segments from either influenza A/goose/Guangdong/1/96 (H5N1) [GD/1], influenza A/Vietnam/1203/2004 (H5N1), or influenza A/Mallard/NL/12/2000 (H7N3) viruses into an influenza A/FPV/Rostock/1934 (H7N1) background by reverse genetics. Cells infected with the virus containing the GD/1 NS segment accumulated more mRNA, cRNA, and vRNA than cells infected with the parental H7N1 virus or the other NS reassortants (150), demonstrating how a heterologous NS segment can alter the efficiency of viral RNA synthesis. Subsequent RNP reconstitution assays suggested that the NS1

protein, in concert with other host or viral factors, was responsible for the observed differences in RNA accumulation.

NS1 can bind to cleavage and polyadenylation specificity factor 30 (CPSF30), a cellular factor involved in processing the 3' ends of cellular pre-mRNAs (151-153). The IAV polymerase complex (PB2, PB1, PA, and NP) was shown to stabilize the binding of NS1 to CPSF30 and, furthermore, PA and NP were responsible for mediating this stability (154). Interestingly, this stabilization could only be achieved with homologous NS1-polymerase components; the polymerase complex of influenza A/Udorn/307/72 (H3N2) virus was unable to stabilize a NS1-CPSF30 complex containing an influenza A/Hong Kong/483/97 (H5N1) virus NS1 protein, and vice versa (154, 155). As successful binding of NS1 to CPSF30 is important for helping control the production of interferon by the host cell, mismatch between NS1 and specific vRNP components can lead to inadequate control of the host immune response in IAV-infected cells.

To examine the fitness of viruses encoding heterologous vRNP and NS proteins, Shelton *et al*. rescued viruses containing PB2/PB1/PA/NP from a pH1N1 virus and an NS segment from either pH1N1, PR8 (H1N1), or influenza A/England/612/2003 (H3N2) viruses. Experiments in A549 cells showed that the viruses containing either heterologous NS produced less vRNA at 7 h and 24 h post-infection compared to the virus containing the homologous NS segment (156). The observed differences in vRNA production could potentially be mediated through either NS1 or NEP function (or both). The authors suggest NS1, since the homologous NS1 lacks the ability to bind to CPSF30. While this inability to bind CPSF30 would lessen control of interferon production by the host cell, the authors argue it could also lead to an increase in polymerase function and therefore an increase in vRNA levels. Additionally, in mice, the virus with the homologous NS produced the most weight loss, the highest viral load and greatest interferon-β production. These

results suggest that NS-vRNP mismatch can lessen virulence by reducing replicative fitness (156). Taken together, mismatch between NS and vRNP components can alter essential viral processes, control of host immune responses, and ultimately decrease the fitness of reassortant progeny.

Additional remarks. Owing to the large number of physical and functional interactions among viral proteins that are critical for maintaining viral fitness, and the diversity of amino acid sequences represented in circulating IAVs, protein mismatch is a complex phenomenon. Although much progress has been made in characterizing mismatch between heterologous viral proteins, results are often seen to depend on the parental strain pairing. While this reality makes predictions of protein compatibility for a given pair of parental strains extremely challenging, documentation of mismatch in reassortant viruses remains a useful tool for deciphering functional interactions occurring throughout the viral life cycle. In other words, where incompatibilities occur, interactions can be detected. Although the same mismatch may not be apparent with a different pairing of parental viruses, the functional interaction identified is likely to be broadly conserved.

Advantages of reassortment between heterologous IAVs

Although often constrained by segment mismatch, reassortment can also facilitate host adaptation, an increase in host range, or evasion from pre-existing immunity (157, 158). Most notably, reassortant viruses that derive a subset of gene segments from non-human hosts were seen to cause the last three pandemics. In this natural situation, post-reassortment adaptive changes were likely needed to achieve high fitness. In addition, however, multiple experimental studies using avian plus human, swine plus human or human plus human IAV strains have demonstrated that, even though some reassortant viruses displayed relatively low fitness, others exhibited high levels of

genetic compatibility and increased pathogenicity or transmissibility when compared to the parental strains in model systems (70, 159-163).

Multiple risk assessment studies to date in the mouse model have demonstrated an increase in IAV virulence following reassortment. For example, incorporation of the PB1 gene from an avian H5N1 virus into a background of human H3N2 internal genes led to increased pathogenicity (92). Based on these results, and the derivation of the PB1 segment from avian IAVs in the 1957 and 1968 pandemic strains, the authors postulated that acquisition of an avian PB1 gene by a human IAV might allow for the reassortant to outcompete currently circulating IAVs (20, 92). In a panel of H5N1 subtype reassortants where each contained one internal H9N2 gene, viruses containing the H9N2 PB2 gene were attenuated in mice compared to the parental virus strains, while viruses containing the H9N2 PA or NP genes were 100% lethal in mice (164). Strikingly, none of the other viruses tested, including the parental strains, caused any mortality. Furthermore, the presence of the H9N2 PA or NP gene conferred a wider tissue tropism in mice and an increase in polymerase activity, while the presence of the H9N2 PB2 gene resulted in a decrease in polymerase activity. Ma *et al.* rescued a H7N1 virus containing a H5N1 NS gene and showed that the reassortant virus could replicate more effectively in cell culture than the wild-type H7N1 virus (165). Additionally, the reassortant virus caused morbidity and mortality in mice, while the wild-type virus was unable to successfully replicate in mice. These data highlight how segment mismatch can limit the fitness of certain reassortant genotypes while other combinations of heterologous segments can confer an advantage in replication or tissue tropism.

Two additional reverse genetics-based risk assessment studies examined the fitness of pH1N1 and H5N1 reassortant viruses. Cline *et al*. demonstrated that a pH1N1 virus containing a H5N1 HA gene was able to replicate more efficiently than both the parental viruses and all other reassortant

viruses tested in MDCK and A549 cells (166). In addition, mice infected with the H5 HA-containing virus exhibited increased pulmonary disease compared to mice infected with either parental strain, but this virus failed to transmit in a ferret model. Generating 127 reassortant viruses between a pH1N1 isolate and a highly pathogenic H5N1 strain, Zhang *et al*. identified single gene reassortants that conferred aerosol transmission in a guinea pig model to the contact-transmissible H5N1 virus (167). Both the pH1N1 PA and NS genes were individually found to allow for respiratory droplet transmission of H5N1 subtype reassortants in guinea pigs.

Taken together, these data offer examples of the wide array of effects a single reassortment event can have on factors such as virus growth, cell tropism, host range, immune evasion, and transmissibility. While segment mismatch often hinders the assembly or subsequent spread of certain reassortant genotypes (Fig. 3), these constraints can sometimes be minimal, enabling the successful evolution of IAV under selective pressure. Importantly, the impact of segment mismatch on IAV reassortment is determined not only by the degree of RNA- and protein-based incompatibilities present between two co-infecting strains, but also by the surrounding host and environmental conditions, which define the selective environment.

Conclusions

When two divergent IAVs co-infect the same cell, the genetic diversity and fitness of reassortant progeny are limited by segment mismatch, or the incompatibilities between heterologous components of parental virus strains. While segment mismatch imposes barriers to reassortment, in some genetic constellations the detrimental effects associated with segment mismatch might be offset by enhancements in immune evasion or host adaptation of the reassortant virus. Due to the complexity of reassortant virus fitness, the models and experimental conditions used successfully

for one study might prove suboptimal for the next. Further studies are therefore needed to more systematically document the underlying mechanisms of segment mismatch. A point of particular interest is the relative contributions of RNA and protein mismatch in determining the outcomes of reassortment between divergent IAV strains. This distinction is important because, once greater mechanistic understanding of IAV genome packaging is achieved, mapping of mismatches among RNA-based packaging signals may allow sequence-based prediction of compatible gene constellations. These studies will yield important contributions towards IAV pandemic preparedness and strengthen efforts to predict and control zoonotic outbreaks.

[a]Dissertation aims

The overarching aim of this dissertation was to determine what effect segment mismatch at the RNA level had on IAV reassortment efficiency. Previous work by others prior to the onset of the experiments contained herein had demonstrated proof of principle that RNA incompatibilities between IAVs were sufficient to limit reassortment. This dissertation expands upon these initial findings, quantifying for the first time the impact of RNA mismatch on IAV reassortment efficiency and showing that the importance of this mismatch in IAV reassortment is segment dependent. We then extend these findings to include IAV strains where reassortment events would raise concern for the emergence of a pandemic virus, such as reassortment between avian and human IAVs. We show that mismatch at the RNA level reduces the likelihood that avian-human IAV reassortment would occur. However, this RNA mismatch is not sufficient to completely prevent the formation of reassortant genotypes, as demonstrated in both cell culture and an intact host. These findings highlight the continued need for IAV surveillance, especially in areas where avian and human IAVs are in close proximity.

Funding information

We acknowledge funding support from the NIAID Centers of Excellence in Influenza Research and Surveillance (CEIRS), contract number HHSN272201400004C, and R01 grants AI125268 and AI099000.

Conflicts of interest

We declare no conflicts of interest.

Figures

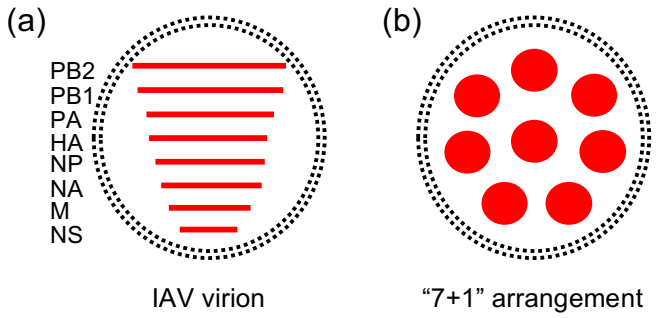

Fig. 1. The influenza A virus genome. (a) Schematic diagram of the IAV genome, with the eight RNA genomic segments organized according to size from largest to smallest. (b) Arrangement of the IAV genome within a virus particle, demonstrating the “7+1” pattern of the eight viral segments as observed via transmission electron microscopy performed by Noda *et al*. One central segment is surrounded by seven outer segments. However, the identity of the segments arranged in this pattern, as well as the precise interaction network between the segments, remains unknown. The glycoproteins present on the viral membrane have been removed for clarity.

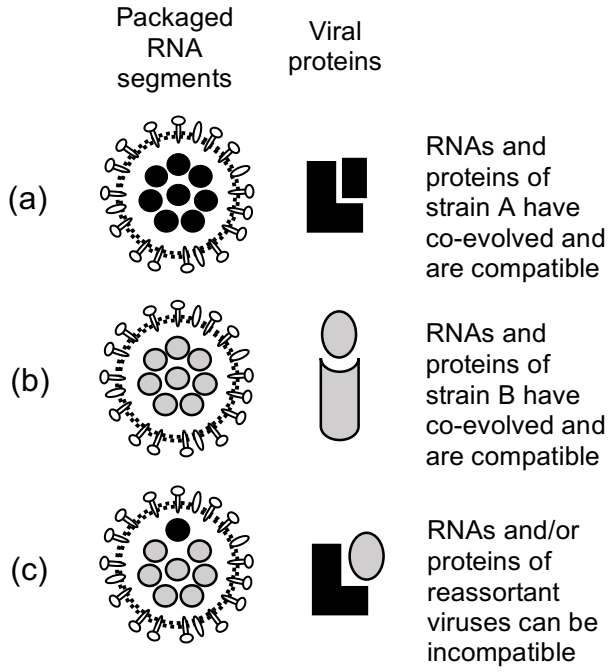

Fig. 2. Reassortant influenza A viruses can have suboptimal RNA and/or protein interactions. During IAV evolution, the genomes and proteins of an individual strain co-evolve alongside one another, resulting in optimal interactions (a and b). During reassortment, the genomes of the two co-infecting strains are mixed. This can result in suboptimal interactions between the genomic segments and/or encoded proteins, leading to viruses that are less fit compared to the parental strains (c).

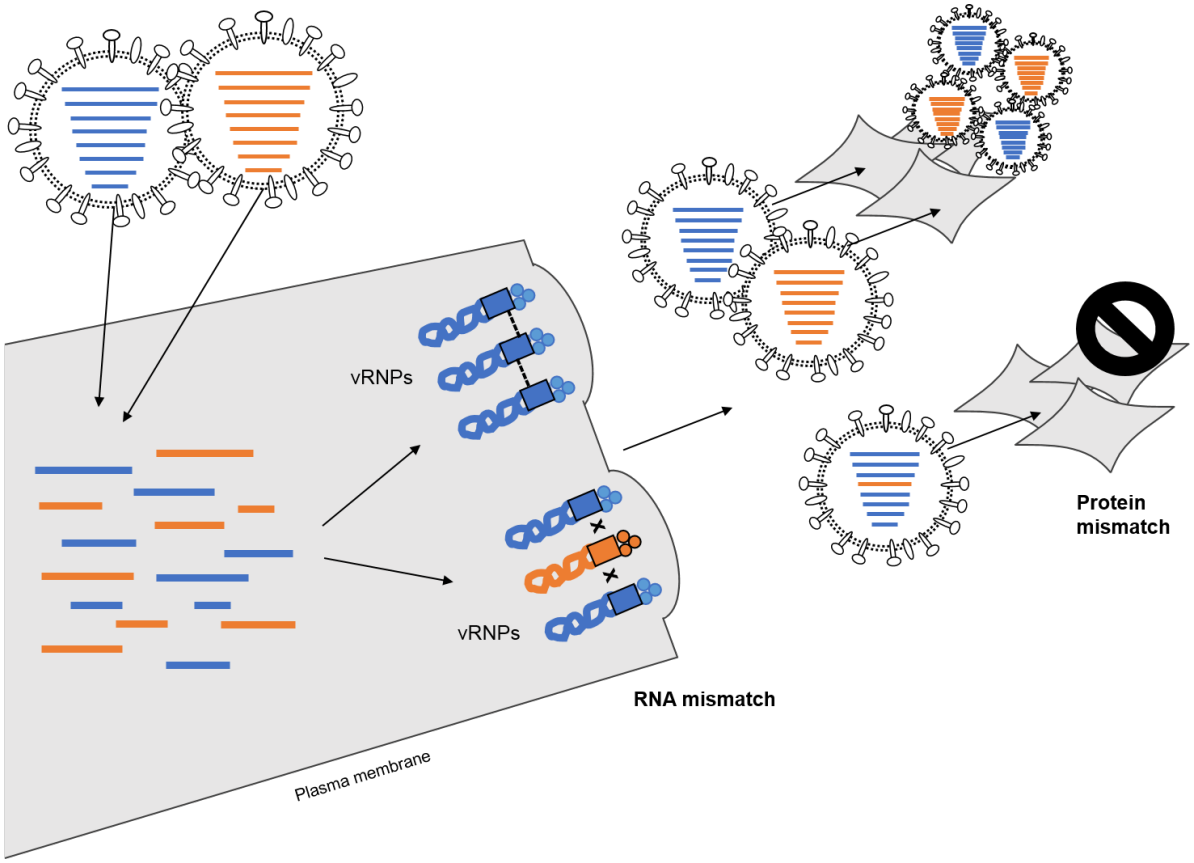

Fig. 3. Manifestations of segment mismatch during the influenza A virus life cycle. When two different IAVs co-infect the same cell, their genomes mix, resulting in the genomic assembly of viral ribonucleoprotein complexes (vRNPs) from either the same virus (as shown in blue) or from different viruses (as shown in blue and orange). The interactions that occur between segments, most likely at the packaging signal regions (dotted lines between colored rectangles), might be optimal when segments originate from the same parental virus, thus facilitating packaging. Conversely, these interactions might be suboptimal or non-existent (black x's) between heterologous segments due to nucleotide differences, and thus formation of these progeny genotypes would be restricted due to RNA mismatch. Protein mismatch manifests later, after reassortant viruses have budded from the host cell and go on to infect new cells. Incompatibilities

between polymerase subunits or HA-NA proteins, among others, can prevent the successful formation of progeny viruses, resulting in an abortive infection. Proteins and RNAs are shown with the same color for clarity; however, in co-infected cells, proteins derived from co-infecting viruses are thought to mix.

References

1. **Shaw ML, Palese P.** 2013. Orthomyxoviridae, p 1151–1185. *In* Knipe D, Howley P (ed), Fields Virology, vol 1. Lippincott Williams & Wilkins, Philadelphia, PA.
2. **Tong S, Li Y, Rivailler P, Conrardy C, Castillo DA, Chen LM, Recuenco S, Ellison JA, Davis CT, York IA, Turmelle AS, Moran D, Rogers S, Shi M, Tao Y, Weil MR, Tang K, Rowe LA, Sammons S, Xu X, Frace M, Lindblade KA, Cox NJ, Anderson LJ, Rupprecht CE, Donis RO.** 2012. A distinct lineage of influenza A virus from bats. Proc Natl Acad Sci U S A **109:**4269-4274.
3. **Tong S, Zhu X, Li Y, Shi M, Zhang J, Bourgeois M, Yang H, Chen X, Recuenco S, Gomez J, Chen LM, Johnson A, Tao Y, Dreyfus C, Yu W, McBride R, Carney PJ, Gilbert AT, Chang J, Guo Z, Davis CT, Paulson JC, Stevens J, Rupprecht CE, Holmes EC, Wilson IA, Donis RO.** 2013. New world bats harbor diverse influenza A viruses. PLoS Pathog **9:**e1003657.
4. **Munster VJ, Baas C, Lexmond P, Waldenstrom J, Wallensten A, Fransson T, Rimmelzwaan GF, Beyer WE, Schutten M, Olsen B, Osterhaus AD, Fouchier RA.** 2007. Spatial, temporal, and species variation in prevalence of influenza A viruses in wild migratory birds. PLoS Pathog **3:**e61.
5. **Webster RG, Bean WJ, Gorman OT, Chambers TM, Kawaoka Y.** 1992. Evolution and ecology of influenza A viruses. Microbiol Rev **56:**152-179.
6. **Holmes EC, Ghedin E, Miller N, Taylor J, Bao Y, St George K, Grenfell BT, Salzberg SL, Fraser CM, Lipman DJ, Taubenberger JK.** 2005. Whole-Genome Analysis of Human Influenza A Virus Reveals Multiple Persistent Lineages and Reassortment among Recent H3N2 Viruses. PLoS Biol **3:**e300.

7. **Nelson MI, Simonsen L, Viboud C, Miller MA, Taylor J, George KS, Griesemer SB, Ghedin E, Sengamalay NA, Spiro DJ, Volkov I, Grenfell BT, Lipman DJ, Taubenberger JK, Holmes EC.** 2006. Stochastic processes are key determinants of short-term evolution in influenza a virus. PLoS Pathog **2:**e125.

8. **Nelson MI, Edelman L, Spiro DJ, Boyne AR, Bera J, Halpin R, Sengamalay N, Ghedin E, Miller MA, Simonsen L, Viboud C, Holmes EC.** 2008. Molecular epidemiology of A/H3N2 and A/H1N1 influenza virus during a single epidemic season in the United States. PLoS Pathog **4:**e1000133.

9. **Westgeest KB, Russell CA, Lin X, Spronken MI, Bestebroer TM, Bahl J, van Beek R, Skepner E, Halpin RA, de Jong JC, Rimmelzwaan GF, Osterhaus AD, Smith DJ, Wentworth DE, Fouchier RA, de Graaf M.** 2014. Genomewide analysis of reassortment and evolution of human influenza A(H3N2) viruses circulating between 1968 and 2011. J Virol **88:**2844-2857.

10. **Rambaut A, Pybus OG, Nelson MI, Viboud C, Taubenberger JK, Holmes EC.** 2008. The genomic and epidemiological dynamics of human influenza A virus. Nature **453:**615-619.

11. **Villa M, Lassig M.** 2017. Fitness cost of reassortment in human influenza. PLoS Pathog **13:**e1006685.

12. **Johnson NP, Mueller J.** 2002. Updating the accounts: global mortality of the 1918-1920 "Spanish" influenza pandemic. Bull Hist Med **76:**105-115.

13. **Viboud C, Simonsen L, Fuentes R, Flores J, Miller MA, Chowell G.** 2016. Global Mortality Impact of the 1957-1959 Influenza Pandemic. J Infect Dis **213:**738-745.

14. **Cockburn WC, Delon PJ, Ferreira W.** 1969. Origin and progress of the 1968-69 Hong Kong influenza epidemic. Bull World Health Organ **41:**345-348.

15. **Simonsen L, Spreeuwenberg P, Lustig R, Taylor RJ, Fleming DM, Kroneman M, Van Kerkhove MD, Mounts AW, Paget WJ, the GCT.** 2013. Global Mortality Estimates for the 2009 Influenza Pandemic from the GLaMOR Project: A Modeling Study. PLoS Med **10:**e1001558.

16. **Worobey M, Han GZ, Rambaut A.** 2014. Genesis and pathogenesis of the 1918 pandemic H1N1 influenza A virus. Proc Natl Acad Sci U S A **111:**8107-8112.

17. **Taubenberger JK, Reid AH, Lourens RM, Wang R, Jin G, Fanning TG.** 2005. Characterization of the 1918 influenza virus polymerase genes. Nature **437:**889-893.

18. **Gibbs MJ, Gibbs AJ.** 2006. Molecular virology: Was the 1918 pandemic caused by a bird flu? Nature **440:**E8-E8.

19. **Kilbourne ED.** 2006. Influenza pandemics of the 20th century. Emerg Infect Dis **12:**9-14.

20. **Kawaoka Y, Krauss S, Webster RG.** 1989. Avian-to-human transmission of the PB1 gene of influenza A viruses in the 1957 and 1968 pandemics. J Virol **63:**4603-4608.

21. **Garten RJ, Davis CT, Russell CA, Shu B, Lindstrom S, Balish A, Sessions WM, Xu X, Skepner E, Deyde V, Okomo-Adhiambo M, Gubareva L, Barnes J, Smith CB, Emery SL, Hillman MJ, Rivailler P, Smagala J, de Graaf M, Burke DF, Fouchier RAM, Pappas C, Alpuche-Aranda CM, López-Gatell H, Olivera H, López I, Myers CA, Faix D, Blair PJ, Yu C, Keene KM, Dotson PD, Boxrud D, Sambol AR, Abid SH, St. George K, Bannerman T, Moore AL, Stringer DJ, Blevins P, Demmler-Harrison GJ, Ginsberg M, Kriner P, Waterman S, Smole S, Guevara HF, Belongia EA, Clark**

PA, Beatrice ST, Donis R, et al. 2009. Antigenic and Genetic Characteristics of Swine-Origin 2009 A(H1N1) Influenza Viruses Circulating in Humans. Science **325:**197-201.

22. **Smith GJD, Vijaykrishna D, Bahl J, Lycett SJ, Worobey M, Pybus OG, Ma SK, Cheung CL, Raghwani J, Bhatt S, Peiris JSM, Guan Y, Rambaut A.** 2009. Origins and evolutionary genomics of the 2009 swine-origin H1N1 influenza A epidemic. Nature **459:**1122-1125.

23. **York I, Donis RO.** 2013. The 2009 pandemic influenza virus: where did it come from, where is it now, and where is it going? Curr Top Microbiol Immunol **370:**241-257.

24. **Ku AS, Chan LT.** 1999. The first case of H5N1 avian influenza infection in a human with complications of adult respiratory distress syndrome and Reye's syndrome. J Paediatr Child Health **35:**207-209.

25. **Chan PK.** 2002. Outbreak of avian influenza A(H5N1) virus infection in Hong Kong in 1997. Clin Infect Dis **34 Suppl 2:**S58-64.

26. **Tran TH, Nguyen TL, Nguyen TD, Luong TS, Pham PM, Nguyen v V, Pham TS, Vo CD, Le TQ, Ngo TT, Dao BK, Le PP, Nguyen TT, Hoang TL, Cao VT, Le TG, Nguyen DT, Le HN, Nguyen KT, Le HS, Le VT, Christiane D, Tran TT, Menno de J, Schultsz C, Cheng P, Lim W, Horby P, Farrar J.** 2004. Avian influenza A (H5N1) in 10 patients in Vietnam. N Engl J Med **350:**1179-1188.

27. **Ungchusak K, Auewarakul P, Dowell SF, Kitphati R, Auwanit W, Puthavathana P, Uiprasertkul M, Boonnak K, Pittayawonganon C, Cox NJ, Zaki SR, Thawatsupha P, Chittaganpitch M, Khontong R, Simmerman JM, Chunsutthiwat S.** 2005. Probable person-to-person transmission of avian influenza A (H5N1). N Engl J Med **352:**333-340.

28. **Gao R, Cao B, Hu Y, Feng Z, Wang D, Hu W, Chen J, Jie Z, Qiu H, Xu K, Xu X, Lu H, Zhu W, Gao Z, Xiang N, Shen Y, He Z, Gu Y, Zhang Z, Yang Y, Zhao X, Zhou L, Li X, Zou S, Zhang Y, Li X, Yang L, Guo J, Dong J, Li Q, Dong L, Zhu Y, Bai T, Wang S, Hao P, Yang W, Zhang Y, Han J, Yu H, Li D, Gao GF, Wu G, Wang Y, Yuan Z, Shu Y.** 2013. Human Infection with a Novel Avian-Origin Influenza A (H7N9) Virus. N Engl J Med **368:**1888-1897.

29. **Fouchier RAM, Schneeberger PM, Rozendaal FW, Broekman JM, Kemink SAG, Munster V, Kuiken T, Rimmelzwaan GF, Schutten M, van Doornum GJJ, Koch G, Bosman A, Koopmans M, Osterhaus ADME.** 2004. Avian influenza A virus (H7N7) associated with human conjunctivitis and a fatal case of acute respiratory distress syndrome. Proc Natl Acad Sci U S A **101:**1356-1361.

30. **WHO.** 2017. Cumulative number of confirmed human cases for avian influenza A(H5N1) reported to WHO, 2003-2017. http://www.who.int/influenza/human_animal_interface/2017_09_27_tableH5N1.pdf?ua=1. Accessed November 11.

31. **WHO.** 2017. Influenza at the human-animal interface. http://www.who.int/influenza/human_animal_interface/Influenza_Summary_IRA_HA_interface_09_27_2017.pdf?ua=1. Accessed November 11.

32. **Lam TT, Wang J, Shen Y, Zhou B, Duan L, Cheung CL, Ma C, Lycett SJ, Leung CY, Chen X, Li L, Hong W, Chai Y, Zhou L, Liang H, Ou Z, Liu Y, Farooqui A, Kelvin DJ, Poon LL, Smith DK, Pybus OG, Leung GM, Shu Y, Webster RG, Webby RJ, Peiris JS, Rambaut A, Zhu H, Guan Y.** 2013. The genesis and source of the H7N9 influenza viruses causing human infections in China. Nature **502:**241-244.

33. **Wu A, Su C, Wang D, Peng Y, Liu M, Hua S, Li T, Gao GF, Tang H, Chen J, Liu X, Shu Y, Peng D, Jiang T.** 2013. Sequential reassortments underlie diverse influenza H7N9 genotypes in China. Cell Host Microbe **14:**446-452.

34. **Li KS, Guan Y, Wang J, Smith GJ, Xu KM, Duan L, Rahardjo AP, Puthavathana P, Buranathai C, Nguyen TD, Estoepangestie AT, Chaisingh A, Auewarakul P, Long HT, Hanh NT, Webby RJ, Poon LL, Chen H, Shortridge KF, Yuen KY, Webster RG, Peiris JS.** 2004. Genesis of a highly pathogenic and potentially pandemic H5N1 influenza virus in eastern Asia. Nature **430:**209-213.

35. **Guan Y, Shortridge KF, Krauss S, Webster RG.** 1999. Molecular characterization of H9N2 influenza viruses: were they the donors of the "internal" genes of H5N1 viruses in Hong Kong? Proc Natl Acad Sci U S A **96:**9363-9367.

36. **Lin YP, Shaw M, Gregory V, Cameron K, Lim W, Klimov A, Subbarao K, Guan Y, Krauss S, Shortridge K, Webster R, Cox N, Hay A.** 2000. Avian-to-human transmission of H9N2 subtype influenza A viruses: relationship between H9N2 and H5N1 human isolates. Proc Natl Acad Sci U S A **97:**9654-9658.

37. **Chen H, Yuan H, Gao R, Zhang J, Wang D, Xiong Y, Fan G, Yang F, Li X, Zhou J, Zou S, Yang L, Chen T, Dong L, Bo H, Zhao X, Zhang Y, Lan Y, Bai T, Dong J, Li Q, Wang S, Zhang Y, Li H, Gong T, Shi Y, Ni X, Li J, Zhou J, Fan J, Wu J, Zhou X, Hu M, Wan J, Yang W, Li D, Wu G, Feng Z, Gao GF, Wang Y, Jin Q, Liu M, Shu Y.** 2014. Clinical and epidemiological characteristics of a fatal case of avian influenza A H10N8 virus infection: a descriptive study. Lancet **383:**714-721.

38. **Zhang Z, Li R, Jiang L, Xiong C, Chen Y, Zhao G, Jiang Q.** 2016. The complexity of human infected AIV H5N6 isolated from China. BMC Infect Dis **16:**600.

39. **Huang Y, Li X, Zhang H, Chen B, Jiang Y, Yang L, Zhu W, Hu S, Zhou S, Tang Y, Xiang X, Li F, Li W, Gao L.** 2015. Human infection with an avian influenza A (H9N2) virus in the middle region of China. J Med Virol **87:**1641-1648.

40. **Yuan J, Zhang L, Kan X, Jiang L, Yang J, Guo Z, Ren Q.** 2013. Origin and molecular characteristics of a novel 2013 avian influenza A(H6N1) virus causing human infection in Taiwan. Clin Infect Dis **57:**1367-1368.

41. **Lubeck MD, Palese P, Schulman JL.** 1979. Nonrandom association of parental genes in influenza A virus recombinants. Virology **95:**269-274.

42. **Greenbaum BD, Li OT, Poon LL, Levine AJ, Rabadan R.** 2012. Viral reassortment as an information exchange between viral segments. Proc Natl Acad Sci U S A **109:**3341-3346.

43. **Pauly MD, Procario MC, Lauring AS.** 2017. A novel twelve class fluctuation test reveals higher than expected mutation rates for influenza A viruses. Elife **6**.

44. **Wrammert J, Koutsonanos D, Li GM, Edupuganti S, Sui J, Morrissey M, McCausland M, Skountzou I, Hornig M, Lipkin WI, Mehta A, Razavi B, Del Rio C, Zheng NY, Lee JH, Huang M, Ali Z, Kaur K, Andrews S, Amara RR, Wang Y, Das SR, O'Donnell CD, Yewdell JW, Subbarao K, Marasco WA, Mulligan MJ, Compans R, Ahmed R, Wilson PC.** 2011. Broadly cross-reactive antibodies dominate the human B cell response against 2009 pandemic H1N1 influenza virus infection. J Exp Med **208:**181-193.

45. **Ekiert DC, Bhabha G, Elsliger MA, Friesen RH, Jongeneelen M, Throsby M, Goudsmit J, Wilson IA.** 2009. Antibody recognition of a highly conserved influenza virus epitope. Science **324:**246-251.

46. **Memoli MJ, Shaw PA, Han A, Czajkowski L, Reed S, Athota R, Bristol T, Fargis S, Risos K, Powers JH, Davey RT, Jr., Taubenberger JK.** 2016. Evaluation of Antihemagglutinin and Antineuraminidase Antibodies as Correlates of Protection in an Influenza A/H1N1 Virus Healthy Human Challenge Model. MBio **7:**e00417-00416.

47. **Gerhard W, Yewdell J, Frankel ME, Webster R.** 1981. Antigenic structure of influenza virus haemagglutinin defined by hybridoma antibodies. Nature **290:**713-717.

48. **Plotkin JB, Dushoff J, Levin SA.** 2002. Hemagglutinin sequence clusters and the antigenic evolution of influenza A virus. Proc Natl Acad Sci U S A **99:**6263-6268.

49. **Smith DJ, Lapedes AS, de Jong JC, Bestebroer TM, Rimmelzwaan GF, Osterhaus ADME, Fouchier RAM.** 2004. Mapping the Antigenic and Genetic Evolution of Influenza Virus. Science **305:**371-376.

50. **Cox NJ, Brammer TL, Regnery HL.** 1994. Influenza: global surveillance for epidemic and pandemic variants. Eur J Epidemiol **10:**467-470.

51. **Nelson MI, Viboud C, Simonsen L, Bennett RT, Griesemer SB, St. George K, Taylor J, Spiro DJ, Sengamalay NA, Ghedin E, Taubenberger JK, Holmes EC.** 2008. Multiple Reassortment Events in the Evolutionary History of H1N1 Influenza A Virus Since 1918. PLoS Pathog **4:**e1000012.

52. **Nelson MI, Holmes EC.** 2007. The evolution of epidemic influenza. Nat Rev Genet **8:**196-205.

53. **Simonsen L, Viboud C, Grenfell BT, Dushoff J, Jennings L, Smit M, Macken C, Hata M, Gog J, Miller MA, Holmes EC.** 2007. The genesis and spread of reassortment human influenza A/H3N2 viruses conferring adamantane resistance. Mol Biol Evol **24:**1811-1820.

54. **Nelson MI, Simonsen L, Viboud C, Miller MA, Holmes EC.** 2009. The origin and global emergence of adamantane resistant A/H3N2 influenza viruses. Virology **388:**270-278.

55. **Wright P, Neumann G, Kawaoka Y.** 2013. Orthomyxoviruses. *In* Knipe D, Howley P (ed), Fields Virology, 6th ed, vol 1. Lippincott Williams & Wilkins.

56. **Ellis JS, Alvarez-Aguero A, Gregory V, Lin YP, Hay A, Zambon MC.** 2003. Influenza AH1N2 viruses, United Kingdom, 2001-02 influenza season. Emerg Infect Dis **9:**304-310.

57. **Chen MJ, La T, Zhao P, Tam JS, Rappaport R, Cheng SM.** 2006. Genetic and phylogenetic analysis of multi-continent human influenza A(H1N2) reassortant viruses isolated in 2001 through 2003. Virus Res **122:**200-205.

58. **Gregory V, Bennett M, Orkhan MH, Al Hajjar S, Varsano N, Mendelson E, Zambon M, Ellis J, Hay A, Lin YP.** 2002. Emergence of influenza A H1N2 reassortant viruses in the human population during 2001. Virology **300:**1-7.

59. **Xu X, Smith CB, Mungall BA, Lindstrom SE, Hall HE, Subbarao K, Cox NJ, Klimov A.** 2002. Intercontinental Circulation of Human Influenza A(H1N2) Reassortant Viruses during the 2001–2002 Influenza Season. J Infect Dis **186:**1490-1493.

60. **Mukherjee TR, Agrawal AS, Chakrabarti S, Chawla-Sarkar M.** 2012. Full genomic analysis of an influenza A (H1N2) virus identified during 2009 pandemic in Eastern India: evidence of reassortment event between co-circulating A(H1N1)pdm09 and A/Brisbane/10/2007-like H3N2 strains. Virol J **9:**1-10.

61. **Rith S, Chin S, Sar B, Y P, Horm SV, Ly S, Buchy P, Dussart P, Horwood PF.** 2015. Natural co-infection of influenza A/H3N2 and A/H1N1pdm09 viruses resulting in a reassortant A/H3N2 virus. J Clin Virol **73:**108-111.

62. **Liu W, Li ZD, Tang F, Wei MT, Tong YG, Zhang L, Xin ZT, Ma MJ, Zhang XA, Liu LJ, Zhan L, He C, Yang H, Boucher CA, Richardus JH, Cao WC.** 2010. Mixed infections of pandemic H1N1 and seasonal H3N2 viruses in 1 outbreak. Clin Infect Dis **50:**1359-1365.

63. **Myers CA, Kasper MR, Yasuda CY, Savuth C, Spiro DJ, Halpin R, Faix DJ, Coon R, Putnam SD, Wierzba TF, Blair PJ.** 2011. Dual infection of novel influenza viruses A/H1N1 and A/H3N2 in a cluster of Cambodian patients. Am J Trop Med Hyg **85:**961-963.

64. **Yamane N, Arikawa J, Odagiri T, Sukeno N, Ishida N.** 1978. Isolation of three different influenza A viruses from an individual after probable double infection with H3N2 and H1N1 viruses. Jpn J Med Sci Biol **31:**431-434.

65. **Falchi A, Arena C, Andreoletti L, Jacques J, Leveque N, Blanchon T, Lina B, Turbelin C, Dorleans Y, Flahault A, Amoros JP, Spadoni G, Agostini F, Varesi L.** 2008. Dual infections by influenza A/H3N2 and B viruses and by influenza A/H3N2 and A/H1N1 viruses during winter 2007, Corsica Island, France. J Clin Virol **41:**148-151.

66. **Kendal AP, Lee DT, Parish HS, Raines D, Noble GR, Dowdle WR.** 1979. Laboratory-based surveillance of influenza virus in the United States during the winter of 1977--1978. II. Isolation of a mixture of A/Victoria- and A/USSR-like viruses from a single person during an epidemic in Wyoming, USA, January 1978. Am J Epidemiol **110:**462-468.

67. **Frank AL, Taber LH, Wells JM.** 1983. Individuals infected with two subtypes of influenza A virus in the same season. J Infect Dis **147:**120-124.

68. **Nishikawa F, Sugiyama T.** 1983. Direct isolation of H1N2 recombinant virus from a throat swab of a patient simultaneously infected with H1N1 and H3N2 influenza A viruses. J Clin Microbiol **18:**425-427.

69. **Phipps KL, Marshall N, Tao H, Danzy S, Onuoha N, Steel J, Lowen AC.** 2017. Seasonal H3N2 and 2009 Pandemic H1N1 Influenza A Viruses Reassort Efficiently but Produce Attenuated Progeny. J Virol **91**.

70. **Schrauwen EJ, Herfst S, Chutinimitkul S, Bestebroer TM, Rimmelzwaan GF, Osterhaus AD, Kuiken T, Fouchier RA.** 2011. Possible increased pathogenicity of pandemic (H1N1) 2009 influenza virus upon reassortment. Emerg Infect Dis **17:**200-208.

71. **Mena I, Nelson MI, Quezada-Monroy F, Dutta J, Cortes-Fernandez R, Lara-Puente JH, Castro-Peralta F, Cunha LF, Trovao NS, Lozano-Dubernard B, Rambaut A, van Bakel H, Garcia-Sastre A.** 2016. Origins of the 2009 H1N1 influenza pandemic in swine in Mexico. Elife **5**.

72. **Ma W, Liu Q, Qiao C, del Real G, Garcia-Sastre A, Webby RJ, Richt JA.** 2014. North American triple reassortant and Eurasian H1N1 swine influenza viruses do not readily reassort to generate a 2009 pandemic H1N1-like virus. MBio **5:**e00919-00913.

73. **Kaverin NV, Gambaryan AS, Bovin NV, Rudneva IA, Shilov AA, Khodova OM, Varich NL, Sinitsin BV, Makarova NV, Kropotkina EA.** 1998. Postreassortment changes in influenza A virus hemagglutinin restoring HA-NA functional match. Virology **244:**315-321.

74. **Ilyushina NA, Rudneva IA, Shilov AA, Klenk HD, Kaverin NV.** 2005. Postreassortment changes in a model system: HA-NA adjustment in an H3N2 avian-human reassortant influenza virus. Arch Virol **150:**1327-1338.

75. **Neverov AD, Lezhnina KV, Kondrashov AS, Bazykin GA.** 2014. Intrasubtype reassortments cause adaptive amino acid replacements in H3N2 influenza genes. PLoS Genet **10:**e1004037.

76. **Steel J, Lowen AC.** 2014. Influenza A virus reassortment. Curr Top Microbiol Immunol **385:**377-401.

77. **Marshall N, Priyamvada L, Ende Z, Steel J, Lowen AC.** 2013. Influenza virus reassortment occurs with high frequency in the absence of segment mismatch. PLoS Pathog **9:**e1003421.

78. **Wittwer CT, Reed GH, Gundry CN, Vandersteen JG, Pryor RJ.** 2003. High-resolution genotyping by amplicon melting analysis using LCGreen. Clin Chem **49:**853-860.

79. **Fonville JM, Marshall N, Tao H, Steel J, Lowen AC.** 2015. Influenza Virus Reassortment Is Enhanced by Semi-infectious Particles but Can Be Suppressed by Defective Interfering Particles. PLoS Pathog **11:**e1005204.

80. **Huang IC, Li W, Sui J, Marasco W, Choe H, Farzan M.** 2008. Influenza A virus neuraminidase limits viral superinfection. J Virol **82:**4834-4843.

81. **Tao H, Steel J, Lowen AC.** 2014. Intrahost dynamics of influenza virus reassortment. J Virol **88:**7485-7492.

82. **Tao H, Li L, White MC, Steel J, Lowen AC.** 2015. Influenza A Virus Coinfection through Transmission Can Support High Levels of Reassortment. J Virol **89:**8453-8461.

83. **Wille M, Tolf C, Avril A, Latorre-Margalef N, Wallerstrom S, Olsen B, Waldenstrom J.** 2013. Frequency and patterns of reassortment in natural influenza A virus infection in a reservoir host. Virology **443:**150-160.

84. **Deng G, Tan D, Shi J, Cui P, Jiang Y, Liu L, Tian G, Kawaoka Y, Li C, Chen H.** 2013. Complex reassortment of multiple subtypes of avian influenza viruses in domestic ducks at the Dongting Lake Region of China. J Virol **87:**9452-9462.

85. **Abolnik C, Gerdes GH, Sinclair M, Ganzevoort BW, Kitching JP, Burger CE, Romito M, Dreyer M, Swanepoel S, Cumming GS, Olivier AJ.** 2010. Phylogenetic analysis of influenza A viruses (H6N8, H1N8, H4N2, H9N2, H10N7) isolated from wild birds, ducks, and ostriches in South Africa from 2007 to 2009. Avian Dis **54:**313-322.

86. **Dugan VG, Chen R, Spiro DJ, Sengamalay N, Zaborsky J, Ghedin E, Nolting J, Swayne DE, Runstadler JA, Happ GM, Senne DA, Wang R, Slemons RD, Holmes EC, Taubenberger JK.** 2008. The evolutionary genetics and emergence of avian influenza viruses in wild birds. PLoS Pathog **4:**e1000076.

87. **Nelson MI, Detmer SE, Wentworth DE, Tan Y, Schwartzbard A, Halpin RA, Stockwell TB, Lin X, Vincent AL, Gramer MR, Holmes EC.** 2012. Genomic reassortment of influenza A virus in North American swine, 1998-2011. J Gen Virol **93:**2584-2589.

88. **Vijaykrishna D, Poon LL, Zhu HC, Ma SK, Li OT, Cheung CL, Smith GJ, Peiris JS, Guan Y.** 2010. Reassortment of pandemic H1N1/2009 influenza A virus in swine. Science **328:**1529.

89. **Rabadan R, Levine AJ, Krasnitz M.** 2008. Non-random reassortment in human influenza A viruses. Influenza Other Respir Viruses **2:**9-22.

90. **Maines TR, Chen LM, Matsuoka Y, Chen H, Rowe T, Ortin J, Falcon A, Nguyen TH, Mai le Q, Sedyaningsih ER, Harun S, Tumpey TM, Donis RO, Cox NJ, Subbarao K,**

Katz JM. 2006. Lack of transmission of H5N1 avian-human reassortant influenza viruses in a ferret model. Proc Natl Acad Sci U S A **103:**12121-12126.

91. **Jackson S, Van Hoeven N, Chen LM, Maines TR, Cox NJ, Katz JM, Donis RO.** 2009. Reassortment between avian H5N1 and human H3N2 influenza viruses in ferrets: a public health risk assessment. J Virol **83:**8131-8140.

92. **Chen LM, Davis CT, Zhou H, Cox NJ, Donis RO.** 2008. Genetic compatibility and virulence of reassortants derived from contemporary avian H5N1 and human H3N2 influenza A viruses. PLoS Pathog **4:**e1000072.

93. **Schrauwen EJ, Bestebroer TM, Rimmelzwaan GF, Osterhaus AD, Fouchier RA, Herfst S.** 2013. Reassortment between Avian H5N1 and human influenza viruses is mainly restricted to the matrix and neuraminidase gene segments. PLoS One **8:**e59889.

94. **Kimble JB, Sorrell E, Shao H, Martin PL, Perez DR.** 2011. Compatibility of H9N2 avian influenza surface genes and 2009 pandemic H1N1 internal genes for transmission in the ferret model. Proc Natl Acad Sci U S A **108:**12084-12088.

95. **Dlugolenski D, Jones L, Howerth E, Wentworth D, Tompkins SM, Tripp RA.** 2015. Swine Influenza Virus PA and Neuraminidase Gene Reassortment into Human H1N1 Influenza Virus Is Associated with an Altered Pathogenic Phenotype Linked to Increased MIP-2 Expression. J Virol **89:**5651-5667.

96. **Ma J, Shen H, Liu Q, Bawa B, Qi W, Duff M, Lang Y, Lee J, Yu H, Bai J, Tong G, Hesse RA, Richt JA, Ma W.** 2015. Pathogenicity and transmissibility of novel reassortant H3N2 influenza viruses with 2009 pandemic H1N1 genes in pigs. J Virol **89:**2831-2841.

97. **Enami M, Sharma G, Benham C, Palese P.** 1991. An influenza virus containing nine different RNA segments. Virology **185:**291-298.

98. **Donald HB, Isaacs A.** 1954. Counts of influenza virus particles. J Gen Microbiol **10:**457-464.

99. **McLain L, Armstrong SJ, Dimmock NJ.** 1988. One defective interfering particle per cell prevents influenza virus-mediated cytopathology: an efficient assay system. J Gen Virol **69 (Pt 6):**1415-1419.

100. **Isaacs A, Donald HB.** 1955. Particle counts of haemagglutinating viruses. J Gen Microbiol **12:**241-247.

101. **Bancroft CT, Parslow TG.** 2002. Evidence for segment-nonspecific packaging of the influenza a virus genome. J Virol **76:**7133-7139.

102. **Gerber M, Isel C, Moules V, Marquet R.** 2014. Selective packaging of the influenza A genome and consequences for genetic reassortment. Trends Microbiol **22:**446-455.

103. **McGeoch D, Fellner P, Newton C.** 1976. Influenza virus genome consists of eight distinct RNA species. Proc Natl Acad Sci U S A **73:**3045-3049.

104. **Nakajima K, Sugiura A.** 1977. Three-factor cross of influenza virus. Virology **81:**486-489.

105. **Bergmann M, Muster T.** 1995. The relative amount of an influenza A virus segment present in the viral particle is not affected by a reduction in replication of that segment. J Gen Virol **76 (Pt 12):**3211-3215.

106. **Smith GL, Hay AJ.** 1982. Replication of the influenza virus genome. Virology **118:**96-108.

107. **Chou YY, Vafabakhsh R, Doganay S, Gao Q, Ha T, Palese P.** 2012. One influenza virus particle packages eight unique viral RNAs as shown by FISH analysis. Proc Natl Acad Sci U S A **109:**9101-9106.

108. **Inagaki A, Goto H, Kakugawa S, Ozawa M, Kawaoka Y.** 2012. Competitive incorporation of homologous gene segments of influenza A virus into virions. J Virol **86:**10200-10202.

109. **Duhaut SD, Dimmock NJ.** 2002. Defective segment 1 RNAs that interfere with production of infectious influenza A virus require at least 150 nucleotides of 5' sequence: evidence from a plasmid-driven system. J Gen Virol **83:**403-411.

110. **Duhaut SD, McCauley JW.** 1996. Defective RNAs Inhibit the Assembly of Influenza Virus Genome Segments in a Segment-Specific Manner. Virology **216:**326-337.

111. **Odagiri T, Tashiro M.** 1997. Segment-specific noncoding sequences of the influenza virus genome RNA are involved in the specific competition between defective interfering RNA and its progenitor RNA segment at the virion assembly step. J Virol **71:**2138-2145.

112. **Odagiri T, Tominaga K, Tobita K, Ohta S.** 1994. An amino acid change in the non-structural NS2 protein of an influenza A virus mutant is responsible for the generation of defective interfering (DI) particles by amplifying DI RNAs and suppressing complementary RNA synthesis. J Gen Virol **75 (Pt 1):**43-53.

113. **Fujii Y, Goto H, Watanabe T, Yoshida T, Kawaoka Y.** 2003. Selective incorporation of influenza virus RNA segments into virions. Proc Natl Acad Sci U S A **100:**2002-2007.

114. **Liang Y, Hong Y, Parslow TG.** 2005. cis-Acting packaging signals in the influenza virus PB1, PB2, and PA genomic RNA segments. J Virol **79:**10348-10355.

115. **Watanabe T, Watanabe S, Noda T, Fujii Y, Kawaoka Y.** 2003. Exploitation of nucleic acid packaging signals to generate a novel influenza virus-based vector stably expressing two foreign genes. J Virol **77:**10575-10583.

116. **Ozawa M, Fujii K, Muramoto Y, Yamada S, Yamayoshi S, Takada A, Goto H, Horimoto T, Kawaoka Y.** 2007. Contributions of two nuclear localization signals of influenza A virus nucleoprotein to viral replication. J Virol **81:**30-41.

117. **Ozawa M, Maeda J, Iwatsuki-Horimoto K, Watanabe S, Goto H, Horimoto T, Kawaoka Y.** 2009. Nucleotide sequence requirements at the 5' end of the influenza A virus M RNA segment for efficient virus replication. J Virol **83:**3384-3388.

118. **Fujii K, Fujii Y, Noda T, Muramoto Y, Watanabe T, Takada A, Goto H, Horimoto T, Kawaoka Y.** 2005. Importance of both the coding and the segment-specific noncoding regions of the influenza A virus NS segment for its efficient incorporation into virions. J Virol **79:**3766-3774.

119. **Cobbin JC, Ong C, Verity E, Gilbertson BP, Rockman SP, Brown LE.** 2014. Influenza virus PB1 and neuraminidase gene segments can cosegregate during vaccine reassortment driven by interactions in the PB1 coding region. J Virol **88:**8971-8980.

120. **Gilbertson B, Zheng T, Gerber M, Printz-Schweigert A, Ong C, Marquet R, Isel C, Rockman S, Brown L.** 2016. Influenza NA and PB1 Gene Segments Interact during the Formation of Viral Progeny: Localization of the Binding Region within the PB1 Gene. Viruses **8**.

121. **Gavazzi C, Yver M, Isel C, Smyth RP, Rosa-Calatrava M, Lina B, Moulès V, Marquet R.** 2013. A functional sequence-specific interaction between influenza A virus genomic RNA segments. Proc Natl Acad Sci U S A **110:**16604-16609.

122. **Moreira EA, Weber A, Bolte H, Kolesnikova L, Giese S, Lakdawala S, Beer M, Zimmer G, Garcia-Sastre A, Schwemmle M, Juozapaitis M.** 2016. A conserved

influenza A virus nucleoprotein code controls specific viral genome packaging. Nat Commun **7:**12861.

123. **Noda T, Sagara H, Yen A, Takada A, Kida H, Cheng RH, Kawaoka Y.** 2006. Architecture of ribonucleoprotein complexes in influenza A virus particles. Nature **439:**490-492.

124. **Nakatsu S, Sagara H, Sakai-Tagawa Y, Sugaya N, Noda T, Kawaoka Y.** 2016. Complete and Incomplete Genome Packaging of Influenza A and B Viruses. MBio **7**.

125. **Noda T, Sugita Y, Aoyama K, Hirase A, Kawakami E, Miyazawa A, Sagara H, Kawaoka Y.** 2012. Three-dimensional analysis of ribonucleoprotein complexes in influenza A virus. Nat Commun **3:**639.

126. **Fournier E, Moules V, Essere B, Paillart JC, Sirbat JD, Cavalier A, Rolland JP, Thomas D, Lina B, Isel C, Marquet R.** 2012. Interaction network linking the human H3N2 influenza A virus genomic RNA segments. Vaccine **30:**7359-7367.

127. **White MC, Steel J, Lowen AC.** 2017. Heterologous Packaging Signals on Segment 4, but Not Segment 6 or Segment 8, Limit Influenza A Virus Reassortment. J Virol **91**.

128. **Baker SF, Nogales A, Finch C, Tuffy KM, Domm W, Perez DR, Topham DJ, Martinez-Sobrido L.** 2014. Influenza A and B Virus Intertypic Reassortment through Compatible Viral Packaging Signals. J Virol **88:**10778-10791.

129. **Essere B, Yver M, Gavazzi C, Terrier O, Isel C, Fournier E, Giroux F, Textoris J, Julien T, Socratous C, Rosa-Calatrava M, Lina B, Marquet R, Moules V.** 2013. Critical role of segment-specific packaging signals in genetic reassortment of influenza A viruses. Proc Natl Acad Sci U S A **110:**E3840-E3848.

130. **Gao Q, Palese P.** 2009. Rewiring the RNAs of influenza virus to prevent reassortment. Proc Natl Acad Sci U S A **106:**15891-15896.

131. **Li C, Hatta M, Watanabe S, Neumann G, Kawaoka Y.** 2008. Compatibility among polymerase subunit proteins is a restricting factor in reassortment between equine H7N7 and human H3N2 influenza viruses. J Virol **82:**11880-11888.

132. **Hatta M, Halfmann P, Wells K, Kawaoka Y.** 2002. Human influenza a viral genes responsible for the restriction of its replication in duck intestine. Virology **295:**250-255.

133. **Song MS, Pascua PN, Lee JH, Baek YH, Park KJ, Kwon HI, Park SJ, Kim CJ, Kim H, Webby RJ, Webster RG, Choi YK.** 2011. Virulence and genetic compatibility of polymerase reassortant viruses derived from the pandemic (H1N1) 2009 influenza virus and circulating influenza A viruses. J Virol **85:**6275-6286.

134. **Octaviani CP, Goto H, Kawaoka Y.** 2011. Reassortment between seasonal H1N1 and pandemic (H1N1) 2009 influenza viruses is restricted by limited compatibility among polymerase subunits. J Virol **85:**8449-8452.

135. **Hara K, Nakazono Y, Kashiwagi T, Hamada N, Watanabe H.** 2013. Co-incorporation of the PB2 and PA polymerase subunits from human H3N2 influenza virus is a critical determinant of the replication of reassortant ribonucleoprotein complexes. J Gen Virol **94:**2406-2416.

136. **Wagner R, Matrosovich M, Klenk H.** 2002. Functional balance between haemagglutinin and neuraminidase in influenza virus infections. Rev Med Virol **12:**159-166.

137. **Rudneva IA, Kovaleva VP, Varich NL, Farashyan VR, Gubareva LV, Yamnikova SS, Popova IA, Presnova VP, Kaverin NV.** 1993. Influenza A virus reassortants with

surface glycoprotein genes of the avian parent viruses: effects of HA and NA gene combinations on virus aggregation. Arch Virol **133:**437-450.

138. **Rudneva IA, Sklyanskaya EI, Barulina OS, Yamnikova SS, Kovaleva VP, Tsvetkova IV, Kaverin NV.** 1996. Phenotypic expression of HA-NA combinations in human-avian influenza A virus reassortants. Arch Virol **141:**1091-1099.

139. **Castrucci MR, Kawaoka Y.** 1993. Biologic importance of neuraminidase stalk length in influenza A virus. J Virol **67:**759-764.

140. **Mitnaul LJ, Matrosovich MN, Castrucci MR, Tuzikov AB, Bovin NV, Kobasa D, Kawaoka Y.** 2000. Balanced hemagglutinin and neuraminidase activities are critical for efficient replication of influenza A virus. J Virol **74:**6015-6020.

141. **García-Sastre A, Egorov A, Matassov D, Brandt S, Levy DE, Durbin JE, Palese P, Muster T.** 1998. Influenza A Virus Lacking the NS1 Gene Replicates in Interferon-Deficient Systems. Virology **252:**324-330.

142. **O'Neill RE, Talon J, Palese P.** 1998. The influenza virus NEP (NS2 protein) mediates the nuclear export of viral ribonucleoproteins. EMBO J **17:**288-296.

143. **Robb NC, Smith M, Vreede FT, Fodor E.** 2009. NS2/NEP protein regulates transcription and replication of the influenza virus RNA genome. J Gen Virol **90:**1398-1407.

144. **Marion RM, Zurcher T, de la Luna S, Ortin J.** 1997. Influenza virus NS1 protein interacts with viral transcription-replication complexes in vivo. J Gen Virol **78 (Pt 10):**2447-2451.

145. **Robb NC, Chase G, Bier K, Vreede FT, Shaw PC, Naffakh N, Schwemmle M, Fodor E.** 2011. The influenza A virus NS1 protein interacts with the nucleoprotein of viral ribonucleoprotein complexes. J Virol **85:**5228-5231.

146. **Min JY, Li S, Sen GC, Krug RM.** 2007. A site on the influenza A virus NS1 protein mediates both inhibition of PKR activation and temporal regulation of viral RNA synthesis. Virology **363:**236-243.

147. **de la Luna S, Fortes P, Beloso A, Ortin J.** 1995. Influenza virus NS1 protein enhances the rate of translation initiation of viral mRNAs. J Virol **69:**2427-2433.

148. **Enami K, Sato TA, Nakada S, Enami M.** 1994. Influenza virus NS1 protein stimulates translation of the M1 protein. J Virol **68:**1432-1437.

149. **Falcon AM, Marion RM, Zurcher T, Gomez P, Portela A, Nieto A, Ortin J.** 2004. Defective RNA replication and late gene expression in temperature-sensitive influenza viruses expressing deleted forms of the NS1 protein. J Virol **78:**3880-3888.

150. **Wang Z, Robb NC, Lenz E, Wolff T, Fodor E, Pleschka S.** 2010. NS reassortment of an H7-type highly pathogenic avian influenza virus affects its propagation by altering the regulation of viral RNA production and antiviral host response. J Virol **84:**11323-11335.

151. **Nemeroff ME, Barabino SM, Li Y, Keller W, Krug RM.** 1998. Influenza virus NS1 protein interacts with the cellular 30 kDa subunit of CPSF and inhibits 3'end formation of cellular pre-mRNAs. Mol Cell **1:**991-1000.

152. **Hale BG, Steel J, Medina RA, Manicassamy B, Ye J, Hickman D, Hai R, Schmolke M, Lowen AC, Perez DR, Garcia-Sastre A.** 2010. Inefficient control of host gene expression by the 2009 pandemic H1N1 influenza A virus NS1 protein. J Virol **84:**6909-6922.

153. **Ayllon J, Domingues P, Rajsbaum R, Miorin L, Schmolke M, Hale BG, Garcia-Sastre A.** 2014. A single amino acid substitution in the novel H7N9 influenza A virus NS1 protein increases CPSF30 binding and virulence. J Virol **88:**12146-12151.

154. **Kuo RL, Krug RM.** 2009. Influenza a virus polymerase is an integral component of the CPSF30-NS1A protein complex in infected cells. J Virol **83:**1611-1616.

155. **Twu KY, Kuo RL, Marklund J, Krug RM.** 2007. The H5N1 influenza virus NS genes selected after 1998 enhance virus replication in mammalian cells. J Virol **81:**8112-8121.

156. **Shelton H, Smith M, Hartgroves L, Stilwell P, Roberts K, Johnson B, Barclay W.** 2012. An influenza reassortant with polymerase of pH1N1 and NS gene of H3N2 influenza A virus is attenuated in vivo. J Gen Virol **93:**998-1006.

157. **Ince WL, Gueye-Mbaye A, Bennink JR, Yewdell JW.** 2013. Reassortment complements spontaneous mutation in influenza A virus NP and M1 genes to accelerate adaptation to a new host. J Virol **87:**4330-4338.

158. **Ma EJ, Hill NJ, Zabilansky J, Yuan K, Runstadler JA.** 2016. Reticulate evolution is favored in influenza niche switching. Proc Natl Acad Sci U S A **113:**5335-5339.

159. **Li C, Hatta M, Nidom CA, Muramoto Y, Watanabe S, Neumann G, Kawaoka Y.** 2010. Reassortment between avian H5N1 and human H3N2 influenza viruses creates hybrid viruses with substantial virulence. Proc Natl Acad Sci U S A **107:**4687-4692.

160. **Octaviani CP, Ozawa M, Yamada S, Goto H, Kawaoka Y.** 2010. High level of genetic compatibility between swine-origin H1N1 and highly pathogenic avian H5N1 influenza viruses. J Virol **84:**10918-10922.

161. **Stincarelli M, Arvia R, De Marco MA, Clausi V, Corcioli F, Cotti C, Delogu M, Donatelli I, Azzi A, Giannecchini S.** 2013. Reassortment ability of the 2009 pandemic H1N1 influenza virus with circulating human and avian influenza viruses: public health risk implications. Virus Res **175:**151-154.

162. **Octaviani CP, Li C, Noda T, Kawaoka Y.** 2011. Reassortment between seasonal and swine-origin H1N1 influenza viruses generates viruses with enhanced growth capability in cell culture. Virus Res **156:**147-150.

163. **Fabrizio TP, Sun Y, Yoon SW, Jeevan T, Dlugolenski D, Tripp RA, Tang L, Webby RJ.** 2016. Virologic Differences Do Not Fully Explain the Diversification of Swine Influenza Viruses in the United States. J Virol **90:**10074-10082.

164. **Hao X, Hu J, Wang J, Xu J, Cheng H, Xu Y, Li Q, He D, Liu X, Wang X, Gu M, Hu S, Xu X, Liu H, Chen S, Peng D, Liu X.** 2016. Reassortant H5N1 avian influenza viruses containing PA or NP gene from an H9N2 virus significantly increase the pathogenicity in mice. Vet Microbiol **192:**95-101.

165. **Ma W, Brenner D, Wang Z, Dauber B, Ehrhardt C, Hogner K, Herold S, Ludwig S, Wolff T, Yu K, Richt JA, Planz O, Pleschka S.** 2010. The NS segment of an H5N1 highly pathogenic avian influenza virus (HPAIV) is sufficient to alter replication efficiency, cell tropism, and host range of an H7N1 HPAIV. J Virol **84:**2122-2133.

166. **Cline TD, Karlsson EA, Freiden P, Seufzer BJ, Rehg JE, Webby RJ, Schultz-Cherry S.** 2011. Increased pathogenicity of a reassortant 2009 pandemic H1N1 influenza virus containing an H5N1 hemagglutinin. J Virol **85:**12262-12270.

167. **Zhang Y, Zhang Q, Kong H, Jiang Y, Gao Y, Deng G, Shi J, Tian G, Liu L, Liu J, Guan Y, Bu Z, Chen H.** 2013. H5N1 hybrid viruses bearing 2009/H1N1 virus genes transmit in guinea pigs by respiratory droplet. Science **340:**1459-1463.

Chapter II: Heterologous Packaging Signals on Segment 4, but not Segment 6 or Segment 8, Limit Influenza A Virus Reassortment

Maria C. White[1], John Steel[1], and Anice C. Lowen[1]

[1]Department of Microbiology and Immunology, Emory University School of Medicine, Atlanta, GA, USA

Published in *Journal of Virology*, 2017, 91(11), e00195-17, PMID: 28331085

All figures were generated by MCW with input from ACL

Abstract

Influenza A virus (IAV) RNA packaging signals serve to direct the incorporation of IAV gene segments into virus particles, and this process is thought to be mediated by segment-segment interactions. These packaging signals are segment- and strain-specific, and as such, they have the potential to impact reassortment outcomes between different IAV strains. Our study aimed to quantify the impact of packaging signal mismatch on IAV reassortment using the human seasonal influenza A/Panama/2007/99 (H3N2) and pandemic influenza A/Netherlands/602/2009 (H1N1) viruses. Focusing on the three most divergent segments, we constructed pairs of viruses that encoded identical proteins but differed in the packaging signal regions on a single segment. We then evaluated the frequency with which segments carrying homologous vs. heterologous packaging signals were incorporated into reassortant progeny viruses. We found that, when the HA segments of co-infecting parental viruses were modified, there was a significant preference for the segment containing matched packaging signals relative to the background of the virus. This preference was apparent even when the homologous HA constituted a minority of the HA segment population available in the cell for packaging. Conversely, when NA or NS segments carried modified packaging signals, there was no significant preference for homologous packaging signals. These data suggest that movement of NA and NS segments between the human H3N2 and H1N1 lineages is unlikely to be restricted by packaging signal mismatch, while movement of the HA segment would be more constrained. Our results indicate that the importance of packaging signals in IAV reassortment is segment dependent.

Importance

Influenza A viruses (IAVs) can exchange genes through reassortment. This process contributes to both the highly diverse population of IAVs found in nature and the formation of novel epidemic and pandemic IAV strains. Our study sought to determine the extent to which IAV packaging signal divergence impacts reassortment between seasonal IAVs. Our knowledge in this area is lacking, and insight into the factors that influence IAV reassortment will inform and strengthen ongoing public health efforts to anticipate the emergence of new viruses. We found that the packaging signals on the HA segment, but not the NA or NS segments, restricted IAV reassortment. Thus, the packaging signals of the HA segment could be an important factor in determining the likelihood that two IAV strains of public health interest will undergo reassortment.

Introduction

Influenza A virus (IAV) is a member of the *Orthomyxoviridae* family and contains a negative-sense, single-stranded RNA genome with eight distinct gene segments (1). During co-infection of a cell with two or more IAVs, the multipartite nature of its genome allows the virus to undergo reassortment (gene segment exchange), resulting in the production of progeny viruses that are genetically distinct from both of the parental viruses (2). Reassortment events gave rise to the last three IAV pandemic strains (3-5), resulting in high mortality as well as increased economic burdens (6-8). In addition, reassortment within an individual IAV subtype, termed intrasubtype reassortment, contributes to the epidemiology and evolution of seasonal IAVs (9-11).

Although the potential for reassortment in nature is high (2, 12-18), when co-infecting viruses are dissimilar, reassortment is constrained by incompatibilities between heterologous viral components, a phenomenon termed segment mismatch (19, 20). RNA mismatch can limit the

number of genotypically distinct viruses that emerge following a co-infection event, while protein mismatch manifests following spread of reassortant progeny viruses to new cells. Several studies focusing on the outcomes of reassortment between phylogenetically distinct IAVs report biases in the genotypes detected and fitness defects associated with a wide range of reassortant genotypes. This body of work includes examination of reassortment between human H3N2 or H1N1 viruses and avian influenza viruses of the H2N2, H5N1, H7N7, and H9N2 subtypes (21-30); between human IAVs and equine or swine IAVs (31-34); and between human H1N1 and human H3N2 viruses (35, 36). In all cases, reduced fitness of certain reassortant genotypes relative to parental viruses is noted. Common sources of mismatch at the protein level include imbalance in HA attachment and NA release functions, and incompatibility among polymerase components (34, 37, 38). Conversely, when co-infecting parental viruses are highly homologous, reassortment occurs readily (39).

RNA packaging signals are segment- and strain-specific regions of IAV viral RNAs (vRNAs) that are comprised of both the untranslated region (UTR) and varying amounts of coding region at both the 3' and 5' ends of each segment, and their purpose is to direct the incorporation of IAV segments into newly-forming virus particles (40-45). It has been proposed that the packaging signal regions encompass two distinct signals: a genome incorporation signal, which allows for packaging of that individual segment, and a genome bundling signal, which allows for the incorporation of all eight IAV segments en masse (46). Bundling signals are thought to mediate specific interactions among vRNA segments that ensure subsequent incorporation of eight distinct segments into virions (47-52). Since the packaging signals on any given segment are not fully conserved across different IAV strains, the hypothesis arises that RNA packaging signal divergence may impact IAV reassortment outcomes. During a reassortment event, segments that contain compatible RNA

packaging signals might be favored in order to maintain optimal segment-segment interactions, thus resulting in a loss of reassortment efficiency.

Two elegant studies have provided proof of principle that incompatibility between RNA packaging signals is sufficient to prevent the formation of particular reassortant genotypes (53, 54). Additionally, it has been shown that rewiring the packaging signals between two segments of a single IAV strain prevents its reassortment with a wild-type IAV (55). However, there is a lack of data on i) the quantitative effects of packaging signal mismatch and ii) which segments are subject to this type of mismatch. Therefore, our study aimed to determine the extent to which packaging signal mismatch interferes with reassortment between a seasonal H3N2 and a 2009 pandemic H1N1 strain, with a focus on the three segments with the least-conserved packaging signal regions: HA, NA, and NS. To accomplish this aim, we adapted our previously described system for measuring reassortment (39). This system relies on the use of two A/Panama/2007/99 [P99]-based parental viruses that differ only by silent nucleotide changes in each segment. These changes between wild-type (WT) and silently-mutated segments (VAR, for variant) allow their differentiation using high-resolution melt (HRM) analysis. Virus isolates can thus be fully genotyped using HRM, eliminating the need for partial or full sequencing of each isolate in order to detect and characterize reassortant progeny. To measure the impact of packaging signals on reassortment, we modified the terminal regions of a single segment in each parental virus so that the WT virus had heterologous packaging signals derived from pandemic influenza A/Netherlands/602/2009 (H1N1) [NL] and the VAR virus had homologous, P99, packaging signals. Both viruses encoded wild-type P99 proteins, so that observed phenotypes could be attributed to the effects of packaging signals alone. Using this well-controlled system, we show

that sequence divergence in the packaging signals of the HA segment, but not the NA or NS segments, significantly influences reassortment.

Materials and Methods

Cells and viruses. Madin-Darby canine kidney (MDCK) cells were maintained in minimum essential medium (Gibco) supplemented with penicillin-streptomycin and 10% fetal bovine serum (FBS). Human embryonic kidney cells (293T) were maintained in Dulbecco's Modified Eagle Medium (Gibco) supplemented with 10% FBS. Reverse genetics-derived influenza A/Panama/2007/99 (H3N2) virus (referred to as P99) was used for this study, and packaging signal regions were taken from P99 as well as from influenza A/Netherlands/602/2009 (H1N1) virus (referred to as NL). Virus stocks were generated in 9-11 day old embryonated hens' eggs (Hy-Line). Viruses with modified HA packaging signals were passaged through eggs once, viruses with modified NA packaging signals were passaged through eggs twice, and virus stocks with modified NS packaging signals were generated by infecting eggs with a plaque isolate derived in MDCK cells from the egg passage 1 stock.

Design of chimeric segments. The three segments examined in this study (HA, NA, and NS) had the lowest percent nucleotide identity in the packaging signal regions of the viruses used (**Table 1**) and were selected for this reason. Chimeric segments were designed as follows, and then synthesized through Genewiz. For HA, NA, and NS, the full P99 open reading frame (ORF) was flanked by 3' and 5' packaging signal regions taken from either P99 or NL. For HA, packaging signals regions constituted 136 nt at each of the 3' and 5' ends; for NA, packaging signal regions constituted 150 nt at the 3' end and 200 nt at the 5' end; and for NS, packaging signal regions constituted 200 nt at each of the 3' and 5' ends. To disrupt the native packaging signals in each

segment, the first and last 60 nt of the ORF were modified via silent mutation of every codon (excluding start, stop, Met and Trp codons). To ensure translation initiation at the appropriate start codon, all ATGs in the added 3' packaging signal region were removed via silent mutation. The constructs were then flanked with BsmBI restriction sites to allow for ligation into the pDP2002 ambisense vector (a generous gift of Daniel Perez, University of Georgia). Construct design was informed by the work of Gao et al. (56) and packaging signal lengths were based on literature compiled by Hutchinson et al. (57).

Generation of modified viruses. The constructs described above were each ligated into the pDP2002 reverse genetics vector (58). A variant (VAR) version of each construct with P99 packaging signals was then generated by introducing up to six silent mutations into the ORF via site-directed mutagenesis (see **Figure 1C**). The mutations introduced correspond to those used in the Pan/99var15 virus described previously (59). These silent mutations allow differentiation of VAR from WT gene segments using HRM analysis and were previously shown to have no detectable effect on viral fitness (39, 59). Plasmids encoding chimeric segments were then used with a pPOL1 P99 reverse genetics system to rescue viruses in a P99 background, following standard procedures (60, 61). Briefly, a 15 plasmid rescue system based on pPOL1 and pCAGGS helper plasmids (PB2, PB1, PA, HA, NP, NA, and NS) was used. At 16-24 hr post-transfection, 293T cells were injected into 9-11 day old embryonated hens' eggs and incubated for 48 hr to generate virus stocks. Stock titers were then determined via plaque assay on MDCK cells. Chimeric WT segments were rescued in a full P99 WT background, and chimeric VAR segments were rescued in a full P99 VAR background. The VAR mutations for all eight segments have been described previously (39, 59) (Pan/99var15 was used in the present study). All rescued viruses contained only one segment with modified packaging signal regions, as follows. One WT virus

and one VAR virus containing P99 packaging signals was generated for each of the three modified segments of interest (HA, NA, or NS), and one WT virus containing NL packaging signals was generated for each of the three modified segments of interest (HA, NA, or NS). Therefore, a total of nine viruses were rescued as illustrated in **Figure 2**.

Sequencing of virus stocks and genotype verification. The full genomes of all nine virus stocks used in this study were sequenced via Illumina next-generation sequencing through the Emory Integrated Genomics Core (EIGC). Sequences of the grafted packaging signals as well as the serially-mutated P99 ORF regions of each modified segment were confirmed via Sanger sequencing (Genewiz), as analysis of the deep sequencing data revealed an inability to map reads within the pseudo-duplicated regions.

Viral growth kinetics. The multi-cycle growth properties of each virus were assessed as follows. Triplicate wells of MDCK cells were infected at a multiplicity of infection (MOI) of 0.01 PFU/cell alongside the P99 wild-type virus as a control. After 1 hr at 33° C, virus inoculum was removed and media containing tosyl phenylalanyl chloromethyl ketone (TPCK)-treated trypsin was added. A sample of medium was collected from each well at 1 hr, 12 hr, 24 hr, 48 hr, and 72 hr post-infection (p.i.), stored at -80° C, and subsequently titered via plaque assay on MDCK cells. Mean titers of the three replicates ± 1 standard deviation (S.D.) were plotted against time. The limit of detection was 50 PFU/mL.

Co-infection of MDCK cells with modified viruses. Triplicate wells of MDCK cells were co-infected at an MOI of 5 PFU/cell for each virus (unless otherwise specified) for a final MOI of 10 PFU/cell to ensure high levels of co-infection. Previously published work from our lab using the same A/Panama/2007/99 WT/VAR system reported a high frequency of co-infected cells (~85% of infected cells) at this MOI (62). The control co-infections used WT and VAR viruses with

matched packaging signals on the segment of interest (P99 for both), and the heterologous co-infections used WT and VAR viruses with mismatched packaging signals on the segment of interest (NL and P99, respectively) as shown in **Figure 2**. Inoculations were performed on ice and, after a 45 min incubation period at 4° C to allow for virus attachment, the virus inoculum was removed and the cells were washed 3x with cold PBS to remove unattached virus. Warm media was then added to allow for synchronized virus entry and the cells were incubated at 33° C for 3 hr. After 3 hr, the media was removed from the cells and replaced with media supplemented with 1M ammonium chloride and HEPES buffer. The absence of TPCK-treated trypsin and the presence of ammonium chloride ensures a single cycle of viral replication. Cells were incubated for an additional 9 hr and then, at 12 hr p.i., supernatants were collected and frozen at -80° C for use in reassortment analyses, and cells were harvested in RNAprotect cell reagent (QIAGEN) for subsequent analysis of RNA by reverse transcription droplet digital PCR (RT ddPCR).

Genotyping viral isolates from co-infected cells. Viruses present in the co-infection supernatants were sampled randomly via plaque-purification on MDCK cells. Well-separated plaque isolates were placed in 150 µL PBS, one isolate per PBS aliquot. Twenty-one virus isolates were picked for each supernatant sample. In total for each set of like co-infections performed, a minimum of 126 plaque isolates were picked. RNA was extracted from the plaque isolates using the Zymo Research ZR-96 Viral RNA kit following the manufacturer's instructions with the following modification: 40 µL water was used for the elution step. Twelve point eight microliters of RNA was reverse-transcribed using Maxima reverse transcriptase (RT) (Fermentas) following the manufacturer's instructions. The resultant cDNA was then diluted in water and used in quantitative PCR (qPCR) with Precision Melt Supermix (Bio-Rad) and primers specific for each of the eight segments of P99 virus (**Table 2**). These primers bind to sequences that do not differ between WT

and VAR viruses, but the ~100 bp amplicons produced contain the region altered in VAR gene segments. qPCR was set up in white, thin-walled, 384-well plates (Bio-Rad) and was run in a CFX384 Real-Time PCR detection system (Bio-Rad). PCR amplification was followed immediately with a melt curve analysis. The conditions of PCR amplification and melt analysis followed the protocol provided with the Precision Melt Supermix. Data were analyzed using Precision Melt Analysis software (Bio-Rad) and comparison to WT and VAR cDNA controls. Thus, the genotype of each segment in each virus isolate was determined to be either WT or VAR depending on which control the melt curves clustered with in the software. Genotype data were analyzed by determining the proportion of genomes that carried the WT version of each of the eight segments. Only reassortant virus isolates were included in these analyses; parental genotypes were excluded due to the possibility that parental-type progeny were produced by singly, rather than co-infected, cells. The data were analyzed using two-way ANOVA with Tukey's multiple comparisons and means ± 1 S.D. were graphed. All co-infections were performed in triplicate two independent times.

Determining heterologous segment availability at 12 hr p.i. The co-infected cells that had been harvested at 12 hr p.i. in RNAprotect cell reagent were either used immediately post-harvest or stored <24 hr at 4° C prior to use. RNA was extracted from the cells using the RNeasy Plus Mini Kit (QIAGEN) following the manufacturer's instructions with the following modifications: homogenization was achieved via vortexing for 2-3 min; 40 µL water was used for the elution step and allowed to incubate on the membranes of the columns for 1-2 min at room temperature; RNA was eluted by spinning the tubes at 11,000 rpm for 2 min in a Beckman Coulter Microfuge 22R centrifuge. Two micrograms of RNA was then reverse-transcribed using Maxima RT (Fermentas). A no-RT control was run in parallel. cDNA was diluted in water and used in droplet digital PCR

(ddPCR). An overview of the ddPCR protocol is outlined in (63). Briefly, cDNAs were diluted to achieve working concentrations within the linear range, and 8.8 μL of diluted cDNA per sample was combined with 13.2 μL master mix (11 μL QX200 ddPCR EvaGreen Supermix (Bio-Rad) + 2.2 μL 4 μM primer set). The primers used were specific for the 3' packaging signal region so that the P99 and NL versions of the modified segment present in co-infected cells could be differentiated. All primers used showed no cross-priming (data not shown). A list of the primers used for ddPCR can be found in **Table 3**. Twenty microliters of each PCR reaction was transferred to a DG8 cartridge (Bio-Rad) alongside 70 μL Droplet Generation Oil for EvaGreen (Bio-Rad) and droplets were generated using a QX200 Droplet Generator (Bio-Rad). Forty microliters of the generated droplets were transferred to a Twin-Tec 96-well PCR plate (Eppendorf) and, after heat-sealing the plate with foil, 40 cycles of PCR were run in a C1000 Touch Thermal Cycler (Bio-Rad) with the following parameters: 95° C for 5 min, [95° C for 30 sec followed by 53.7° C for 1 min] x40, 4° C for 5 min, 90° C for 5 min, and a final hold at 4° C. The ramp rate for all steps was set at 2° C/sec as recommended by the manufacturer. The plate was then read in a QX200 Droplet Reader (Bio-Rad). No-RT control samples were included in the ddPCR analysis as negative controls. ddPCR was run with two technical replicates per sample. The copy number of each segment of interest (segments with modified packaging signal regions) in each sample was determined using QuantaSoft software (Bio-Rad). The total copy number of each segment present in each well of co-infected cells was then calculated and data were graphed as means ± 1 S.D. For HA and NS, ddPCR was performed in parallel with the reassortment analyses (i.e. the same co-infections were used); for NA, ddPCR was performed using co-infections that had been set up under the same conditions and using the same virus stocks as those used to generate the reassortment data.

Replication efficiencies of heterologous segments. In order to calculate the replication efficiencies of the chimeric packaging signal segments, co-infected cells were harvested at 12 hr p.i. and processed for RT ddPCR as described above. In addition, viral RNA was extracted from the inoculum used for the co-infections immediately following infection using the QIAamp Viral RNA kit (QIAGEN) according to the manufacturer's instructions with the following modifications: carrier RNA was not added to the Buffer AVL; 40 µL water was used for the elution, and tubes were spun for 2 min instead of 1 min in a Beckman Coulter Microfuge 22R centrifuge to elute the RNA. Twelve microliters of RNA was reverse-transcribed using Maxima RT (Fermentas). A no-RT control was included in parallel. cDNA was diluted in water and used in ddPCR as described above with the primers listed in **Table 3**. The copy number of each segment of interest in both the inoculum (input) and the cellular extracts (output) were determined using QuantaSoft software (Bio-Rad), taking into account the dilutions performed to ensure that each cDNA was within the linear range of the assay. The ratio of output to input values for each replicate was then determined, and the means ± 1 S.D. across 2-4 biological replicates performed in triplicate were graphed. Data were analyzed using Student's *t*-test.

Statistical analyses. All statistical analyses were performed in GraphPad Prism v7.02.

Results

Generation of chimeric IAV segments with identical protein coding regions but differing packaging signal regions. Broad regions of each of the eight vRNAs that support efficient incorporation into virions have been mapped and include the UTRs as well as varying amounts of 3' and 5' coding region, depending on the segment (40-45). To evaluate the impact of heterologous packaging signals on IAV reassortment, we generated WT/VAR virus pairs in the P99 background

in which the WT virus carried NL packaging signals on a single segment. By retaining all P99 ORFs, we aimed to ensure that any bias in reassortment was due to packaging signals rather than incompatibilities occurring at the protein level. In addition, to control for any effects of the engineering that we performed, we produced control segments that carried P99 packaging signals flanking the corresponding P99 ORF. Our chimeric segment design was informed by Gao et al. (56) and included the following three features (see **Figure 1**). i) The first 60 nt of the 3' end and the last 60 nt of the 5' end of the P99 ORF were modified via silent mutation of every codon (excluding start, stop, Met and Trp codons). This step was demonstrated by Gao et al. to be necessary to disrupt native packaging signal function. ii) The ORFs were flanked with packaging signal regions from either P99 or NL. The terminal sequences added on to the HA, NA and NS segments were at least 100 nt in length at either end and were selected based on conservative estimates of the packaging signal locations as mapped by others (see (57) for review). iii) The ATG codons upstream of the true start codon were disrupted via silent mutation, so that translation would result in production of wild-type P99 protein. Each of these chimeric segments was incorporated into a P99 strain background via reverse genetics to produce a total of nine viruses (**Figure 2**). For each of the segments examined, three viruses were made: i) a WT virus with P99 packaging signals on the segment of interest (e.g. P99wt HA_P99PS), ii) a WT virus with NL packaging signals on the segment of interest (e.g. P99wt HA_NLPS), and iii) a VAR virus with P99 packaging signals on the segment of interest (e.g. P99var15 HA_P99PS) (**Figure 2**). Labeling as WT or VAR refers to the absence or presence, respectively, of silent genetic tags in each segment (39).

Viruses with altered packaging signal regions exhibited similar growth kinetics. To assess whether introduced mutations and added packaging signals affected virus growth, we performed

multi-cycle growth analyses. As fitness differences within each set of three viruses could skew reassortment outcomes, we wanted to ensure that each set of viruses exhibited comparable growth. The P99 wild-type virus (recombinant A/Panama/2007/99, or P99wt) was included as a control in parallel with each set of three chimeric packaging signal viruses rescued per segment. Triplicate wells of MDCK cells were infected with each virus and output titers over time were determined by plaque assay. Compared to the P99wt control, we saw no attenuation of growth due to modification of the HA segment and, at the later time points, two of the modified HA_PS viruses produced higher titers than the control (**Figure 3A**). In contrast, compared to the P99wt control, we saw ~10-fold attenuation in growth for all of the NA_PS viruses (**Figure 3B**) and NS_PS viruses (**Figure 3C**). However, since all three of the modified viruses for each segment exhibited comparable growth phenotypes, we concluded that fitness differences would not bias our co-infection experiments.

Heterologous segments showed varying efficiencies of replication. We next addressed how efficiently the heterologous segments within each set of viruses were replicated. The growth curves in **Figure 3** suggested that the viruses had approximately equal growth properties; however, these experiments i) involved single infections done under multi-cycle growth conditions, whereas experiments to assess reassortment would use co-infection under single cycle conditions, and ii) growth curves are not a sensitive way to assess replication of a single segment. We therefore applied RT ddPCR to quantify the vRNA copy number of each chimeric segment in the context of co-infection with WT NLPS and VAR P99PS viruses. RNA was extracted from the inoculum (0 hr p.i.) and from the co-infected cells (12 hr p.i.), yielding samples representative of the input vRNA and the output vRNA, respectively. RT ddPCR with primers specific for each chimeric segment (**Table 3**) was then used to quantify segment copy numbers in each sample. To evaluate

replication efficiency, the fold-increase was calculated as the copy number of output vRNA / input vRNA. For the heterologous HA segments, HA_P99PS was replicated ~2.1x more efficiently than HA_NLPS (**Figure 4A**). The heterologous NA segments were replicated with comparable efficiency: NA_NLPS had a ~1.2x advantage over NA_P99PS (**Figure 4B**). For the heterologous NS segments, NS_P99PS was replicated ~2.1x more efficiently than NS_NLPS (**Figure 4C**). Although the differences in replication for the HA_PS and NS_PS segments are moderate, they could potentially impact reassortment outcomes. For example, if less of the NLPS-containing segment was present in co-infected cells, then the P99PS segment might predominate in reassortant progeny viruses due to its greater availability rather than a preference for homologous packaging signals during genome assembly. As indicated below, we corrected for unequal replication of P99PS and NLPS segments where necessary by altering the input ratio of the co-infecting viruses such that equal or greater amounts of the NLPS segment were present in cells at 12 hr p.i. In this way, if the P99PS segment was favored for incorporation, then the phenotype could be confidently attributed to a packaging defect of the NLPS segment and not to a difference in availability.

HA segments containing matched packaging signals relative to the background of the virus were significantly favored for incorporation into new virus particles. To assess whether the packaging signals on the HA segment affected IAV reassortment outcomes, we performed co-infections in MDCK cells with i) P99wt HA_P99PS and P99var15 HA_P99PS viruses as a control, or ii) P99var15 HA_P99PS and P99wt HA_NLPS viruses (see **Figure 2**). For the control co-infection, 5 PFU/cell of each virus was used. Due to the differences in replication of HA_P99PS and HA_NLPS segments outlined above, the inoculum for the heterologous co-infection was formulated to contain 5 PFU/cell of the P99var15 HA_P99PS virus and >5 PFU/cell of the P99wt HA_NLPS virus. Both co-infections were performed in triplicate on two separate occasions and

limited to a single round of replication by adding ammonium chloride to the medium. At 12 hr p.i. the cell culture supernatants and the infected cell monolayers were harvested. The cells were used to quantify the total number of each modified HA segment available within co-infected cells at 12 hr p.i. Plaque isolates derived from the collected supernatants were genotyped to evaluate reassortment outcomes. Genotype data averaged across all six replicate co-infections are presented in **Figure 5A**. For each segment, the percentage of virus isolates containing a WT segment was plotted. Reassortment efficiency for these experiments was high: for the heterologous co-infections, 94-100% of isolates had reassortant genotypes.

Since the viruses used in the control co-infection contained P99 packaging signals on all eight segments, we expected an approximate 50:50 distribution of WT:VAR for each segment. We did indeed see this distribution in our data set (black bars, **Figure 5A**). Similarly, all segments in the viruses used in the heterologous co-infection with the exception of the HA segment had P99 packaging signals. We therefore also expected to see approximately equal incorporation of WT and VAR versions of these seven segments in reassortant progeny, and again this expected result was observed (gray bars, **Figure 5A**). In the heterologous co-infection, the WT HA segment had NL packaging signals and the VAR HA segment had P99 packaging signals. Our data show that 15% of isolates genotyped contained a WT HA_NLPS segment (**Figure 5A**). Conversely, in the control co-infection, 60% of isolates genotyped contained a WT HA_P99PS segment. **Figure 5B** shows that there was on average 3.9x more HA_NLPS than HA_P99PS available in the cells at 12 hr p.i. (gray bars, **Figure 5A**). Taken together, these data show a clear preference for incorporation of HA segments containing packaging signals that match those of the other seven segments, and this phenotype is due to inefficient incorporation of the HA_NLPS segment and not due to lower availability of the HA_NLPS segment in the cell.

The NA segment with heterologous packaging signals is not disfavored during reassortment. Based on low sequence identity in the packaging signal regions (**Table 1**), we hypothesized that introduction of NLPS sequences onto the P99 NA segment would disfavor its incorporation, as was seen for HA. However, contrary to our hypothesis, we did not see a significant difference in the incorporation of NA_P99PS vs. NA_NLPS (**Figure 6**). Co-infections of MDCK cells, genotyping of virus isolates, and enumeration of the NA_PS segments present in the cells at 12 hr p.i. were carried out as described for the HA segment above. For the NA_PS viruses, a 1:1 input ratio of VAR:WT viruses in the control co-infection yielded an approximate 50:50 distribution of WT:VAR for each segment as expected (black bars in **Figure 6**). However, a 1:1 input ratio of VAR:WT viruses in the heterologous co-infection showed an overrepresentation of VAR across all eight segments (gray bars, **Figure 6A**), even though there were equal amounts of NA_P99PS and NA_NLPS segments available in the cells at 12 hr p.i. (**Figure 6B**). As explained above, we expected to see an approximate 50:50 distribution of WT:VAR in all unmodified segments for the heterologous co-infection, since all unmodified segments have P99 packaging signals. Therefore, we repeated the heterologous co-infection experiments using a 1:1.5 input ratio of VAR:WT viruses. After this correction, we saw an approximate 50:50 WT:VAR distribution across the unmodified segments as expected (gray bars, **Figure 6C**). Focusing on the NA segment, we observed a slight preference for incorporation of the segment containing matched packaging signals, but this bias was not significant (**Figure 6C**). We observed 1.5x more NA_NLPS than NA_P99PS available in the cells at 12 hr p.i. (**Figure 6D**), reflecting the adjusted WT input. Taken together, these data suggest that packaging signal divergence on the NA segment does not significantly affect reassortment outcomes between the IAV strains tested.

Packaging signals on the NS segment do not impact IAV reassortment outcomes. Compared to the HA and NA segments, the NS segment has a higher percent nucleotide identity in the packaging signal regions of P99 and NL viruses (**Table 1**). However, it is important to note that the precise nucleotides within these regions that are important for IAV segment incorporation have not been identified; thus, the 17% difference in nucleotide sequence could impact NS segment packaging in the context of a heterologous co-infection. The MDCK cell co-infections, genotyping of virus isolates, and quantification of the NS_PS segments present in co-infected cells at 12 hr p.i. were performed as described above for the HA segment. Somewhat similar to the NA segment co-infections, we found that a 1:1 input ratio of VAR:WT viruses resulted in an overrepresentation of VAR across all eight segments in the control co-infection as well as across all unmodified segments in the heterologous co-infection (**Figure 7A**). However, even under these conditions, it was clear that the NS_NLPS segment was packaged efficiently, as the % WT for the NS segment was one of the higher values calculated (**Figure 7A**). Interestingly, this phenotype was observed even though there was less of the NS_NLPS segment available in the cells at 12 hr p.i. when compared to the NS_P99PS segment (**Figure 7B**).

To verify these data, we repeated the co-infection experiments, this time increasing the amount of WT virus used in both the control (25% increase) and heterologous (50% increase) co-infections but keeping the amount of VAR virus constant. Under these conditions, we observed an approximate 50:50 WT:VAR distribution for all segments in the control co-infection and for all unmodified segments in the heterologous co-infection as expected (**Figure 7C**). This second set of co-infections confirmed our original findings: the heterologous NS_NLPS segment was not underrepresented when compared to the unmodified segments of the same co-infection (gray bars, **Figure 7C**) or to the NS_P99PS counterpart in the control co-infection. In this repeat experiment,

approximately equal amounts of the heterologous NS segments were available in the cells at 12 hr p.i. (**Figure 7D**). Taken together, our data show that packaging signal divergence on the NS segment does not impact IAV reassortment, at least for the strains tested.

Discussion

This study aimed to quantify the impact of packaging signal divergence on IAV reassortment. Toward generating results relevant for currently circulating IAVs, we used human IAV strains of the seasonal H3N2 and pandemic H1N1 lineages. We focused on the HA, NA, and NS segments due to the degree of divergence in the packaging signal regions, between the two strains selected for our experiments and also more generally among IAVs (64). Our knowledge to date on how incompatibilities among vRNAs affect IAV reassortment is limited, in part due to the challenge of finding a system that allows for examination of RNA mismatch in the absence of other confounding factors. To overcome this problem, we applied our previously described WT/VAR system to isolate the effects of mismatch among RNA packaging signals from those of protein mismatch (39).

Our results show that HA segments containing homologous packaging signals were preferentially packaged into P99-based viruses. Under single cycle conditions, 85% of progeny viruses were found to have incorporated the homologous HA_P99PS segment, while 15% of progeny viruses incorporated the heterologous HA_NLPS segment. This preference was observed even when HA segments with heterologous packaging signals constituted a majority of the HA segment pool in the co-infected cells, indicating that the favored incorporation was directed by packaging signals and not by abundance in the cell. Our data are consistent with the observations of Essere et al. (53), and confirm that heterologous packaging signals can limit reassortment. These findings are of

particular interest given the relevance of HA segment reassortment for the formation of antigenically novel IAVs.

In contrast to the HA segment, introduction of NL packaging signals onto the NA or NS segment of P99 virus did not result in a detectable bias in reassortment patterns. These results were unexpected based on our own findings for HA and those of Essere et al., and the low sequence identity between P99 and NL viruses in NS and particularly NA packaging signal regions. Several possible explanations exist. The first is that, despite differences in nucleotide sequence over the broad terminal regions examined, the RNA signals on NA and NS that mediate segment bundling may not differ substantially between NL and P99 viruses. For NS, which has ~83% nucleotide identity between P99 and NL viruses in the packaging signal regions, it is reasonable to propose that the particular nucleotides involved in packaging are conserved (65). For NA, which has ~57% identity in packaging regions, this explanation is less satisfactory. Potentially, however, secondary structures formed by the RNA are critical for packaging, and nucleotide differences between P99 and NL may not disrupt these structures in the NA and NS segments. It has been proposed that interactions between segments during packaging occur through complementary sequences found on local RNA structures, or RNA loops, which are exposed from the viral ribonucleoprotein complexes (vRNPs) (66-69). If the molecular cues for genome assembly found on certain segments are conserved among divergent IAVs, it follows that these signals would be unlikely to restrict heterologous reassortment.

A second possible explanation for the absence of a packaging phenotype for NA and NS is the existence of packaging signals that are outside of the currently mapped terminal regions. A recent study demonstrated that the influenza A/Udorn/307/72 virus PB1 and NA segments were preferentially co-packaged during reassortment with A/Puerto Rico/8/34 virus. The interaction

between these two segments was mapped to an internal region of PB1 comprising nucleotides 1776-2070 (70, 71). Additionally, NS and PB1 from influenza A/Finch/England/2051/91 have been shown to interact via complementary sequences that are located within internal regions of both segments (51). As our study examined only terminal packaging signal regions, we cannot discount the possibility that the P99 NA and/or NS assemble with other segments via sequences within the inner coding region. Similarly, is it formally possible that serial mutation within the terminal ~60 nt of the P99 ORF did not disrupt the nucleotides important for NA and NS packaging, such that P99 sequences directed incorporation of segments, rather than NL-derived terminal sequences. However, Gao et al. demonstrated that a similar strategy was sufficient to disrupt packaging in a PR8 background (56). It is also important to note that multiple reports have documented a key role for the terminal regions in packaging of NA and NS gene segments (41, 45, 49).

A third reason why heterologous packaging signals on NA or NS segments were not found to bias reassortment could be that these two segments are relatively unimportant in the selective process that results in segment bundling. The existence of a hierarchy in which the packaging signals of certain segments have a dominant role in genome assembly has been noted (56, 72). Gao et al. were furthermore able to rescue a seven-segmented IAV that expressed an influenza C virus glycoprotein flanked with HA-specific packaging signals in the place of the HA and NA segments. This virus was stable over multiple passages in eggs despite the lack of NA packaging signals, suggesting that the NA sequences are not critical for incorporation of the other seven segments (73). A subsequent study demonstrated that deleting the packaging signals of the NS segment had no effect on recombinant virus growth, implying that NS packaging signals might also be of lesser importance during genome packaging (56).

It is now well-accepted that packaging of the IAV genome is a selective process (19, 50, 74-77). Since an IAV particle typically does not carry more than eight segments and must carry one copy of each segment to be infectious, high fidelity packaging is needed to ensure viability (52, 78). However, there is a trade-off between infectivity and evolutionary capacity: a very stringent selective packaging mechanism would limit reassortment among IAVs that differ in their packaging signals. In other words, a more flexible packaging mechanism may offer an evolutionary advantage by allowing greater genetic diversification through reassortment (52). Our findings show that movement of the antigenically important HA segment between two human IAV subtypes was disfavored at the level of packaging, while the movement of NS and NA (which also has antigenic properties) was relatively free. These results suggest that packaging is relatively flexible, but that this property varies with segment (and likely also virus strain). Although our data revealed a preference for the HA segment containing homologous packaging signals, the HA segment with heterologous packaging signals was present in 15% of P99-based progeny viruses. In other words, packaging signal mismatch reduced but did not completely block HA reassortment. Low levels of reassortment are expected to be epidemiologically significant if certain reassortant genotypes have a selective advantage, such as immunological novelty (79).

It will be of interest to determine whether the reassortment patterns observed herein extend to other strain pairings. Detailed knowledge of the segment interactions that occur during packaging is currently limited and, importantly, the extent to which the process of IAV genome assembly is conserved among strains remains unclear. As discussed above, sequences or structures involved in packaging may differ between divergent IAVs. In the HA and NA segments in particular, the degree of sequence conservation within mapped packaging signal regions among subtypes is low. In addition, the order in which segments are bundled and the pairwise interactions that make up

the full network of eight vRNPs may not be conserved. Without this detailed knowledge, it is difficult to predict how packaging might shape reassortment between a given pairing of parental viruses. A key question is whether the preference for matched packaging signals on HA holds true across subtypes. The compatibility of zoonotic H5 and H7 subtype strains with seasonal human IAVs is of particular relevance since a reassortment event could lead to the formation of a pandemic strain. Our system is well-suited to give quantitative answers to these important questions.

In summary, the data presented here suggest that movement of the NA and NS segments from viruses of the 2009 pandemic H1N1 lineage into a seasonal H3N2 background would not be significantly restricted by packaging signal mismatch, while movement of the H1 HA segment would be constrained at the level of genome assembly. Thus, our data reveal that the impact of packaging signals on reassortment is segment dependent.

Acknowledgments

We thank Daniel Perez for the kind gift of the pDP2002 plasmid. We thank Christopher Scharer, Bhanu Gandham, and Ramya Govindarajan for their assistance and expertise with the analysis of the whole genome sequencing data.

This study was supported in part by the Emory Integrated Genomics Core (EIGC), which is subsidized by the Emory University School of Medicine and is one of the Emory Integrated Core Facilities. Additional support was provided by the National Center for Advancing Translational Sciences of the National Institutes of Health under Award Number UL1TR000454. The content is solely the responsibility of the authors and does not necessarily reflect the official views of the National Institutes of Health.

The authors declare no conflicts of interest.

Funding Information

This work was funded in part by the NIAID Centers of Excellence in Influenza Research and Surveillance (CEIRS), contract number HHSN272201400004C to A.C.L. and J.S. and by R01 grants AI125268 and AI099000 to A.C.L.

Figures

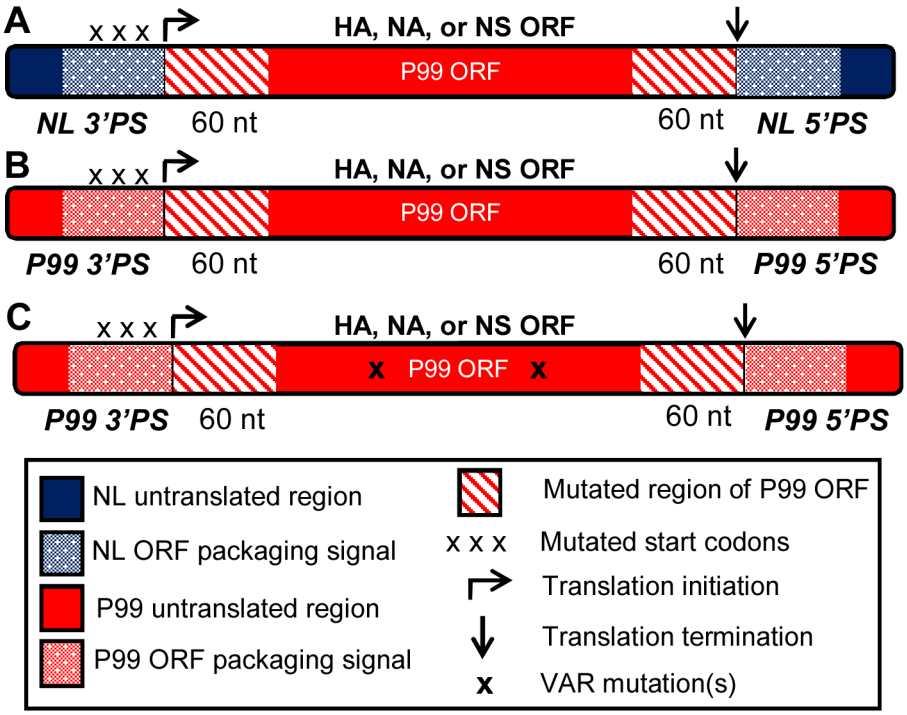

Figure 1. Chimeric IAV segments have the same protein coding regions but different packaging signal regions. HA, NA, and NS segments with either NL (H1N1) (**A**) or P99 (H3N2) (**B**) packaging signals were constructed around the P99 open reading frame (ORF) for that segment. Silent mutations were introduced into the packaging signal regions of the ORF so that packaging would be directed only by the sequences flanking the 3' and 5' ends of the ORF. Start codons within the added 3' packaging signal region were mutated so that translation would result in the production of full-length wild-type protein. A variant, or VAR, version of **B** was generated via silent nucleotide changes in the ORF (**C**). Segments are shown in positive sense for clarity. Chimeric segments were then cloned into the pDP2002 ambisense vector to allow for recovery of infectious virus from cDNA.

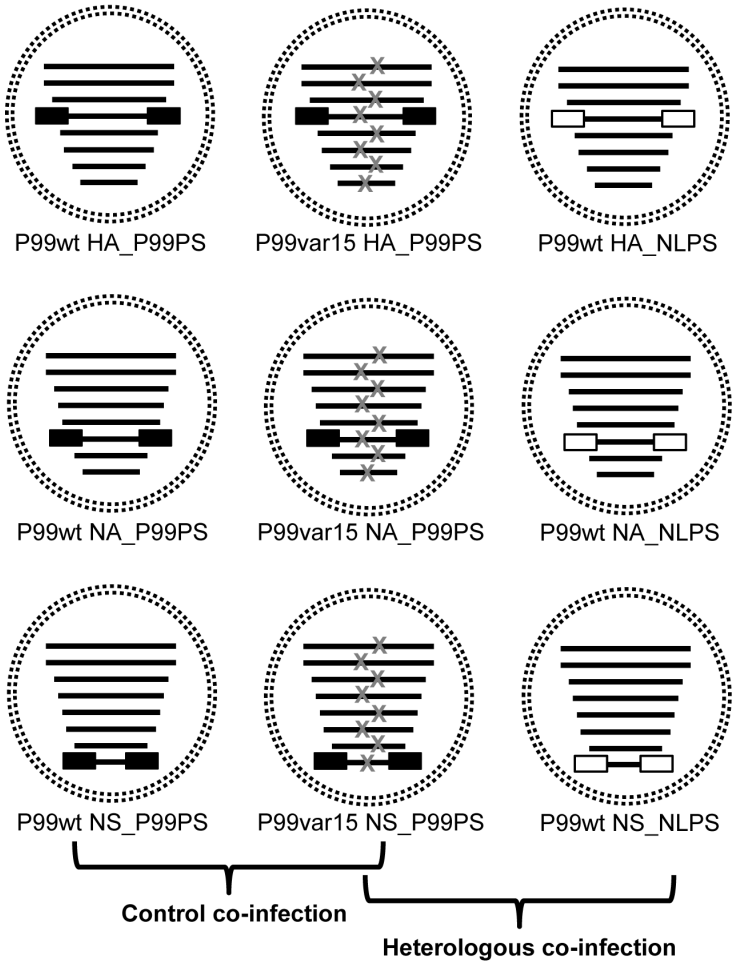

Figure 2. Viruses generated to evaluate the effects of packaging signal divergence on IAV reassortment. Viruses were rescued in a P99 background (black segments) with either P99 packaging signals (black boxes) or NL packaging signals (white boxes) on the HA, NA, or NS segments. Each virus contained one segment with modified packaging signals, and three viruses were rescued for each segment examined. Within each set of three viruses, one carried the silent VAR mutations that act as genetic tags for genotyping (gray x's), and the remaining two were WT (no genetic tags). Brackets indicate the virus pairs used for the control and heterologous co-infections. The same VAR virus was part of both virus pairings.

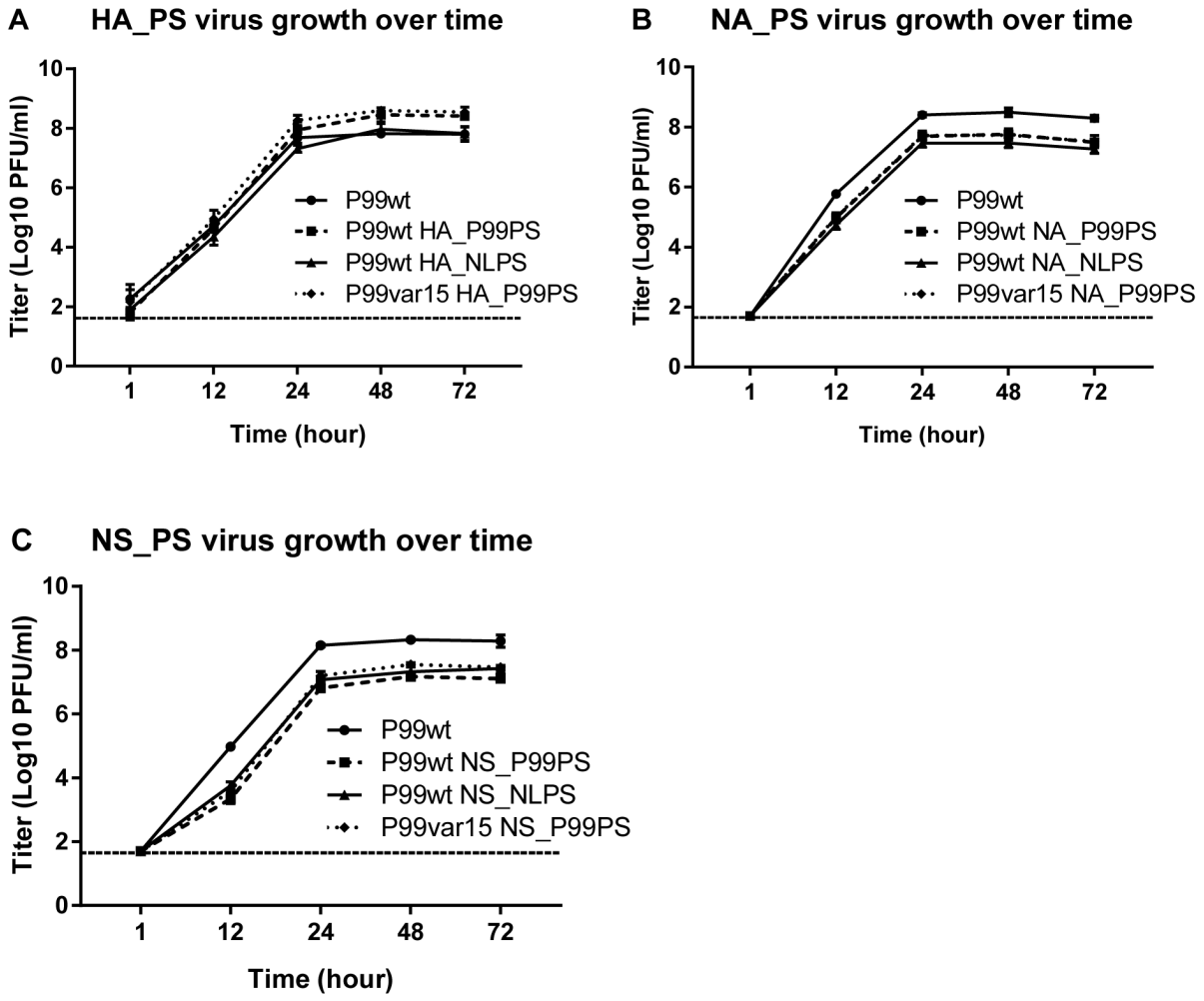

Figure 3. P99-based viruses with chimeric segments exhibited comparable growth phenotypes. Viruses containing chimeric HA (**A**), NA (**B**), or NS (**C**) segments were used to infect triplicate wells of MDCK cells at an MOI of 0.01 PFU/cell and output titers over time were compared to the P99 wild-type (P99wt) control virus. Data are represented as the means ± 1 S.D. The limit of detection was 50 PFU/mL and is indicated by a dashed line.

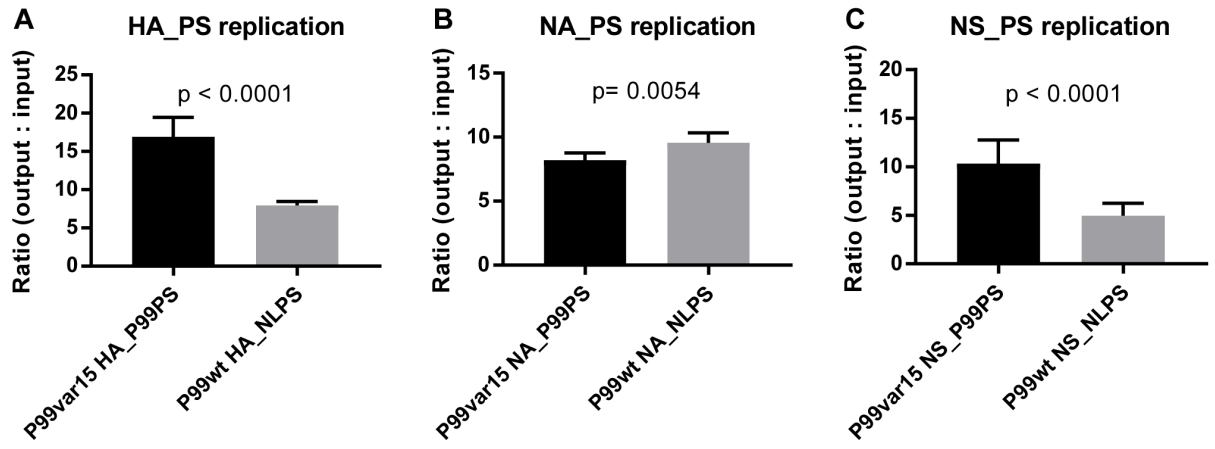

Figure 4. Segments with different packaging signal regions were replicated with varying efficiencies. MDCK cells were co-infected at a high MOI with P99-based viruses containing chimeric HA (**A**), NA (**B**), or NS (**C**) segments. RNA was extracted from both the inoculum (0 hr p.i.) and the cells (12 hr p.i.) and reverse-transcribed into cDNA, which was used as template in ddPCR with primers specific for the 3' packaging signal region of each segment of interest. The copy number of each segment in the cells (output) was divided by the copy number of each segment in the inoculum (input). Data were analyzed using Student's *t*-test. Data are represented as the means ± 1 S.D. for 2-4 biological replicates performed in triplicate.

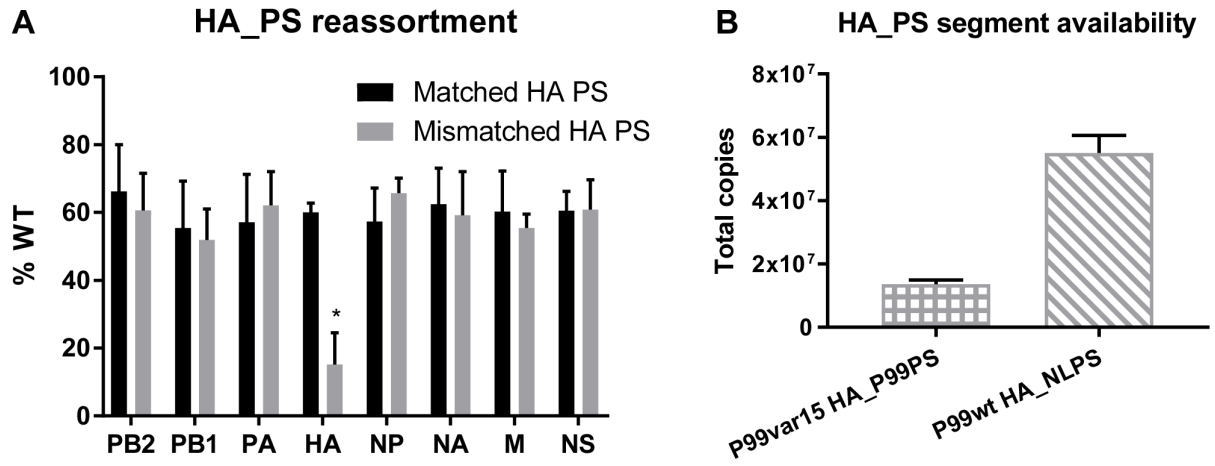

Figure 5. HA segments with matched packaging signals were preferentially incorporated into new virus particles. A. MDCK cells were co-infected at a high MOI with P99-based viruses containing chimeric HA segments and the genotypes of progeny viruses collected at 12 hr p.i. after one cycle of replication were determined. The percentage of viruses that contained a WT segment (as opposed to VAR) is plotted on the y-axis. The WT HA segment has matched packaging signals for the control co-infection (black bars) and mismatched packaging signals for the heterologous co-infection (gray bars). For all other segments, both WT and VAR contain matched packaging signals. *$p < 0.0001$ compared to all other values using two-way ANOVA with Tukey's multiple comparisons. Data are represented as the means ± 1 S.D. for two biological replicates performed in triplicate. **B.** RT ddPCR was used to quantify the number of each HA segment available in the co-infected cells at 12 hr p.i. using primers specific for the 3' packaging signal region of each segment. The total number of HA copies in each well was calculated and graphed. Data are represented as the means ± 1 S.D.

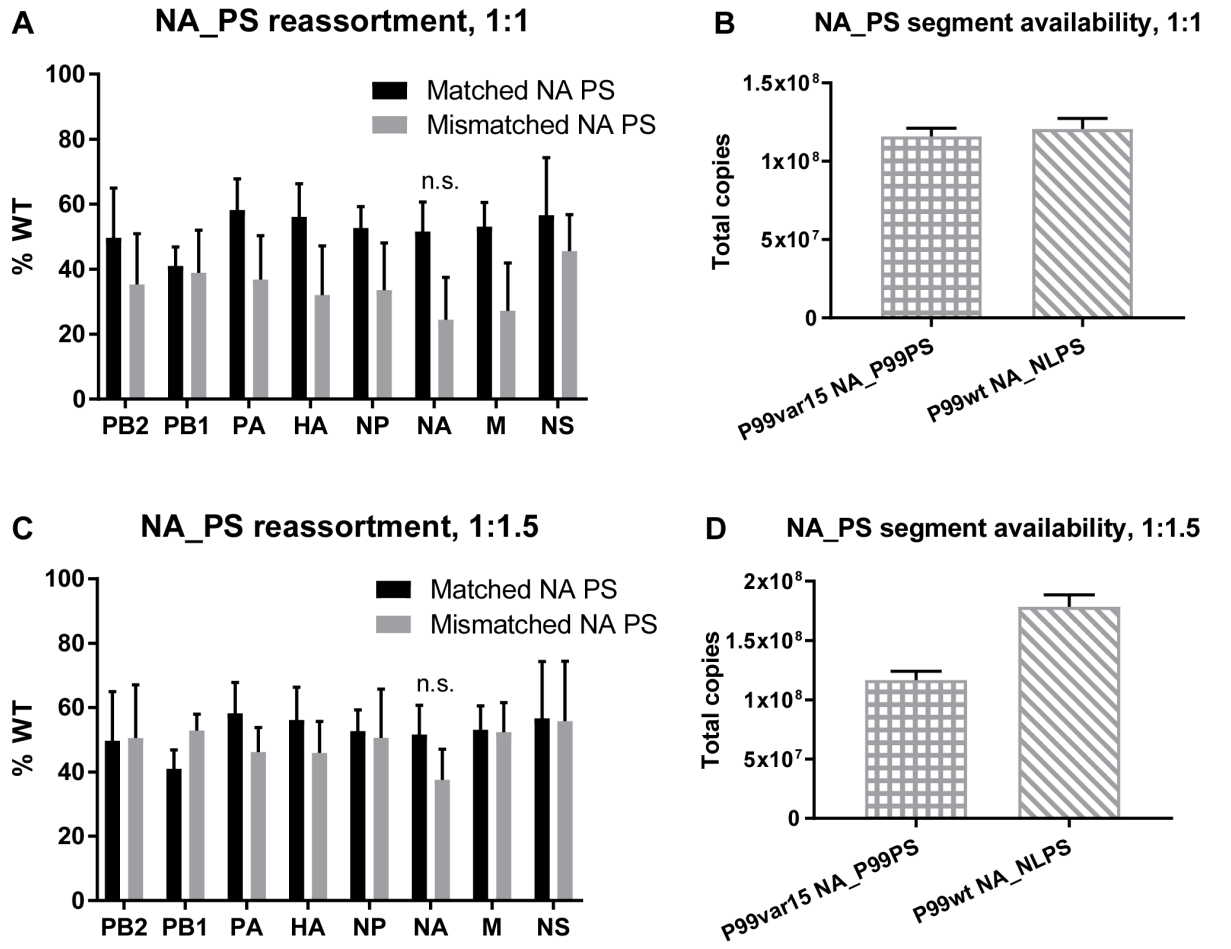

Figure 6. NA segments with matched packaging signals were not significantly favored for incorporation. MDCK cells were co-infected at a high MOI with P99-based viruses containing chimeric NA segments in either a 1:1 input ratio of VAR:WT (**A**) or a 1:1 input ratio of VAR:WT for the control co-infection and a 1:1.5 input ratio of VAR:WT for the heterologous co-infection (**C**). The genotypes of progeny viruses collected at 12 hr p.i. after a single cycle of replication were then analyzed via HRM analysis. The percentage of viruses that contained a WT segment (as opposed to VAR) is plotted on the y-axis. The WT NA segment has matched packaging signals for the control co-infection (black bars) and mismatched packaging signals for the heterologous co-infection (gray bars). For all other segments, both WT and VAR contain matched packaging

signals. n.s. = not significant using two-way ANOVA with Tukey's multiple comparisons. Data are represented as the means ± 1 S.D. for two biological replicates performed in triplicate for each condition. The data sets used for the control co-infections in (**A**) and (**C**) are the same. **B and D.** RT ddPCR was used to quantify the number of each NA segment available in the co-infected cells at 12 hr p.i. using primers specific for the 3' packaging signal region of each segment. The total number of NA copies in each well was calculated and graphed. 1:1 input ratio of VAR:WT (**B**), 1:1.5 input ratio of VAR:WT (**D**). Data are represented as the means ± 1 S.D.

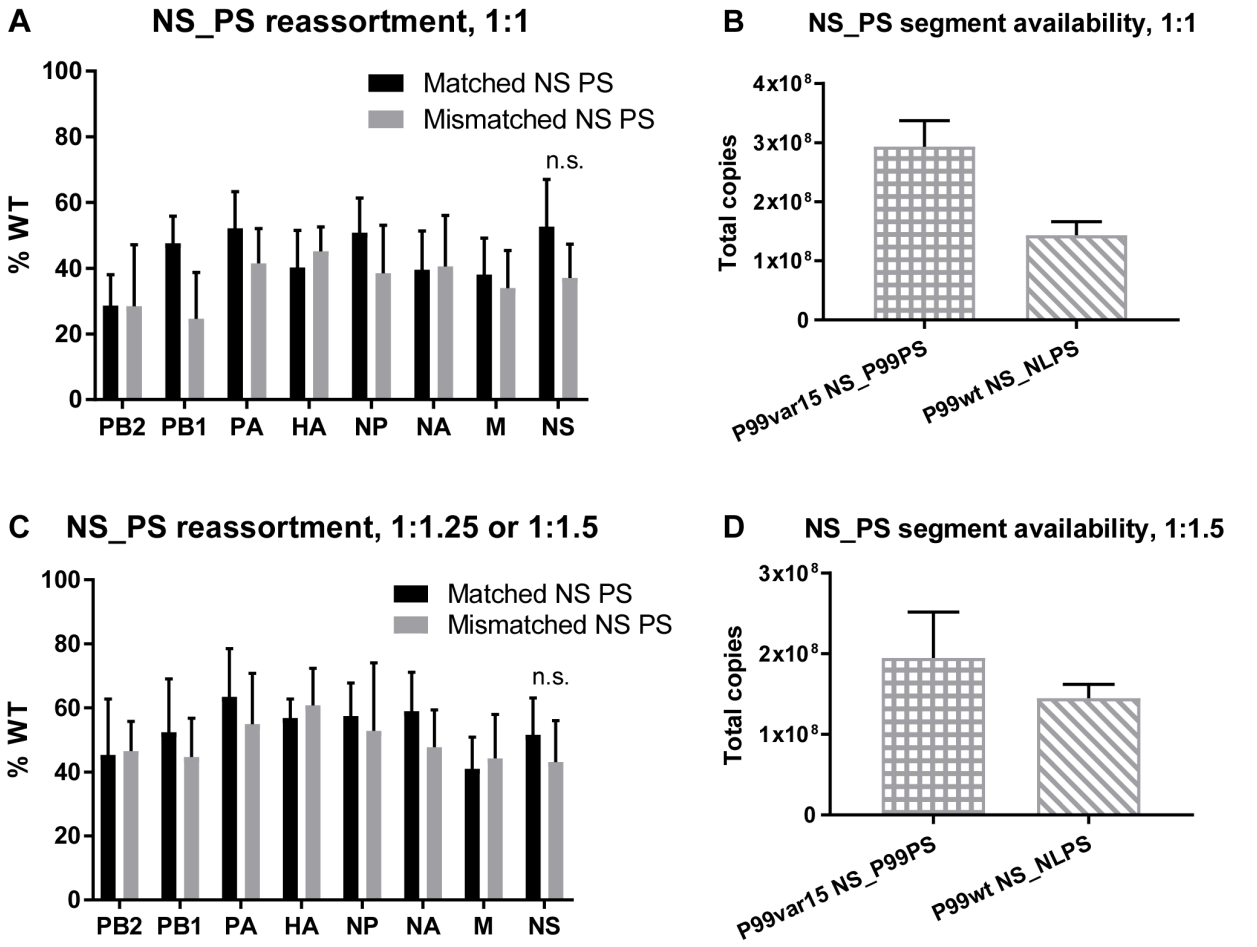

Figure 7. NS segments with heterologous packaging signals assorted randomly. MDCK cells were co-infected at a high MOI with P99-based viruses containing chimeric NS segments in either a 1:1 input ratio of VAR:WT (**A**) or a 1:1.25 input ratio of VAR:WT for the control co-infection and a 1:1.5 input ratio of VAR:WT for the heterologous co-infection (**C**). The genotypes of progeny viruses collected at 12 hr p.i. after one cycle of replication were then analyzed via HRM analysis. The percentage of viruses that contained a WT segment (as opposed to VAR) is plotted on the y-axis. The WT NS segment has matched packaging signals for the control co-infection (black bars) and mismatched packaging signals for the heterologous co-infection (gray bars). For all other segments, both WT and VAR contain matched packaging signals. n.s. = not significant using two-way ANOVA with Tukey's multiple comparisons. Data are represented as the means ±

1 S.D. for two biological replicates performed in triplicate for each condition. **B and D.** RT ddPCR was used to quantify the number of each NS segment available in the co-infected cells at 12 hr p.i. using primers specific for the 3' packaging signal region of each segment. The total number of NS copies in each well was calculated and graphed. 1:1 input ratio of VAR:WT (**B**), 1:1.5 input ratio of VAR:WT (**D**). Data are represented as the means ± 1 S.D.

Tables

Table 1. % Nucleotide identity in packaging signal regions, P99 (H3N2) vs. NL (H1N1)[a]

Segment	*% Nucleotide Identity*	*3' PS Length (UTR + coding)*	*5' PS Length (UTR + coding)*
PB2	89.7	177 nt	184 nt
PB1	96.9	174 nt	193 nt
PA	89.8	174 nt	208 nt
HA	**50.0**	**136 nt**	**136 nt**
NP	87.5	195 nt	174 nt
NA	**56.6**	**150 nt**	**200 nt**
M	90.1	275 nt	270 nt
NS	**83.3**	**200 nt**	**200 nt**

[a]Regions analyzed are conservative estimates of packaging signal lengths, based on data compiled by Hutchinson et al.

Table 2. Nucleotide sequences of P99-specific primers used for HRM analysis

Segment	*Forward Primer*	*Reverse Primer*
PB2	TGGAATAGAAATGGACCTGTGA	GGTTCCATGTTTTAACCTTTCG
PB1	AGGCTAATAGATTTCCTCAAGGATG	ACTCTCCTTTTTCTTTGAAAGTGTG
PA	TGCAACACTACTGGAGCTGAG	CTCCTTGTCACTCCAATTTCG
HA	CCTTGATGGAGAAAACTGCAC	CAACAAAAAGGTCCCATTCC
NP	CAACATACCAGAGGACAAGAGC	ACCTTCTAGGGAGGGTCGAG
NA	TCATGCGATCCTGACAAGTG	TGTCATTTGAATGCCTGTTG
M	GTTTTGGCCAGCACTACAGC	CCATTTGCCTGGCCTGACTA
NS	ACCTGCTTCGCGATACATAAC	AGGGGTCCTTCCACTTTTTG

Table 3. Nucleotide sequences of primers used for RT ddPCR

Segment	*Forward Primer*	*Reverse Primer*
HA_P99PS	AAGACTATCATTGCTTTGAGCTAC	GTTGCCGTGCTGTTGTAAT
HA_NLPS	GTTCTGCTATATACATTTGCAACC	GTGTCTACAGTGTCTGTTGAAT
NA_P99PS	CGATTGGCTCTGTTTCTCTC	TGCTTGAAATGCAATGTTACAG
NA_NLPS	CCATTGGTTCGGTCTGTTTG	CCAAGTTGAATTGAGTGGCTAA
NS_P99PS	CCAACACTGTGTCAAGTTTC	AACACTCAGTTCTTGGTCTAC
NS_NLPS	CAACACCTTGTCAAGCTTT	GCAACACCCAATCCAATG

References

1. **Shaw ML, Palese P.** 2013. Orthomyxoviridae, p 1151–1185. *In* Knipe D, Howley P (ed), Fields Virology, vol 1. Lippincott Williams & Wilkins, Philadelphia, PA.
2. **Desselberger U, Nakajima K, Alfino P, Pedersen FS, Haseltine WA, Hannoun C, Palese P.** 1978. Biochemical evidence that "new" influenza virus strains in nature may arise by recombination (reassortment). Proc Natl Acad Sci U S A **75:**3341-3345.
3. **Kawaoka Y, Krauss S, Webster RG.** 1989. Avian-to-human transmission of the PB1 gene of influenza A viruses in the 1957 and 1968 pandemics. Journal of Virology **63:**4603-4608.
4. **Garten RJ, Davis CT, Russell CA, Shu B, Lindstrom S, Balish A, Sessions WM, Xu X, Skepner E, Deyde V, Okomo-Adhiambo M, Gubareva L, Barnes J, Smith CB, Emery SL, Hillman MJ, Rivailler P, Smagala J, de Graaf M, Burke DF, Fouchier RAM, Pappas C, Alpuche-Aranda CM, López-Gatell H, Olivera H, López I, Myers CA, Faix D, Blair PJ, Yu C, Keene KM, Dotson PD, Boxrud D, Sambol AR, Abid SH, St. George K, Bannerman T, Moore AL, Stringer DJ, Blevins P, Demmler-Harrison GJ, Ginsberg M, Kriner P, Waterman S, Smole S, Guevara HF, Belongia EA, Clark PA, Beatrice ST, Donis R, et al.** 2009. Antigenic and Genetic Characteristics of Swine-Origin 2009 A(H1N1) Influenza Viruses Circulating in Humans. Science **325:**197-201.
5. **Kilbourne ED.** 2006. Influenza pandemics of the 20th century. Emerg Infect Dis **12:**9-14.
6. **Viboud C, Simonsen L, Fuentes R, Flores J, Miller MA, Chowell G.** 2016. Global Mortality Impact of the 1957-1959 Influenza Pandemic. J Infect Dis **213:**738-745.
7. **Simonsen L, Spreeuwenberg P, Lustig R, Taylor RJ, Fleming DM, Kroneman M, Van Kerkhove MD, Mounts AW, Paget WJ, the GCT.** 2013. Global Mortality Estimates for

the 2009 Influenza Pandemic from the GLaMOR Project: A Modeling Study. PLoS Med **10:**e1001558.

8. **Nguyen-Van-Tam JS, Hampson AW.** 2003. The epidemiology and clinical impact of pandemic influenza. Vaccine **21:**1762-1768.

9. **Nelson MI, Viboud C, Simonsen L, Bennett RT, Griesemer SB, St. George K, Taylor J, Spiro DJ, Sengamalay NA, Ghedin E, Taubenberger JK, Holmes EC.** 2008. Multiple Reassortment Events in the Evolutionary History of H1N1 Influenza A Virus Since 1918. PLoS Pathog **4:**e1000012.

10. **Holmes EC, Ghedin E, Miller N, Taylor J, Bao Y, St George K, Grenfell BT, Salzberg SL, Fraser CM, Lipman DJ, Taubenberger JK.** 2005. Whole-Genome Analysis of Human Influenza A Virus Reveals Multiple Persistent Lineages and Reassortment among Recent H3N2 Viruses. PLoS Biology **3:**e300.

11. **Westgeest KB, de Graaf M, Fourment M, Bestebroer TM, van Beek R, Spronken MI, de Jong JC, Rimmelzwaan GF, Russell CA, Osterhaus AD, Smith GJ, Smith DJ, Fouchier RA.** 2012. Genetic evolution of the neuraminidase of influenza A (H3N2) viruses from 1968 to 2009 and its correspondence to haemagglutinin evolution. J Gen Virol **93:**1996-2007.

12. **Wille M, Tolf C, Avril A, Latorre-Margalef N, Wallerstrom S, Olsen B, Waldenstrom J.** 2013. Frequency and patterns of reassortment in natural influenza A virus infection in a reservoir host. Virology **443:**150-160.

13. **Deng G, Tan D, Shi J, Cui P, Jiang Y, Liu L, Tian G, Kawaoka Y, Li C, Chen H.** 2013. Complex reassortment of multiple subtypes of avian influenza viruses in domestic ducks at the Dongting Lake Region of China. J Virol **87:**9452-9462.

14. **Abolnik C, Gerdes GH, Sinclair M, Ganzevoort BW, Kitching JP, Burger CE, Romito M, Dreyer M, Swanepoel S, Cumming GS, Olivier AJ.** 2010. Phylogenetic analysis of influenza A viruses (H6N8, H1N8, H4N2, H9N2, H10N7) isolated from wild birds, ducks, and ostriches in South Africa from 2007 to 2009. Avian Dis **54:**313-322.

15. **Steel J, Lowen AC.** 2014. Influenza A virus reassortment. Curr Top Microbiol Immunol **385:**377-401.

16. **Vijaykrishna D, Poon LL, Zhu HC, Ma SK, Li OT, Cheung CL, Smith GJ, Peiris JS, Guan Y.** 2010. Reassortment of pandemic H1N1/2009 influenza A virus in swine. Science **328:**1529.

17. **Nelson MI, Detmer SE, Wentworth DE, Tan Y, Schwartzbard A, Halpin RA, Stockwell TB, Lin X, Vincent AL, Gramer MR, Holmes EC.** 2012. Genomic reassortment of influenza A virus in North American swine, 1998-2011. J Gen Virol **93:**2584-2589.

18. **Dugan VG, Chen R, Spiro DJ, Sengamalay N, Zaborsky J, Ghedin E, Nolting J, Swayne DE, Runstadler JA, Happ GM, Senne DA, Wang R, Slemons RD, Holmes EC, Taubenberger JK.** 2008. The evolutionary genetics and emergence of avian influenza viruses in wild birds. PLoS Pathog **4:**e1000076.

19. **Lubeck MD, Palese P, Schulman JL.** 1979. Nonrandom association of parental genes in influenza A virus recombinants. Virology **95:**269-274.

20. **Greenbaum BD, Li OT, Poon LL, Levine AJ, Rabadan R.** 2012. Viral reassortment as an information exchange between viral segments. Proc Natl Acad Sci U S A **109:**3341-3346.

21. **Maines TR, Chen LM, Matsuoka Y, Chen H, Rowe T, Ortin J, Falcon A, Nguyen TH, Mai le Q, Sedyaningsih ER, Harun S, Tumpey TM, Donis RO, Cox NJ, Subbarao K, Katz JM.** 2006. Lack of transmission of H5N1 avian-human reassortant influenza viruses in a ferret model. Proc Natl Acad Sci U S A **103:**12121-12126.

22. **Jackson S, Van Hoeven N, Chen LM, Maines TR, Cox NJ, Katz JM, Donis RO.** 2009. Reassortment between avian H5N1 and human H3N2 influenza viruses in ferrets: a public health risk assessment. J Virol **83:**8131-8140.

23. **Chen LM, Davis CT, Zhou H, Cox NJ, Donis RO.** 2008. Genetic compatibility and virulence of reassortants derived from contemporary avian H5N1 and human H3N2 influenza A viruses. PLoS Pathog **4:**e1000072.

24. **Hatta M, Halfmann P, Wells K, Kawaoka Y.** 2002. Human influenza a viral genes responsible for the restriction of its replication in duck intestine. Virology **295:**250-255.

25. **Kimble JB, Sorrell E, Shao H, Martin PL, Perez DR.** 2011. Compatibility of H9N2 avian influenza surface genes and 2009 pandemic H1N1 internal genes for transmission in the ferret model. Proc Natl Acad Sci U S A **108:**12084-12088.

26. **Schrauwen EJ, Bestebroer TM, Rimmelzwaan GF, Osterhaus AD, Fouchier RA, Herfst S.** 2013. Reassortment between Avian H5N1 and human influenza viruses is mainly restricted to the matrix and neuraminidase gene segments. PLoS One **8:**e59889.

27. **Cline TD, Karlsson EA, Freiden P, Seufzer BJ, Rehg JE, Webby RJ, Schultz-Cherry S.** 2011. Increased pathogenicity of a reassortant 2009 pandemic H1N1 influenza virus containing an H5N1 hemagglutinin. J Virol **85:**12262-12270.

28. **Li C, Hatta M, Nidom CA, Muramoto Y, Watanabe S, Neumann G, Kawaoka Y.** 2010. Reassortment between avian H5N1 and human H3N2 influenza viruses creates hybrid viruses with substantial virulence. Proc Natl Acad Sci U S A **107:**4687-4692.

29. **Octaviani CP, Ozawa M, Yamada S, Goto H, Kawaoka Y.** 2010. High level of genetic compatibility between swine-origin H1N1 and highly pathogenic avian H5N1 influenza viruses. J Virol **84:**10918-10922.

30. **Zhang Y, Zhang Q, Kong H, Jiang Y, Gao Y, Deng G, Shi J, Tian G, Liu L, Liu J, Guan Y, Bu Z, Chen H.** 2013. H5N1 hybrid viruses bearing 2009/H1N1 virus genes transmit in guinea pigs by respiratory droplet. Science **340:**1459-1463.

31. **Ma W, Liu Q, Qiao C, del Real G, Garcia-Sastre A, Webby RJ, Richt JA.** 2014. North American triple reassortant and Eurasian H1N1 swine influenza viruses do not readily reassort to generate a 2009 pandemic H1N1-like virus. MBio **5:**e00919-00913.

32. **Ma J, Shen H, Liu Q, Bawa B, Qi W, Duff M, Lang Y, Lee J, Yu H, Bai J, Tong G, Hesse RA, Richt JA, Ma W.** 2015. Pathogenicity and transmissibility of novel reassortant H3N2 influenza viruses with 2009 pandemic H1N1 genes in pigs. J Virol **89:**2831-2841.

33. **Dlugolenski D, Jones L, Howerth E, Wentworth D, Tompkins SM, Tripp RA.** 2015. Swine Influenza Virus PA and Neuraminidase Gene Reassortment into Human H1N1 Influenza Virus Is Associated with an Altered Pathogenic Phenotype Linked to Increased MIP-2 Expression. J Virol **89:**5651-5667.

34. **Li C, Hatta M, Watanabe S, Neumann G, Kawaoka Y.** 2008. Compatibility among polymerase subunit proteins is a restricting factor in reassortment between equine H7N7 and human H3N2 influenza viruses. J Virol **82:**11880-11888.

35. **Schrauwen EJ, Herfst S, Chutinimitkul S, Bestebroer TM, Rimmelzwaan GF, Osterhaus AD, Kuiken T, Fouchier RA.** 2011. Possible increased pathogenicity of pandemic (H1N1) 2009 influenza virus upon reassortment. Emerg Infect Dis **17:**200-208.

36. **Song MS, Pascua PN, Lee JH, Baek YH, Park KJ, Kwon HI, Park SJ, Kim CJ, Kim H, Webby RJ, Webster RG, Choi YK.** 2011. Virulence and genetic compatibility of polymerase reassortant viruses derived from the pandemic (H1N1) 2009 influenza virus and circulating influenza A viruses. J Virol **85:**6275-6286.

37. **Wagner R, Matrosovich M, Klenk H.** 2002. Functional balance between haemagglutinin and neuraminidase in influenza virus infections. Reviews in Medical Virology **12:**159-166.

38. **Octaviani CP, Goto H, Kawaoka Y.** 2011. Reassortment between seasonal H1N1 and pandemic (H1N1) 2009 influenza viruses is restricted by limited compatibility among polymerase subunits. J Virol **85:**8449-8452.

39. **Marshall N, Priyamvada L, Ende Z, Steel J, Lowen AC.** 2013. Influenza virus reassortment occurs with high frequency in the absence of segment mismatch. PLoS Pathog **9:**e1003421.

40. **Liang Y, Hong Y, Parslow TG.** 2005. cis-Acting packaging signals in the influenza virus PB1, PB2, and PA genomic RNA segments. J Virol **79:**10348-10355.

41. **Fujii Y, Goto H, Watanabe T, Yoshida T, Kawaoka Y.** 2003. Selective incorporation of influenza virus RNA segments into virions. Proceedings of the National Academy of Sciences of the United States of America **100:**2002-2007.

42. **Watanabe T, Watanabe S, Noda T, Fujii Y, Kawaoka Y.** 2003. Exploitation of nucleic acid packaging signals to generate a novel influenza virus-based vector stably expressing two foreign genes. J Virol **77:**10575-10583.

43. **Ozawa M, Fujii K, Muramoto Y, Yamada S, Yamayoshi S, Takada A, Goto H, Horimoto T, Kawaoka Y.** 2007. Contributions of two nuclear localization signals of influenza A virus nucleoprotein to viral replication. J Virol **81:**30-41.

44. **Ozawa M, Maeda J, Iwatsuki-Horimoto K, Watanabe S, Goto H, Horimoto T, Kawaoka Y.** 2009. Nucleotide sequence requirements at the 5' end of the influenza A virus M RNA segment for efficient virus replication. J Virol **83:**3384-3388.

45. **Fujii K, Fujii Y, Noda T, Muramoto Y, Watanabe T, Takada A, Goto H, Horimoto T, Kawaoka Y.** 2005. Importance of both the coding and the segment-specific noncoding regions of the influenza A virus NS segment for its efficient incorporation into virions. J Virol **79:**3766-3774.

46. **Goto H, Muramoto Y, Noda T, Kawaoka Y.** 2013. The Genome-Packaging Signal of the Influenza A Virus Genome Comprises a Genome Incorporation Signal and a Genome-Bundling Signal. Journal of Virology **87:**11316-11322.

47. **Noda T, Sugita Y, Aoyama K, Hirase A, Kawakami E, Miyazawa A, Sagara H, Kawaoka Y.** 2012. Three-dimensional analysis of ribonucleoprotein complexes in influenza A virus. Nat Commun **3:**639.

48. **Fournier E, Moules V, Essere B, Paillart J-C, Sirbat J-D, Isel C, Cavalier A, Rolland J-P, Thomas D, Lina B, Marquet R.** 2012. A supramolecular assembly formed by influenza A virus genomic RNA segments. Nucleic Acids Research **40:**2197-2209.

49. **Fournier E, Moules V, Essere B, Paillart JC, Sirbat JD, Cavalier A, Rolland JP, Thomas D, Lina B, Isel C, Marquet R.** 2012. Interaction network linking the human H3N2 influenza A virus genomic RNA segments. Vaccine **30:**7359-7367.

50. **Chou YY, Vafabakhsh R, Doganay S, Gao Q, Ha T, Palese P.** 2012. One influenza virus particle packages eight unique viral RNAs as shown by FISH analysis. Proc Natl Acad Sci U S A **109:**9101-9106.

51. **Gavazzi C, Yver M, Isel C, Smyth RP, Rosa-Calatrava M, Lina B, Moulès V, Marquet R.** 2013. A functional sequence-specific interaction between influenza A virus genomic RNA segments. Proceedings of the National Academy of Sciences of the United States of America **110:**16604-16609.

52. **Nakatsu S, Sagara H, Sakai-Tagawa Y, Sugaya N, Noda T, Kawaoka Y.** 2016. Complete and Incomplete Genome Packaging of Influenza A and B Viruses. MBio **7**.

53. **Essere B, Yver M, Gavazzi C, Terrier O, Isel C, Fournier E, Giroux F, Textoris J, Julien T, Socratous C, Rosa-Calatrava M, Lina B, Marquet R, Moules V.** 2013. Critical role of segment-specific packaging signals in genetic reassortment of influenza A viruses. Proceedings of the National Academy of Sciences **110:**E3840-E3848.

54. **Baker SF, Nogales A, Finch C, Tuffy KM, Domm W, Perez DR, Topham DJ, Martinez-Sobrido L.** 2014. Influenza A and B Virus Intertypic Reassortment through Compatible Viral Packaging Signals. Journal of Virology **88:**10778-10791.

55. **Gao Q, Palese P.** 2009. Rewiring the RNAs of influenza virus to prevent reassortment. Proceedings of the National Academy of Sciences **106:**15891-15896.

56. **Gao Q, Chou Y-Y, Doğanay S, Vafabakhsh R, Ha T, Palese P.** 2012. The Influenza A Virus PB2, PA, NP, and M Segments Play a Pivotal Role during Genome Packaging. Journal of Virology **86:**7043-7051.

57. **Hutchinson EC, von Kirchbach JC, Gog JR, Digard P.** 2010. Genome packaging in influenza A virus. Journal of General Virology **91:**313-328.

58. **Chen H, Ye J, Xu K, Angel M, Shao H, Ferrero A, Sutton T, Perez DR.** 2012. Partial and full PCR-based reverse genetics strategy for influenza viruses. PLoS One **7:**e46378.

59. **Tao H, Li L, White MC, Steel J, Lowen AC.** 2015. Influenza A Virus Coinfection through Transmission Can Support High Levels of Reassortment. J Virol **89:**8453-8461.

60. **Fodor E, Devenish L, Engelhardt OG, Palese P, Brownlee GG, García-Sastre A.** 1999. Rescue of Influenza A Virus from Recombinant DNA. Journal of Virology **73:**9679-9682.

61. **Steel J, Lowen AC, Mubareka S, Palese P.** 2009. Transmission of influenza virus in a mammalian host is increased by PB2 amino acids 627K or 627E/701N. PLoS Pathog **5:**e1000252.

62. **Fonville JM, Marshall N, Tao H, Steel J, Lowen AC.** 2015. Influenza Virus Reassortment Is Enhanced by Semi-infectious Particles but Can Be Suppressed by Defective Interfering Particles. PLoS Pathog **11:**e1005204.

63. **Schwartz SL, Lowen AC.** 2016. Droplet digital PCR: A novel method for detection of influenza virus defective interfering particles. J Virol Methods **237:**159-165.

64. **Chen R, Holmes EC.** 2010. Hitchhiking and the population genetic structure of avian influenza virus. J Mol Evol **70:**98-105.

65. **Gog JR, Afonso EDS, Dalton RM, Leclercq I, Tiley L, Elton D, von Kirchbach JC, Naffakh N, Escriou N, Digard P.** 2007. Codon conservation in the influenza A virus genome defines RNA packaging signals. Nucleic Acids Research **35:**1897-1907.

66. **Gerber M, Isel C, Moules V, Marquet R.** 2014. Selective packaging of the influenza A genome and consequences for genetic reassortment. Trends in Microbiology **22:**446-455.

67. **Gultyaev AP, Spronken MI, Richard M, Schrauwen EJ, Olsthoorn RC, Fouchier RA.** 2016. Subtype-specific structural constraints in the evolution of influenza A virus hemagglutinin genes. Sci Rep **6:**38892.

68. **Baudin F, Bach C, Cusack S, Ruigrok RW.** 1994. Structure of influenza virus RNP. I. Influenza virus nucleoprotein melts secondary structure in panhandle RNA and exposes the bases to the solvent. Embo j **13:**3158-3165.

69. **Arranz R, Coloma R, Chichon FJ, Conesa JJ, Carrascosa JL, Valpuesta JM, Ortin J, Martin-Benito J.** 2012. The structure of native influenza virion ribonucleoproteins. Science **338:**1634-1637.

70. **Cobbin JC, Ong C, Verity E, Gilbertson BP, Rockman SP, Brown LE.** 2014. Influenza virus PB1 and neuraminidase gene segments can cosegregate during vaccine reassortment driven by interactions in the PB1 coding region. J Virol **88:**8971-8980.

71. **Gilbertson B, Zheng T, Gerber M, Printz-Schweigert A, Ong C, Marquet R, Isel C, Rockman S, Brown L.** 2016. Influenza NA and PB1 Gene Segments Interact during the Formation of Viral Progeny: Localization of the Binding Region within the PB1 Gene. Viruses **8**.

72. **Marsh GA, Rabadan R, Levine AJ, Palese P.** 2008. Highly conserved regions of influenza a virus polymerase gene segments are critical for efficient viral RNA packaging. J Virol **82:**2295-2304.

73. **Gao Q, Brydon EW, Palese P.** 2008. A seven-segmented influenza A virus expressing the influenza C virus glycoprotein HEF. J Virol **82:**6419-6426.

74. **Nakajima K, Sugiura A.** 1977. Three-factor cross of influenza virus. Virology **81:**486-489.

75. **Bergmann M, Muster T.** 1995. The relative amount of an influenza A virus segment present in the viral particle is not affected by a reduction in replication of that segment. J Gen Virol **76 (Pt 12):**3211-3215.

76. **Smith GL, Hay AJ.** 1982. Replication of the influenza virus genome. Virology **118:**96-108.

77. **Inagaki A, Goto H, Kakugawa S, Ozawa M, Kawaoka Y.** 2012. Competitive incorporation of homologous gene segments of influenza A virus into virions. J Virol **86:**10200-10202.

78. **Enami M, Sharma G, Benham C, Palese P.** 1991. An influenza virus containing nine different RNA segments. Virology **185:**291-298.

79. **Ince WL, Gueye-Mbaye A, Bennink JR, Yewdell JW.** 2013. Reassortment complements spontaneous mutation in influenza A virus NP and M1 genes to accelerate adaptation to a new host. J Virol **87:**4330-4338.

Chapter III: Serial Passage of an Influenza A Virus Containing Heterologous Packaging Signals on Segment 4

Maria C. White[1], John Steel[1], and Anice C. Lowen[1]

[1]Department of Microbiology and Immunology, Emory University School of Medicine, Atlanta, GA, USA

Data currently unpublished

All figures were generated by MCW with input from ACL

Abstract

Influenza A virus (IAV) contains eight distinct genomic segments. For a virus particle to be infectious, it must contain one copy of each segment. During virus assembly, terminal regions of the segments termed packaging signals allow for differentiation of the eight segments. The current working model is that interactions between segments occur during assembly at the packaging signal regions; however, it is unknown which nucleotides of each segment are important for mediating this packaging process. This study aimed to identify nucleotides that are critical for directing packaging of the hemagglutinin (HA) segment. Influenza A/Panama/2007/99 (P99; H3N2)-based viruses were rescued with P99 HA open reading frames carrying either influenza A/Netherlands/602/2009 (NL; H1N1) packaging signals or P99 packaging signals as a control. These two viruses were then serially passaged ten times in MDCK cells, and compensatory mutations in the heterologous H1N1 HA packaging signals that were absent in the control HA segment were identified via Sanger sequencing. A single mutation in the 5' HA packaging signal region, T1864C, was identified in all three independent heterologous lineages post-passage. However, despite being selected for three independent times, this mutation did not confer an increase in packaging efficiency to the passaged heterologous HA segment. A recombinant unpassaged virus containing the T1864C mutation was then generated, and experiments with this recombinant virus failed to show an increase in HA packaging efficiency or virus growth compared to the control virus lacking the mutation. Overall, our approach was unable to identify nucleotides that are important for directing packaging of a HA segment. However, the T1864C mutation could have a yet unidentified role in easing segment mismatch when a H1N1 HA segment enters a H3N2 virus.

Introduction

Influenza A virus (IAV) is a negative sense, single-stranded RNA virus (1). IAV contains eight gene segments which encode a minimum of twelve proteins. The glycoprotein hemagglutinin (HA) is encoded by segment 4 and is one of the major glycoproteins embedded in outer membrane of the virus. HA binds the IAV sialic acid receptor and allows fusion between the viral membrane and the endosomal membrane to mediate infection of a host cell (2).

As a segmented virus, IAV can undergo reassortment, or gene segment exchange, within a cell infected with two or more IAVs. The process of reassortment plays a major role in both epidemic and pandemic influenza. Reassortment among co-circulating strains of the same IAV lineage, such as the H3N2 seasonal lineage, occurs and can result in the formation of new strains of epidemiological significance (3, 4). Additionally, the last three pandemic strains were produced through one or multiple reassortment events involving IAV of distinct lineages (5-7). Of note, the introduction of a novel HA segment was a common factor in each of these pandemics.

The efficiency of reassortment between different IAV strains is likely limited by incompatibilities between the co-infecting viruses at both the RNA and protein levels, a phenomenon termed segment mismatch (8, 9). Indeed, multiple studies to date have demonstrated that heterologous RNAs and heterologous proteins result in a decrease in reassortment efficiency (10-15). Segment mismatch at the RNA level occurs at the packaging signal regions of each IAV segment. These packaging signals are specific to each segment, and direct the incorporation and bundling of the segments during virus assembly (16). Interactions between the segments occur at the packaging signal regions; however, the nature of these interactions has yet to be definitively determined (17, 18). Likewise, the nucleotides that are critical for mediating packaging of each segment and segment-segment interactions are largely unknown to date.

The aim of this study was to identify nucleotides that are critical for mediating packaging of the HA segment. Previous data from our lab showed that heterologous packaging signals on the HA segment limited reassortment efficiency between otherwise similar IAV strains (12). To accomplish this aim, we passaged our previously described viruses (12) in MDCK cells. Briefly, these viruses were influenza A/Panama/2007/99 (P99; H3N2)-based, with the HA segment of each virus carrying either P99 packaging signals or influenza A/Netherlands/602/2009 (NL; H1N1) packaging signals introduced onto the H3N2 HA open reading frame (ORF). During these serial passages, we predicted that mutations would arise in the heterologous packaging signals that would ease segment mismatch, thus allowing better packaging of the HA segment carrying H1 packaging signals into a H3N2 virus. Thus, post-passage we sequenced the HA packaging signal regions of both viruses, looking for compensatory mutations that arose in the heterologous packaging signals but not the homologous packaging signals. We identified a single mutation, T1864C, which did not appear to ease the packaging constraint of the heterologous segment, but could have a currently unidentified role in alleviating segment mismatch between the H1 HA segment and the P99 strain background.

Results

Serial passage of viruses carrying heterologous packaging signals on HA identified possible compensatory mutations. In order to identify nucleotides important for mediating packaging of the HA segment, a serial passage assay was designed. Briefly, P99-based viruses carrying either homologous (P99) or heterologous (NL) packaging signals on HA were passaged ten times in triplicate in MDCK cells (**Fig. 1**). Post-passage, the packaging signal regions of both HA segments were sequenced, and mutations that arose in the NL but not P99 packaging signal regions were

identified (**Table 1**). Interestingly, no mutations were observed in the homologous HA segment after ten passages; the introduced packaging signal regions as well as the introduced silent mutations to disrupt native packaging signal function in the HA ORF remained unchanged and intact, respectively (12). Conversely, several mutations were found in the heterologous packaging signal regions; some were partial mutations and some were full conversions (**Table 1**). A single mutation, T1864C, was identified in all three lineages of the passaged P99 HA_NLPS virus. Position 1864 of this modified HA segment corresponds to position 1668 of the NL/09 HA segment. This mutation lies within the previously mapped 5' packaging signal region of the HA segment (19). Thus, the nucleotide at position 1864 (1668 of NL/09) could be involved in packaging of the HA segment. Sanger sequencing analysis of the seed virus used for the serial passage inoculation was unable to detect the T1864C mutation in the original virus stock (data not shown). Therefore, this mutation was positively selected for during passage of all three lineages.

We then aligned the area of the HA segment containing the identified mutation to other H1 HA segments from well-characterized IAVs (influenza A/PR8/34 and influenza A/WSN/33, with influenza A/Netherlands/602/2009 [NL/09] as a control). The T at this position was 100% conserved (**Table 2**). Next, we aligned this area to representative IAV isolates sampled over the past 100 years, including 1918 H1N1 viruses, seasonal H1N1 viruses, 2009 pandemic H1N1 viruses, avian H1N1 viruses, swine H1N1 viruses, and H3N2 viruses (data not shown). The T at position 1864 (1668 of NL/09) was found to be 100% conserved across these IAV lineages over time, suggesting an importance in nature for maintaining a T at this position.

Serial passage of viruses carrying heterologous packaging signals on HA did not increase HA packaging efficiency. To assess whether serial passage (and the accompanying mutations) conferred an increase in packaging efficiency for the HA segment carrying heterologous H1

packaging signals, we performed a series of co-infection experiments. MDCK cells were co-infected with WT-VAR virus pairs in the P99 background. The WT-VAR virus system has been described previously (20). Briefly, this system utilizes P99-based viruses that differ only in silent mutations introduced into each of the eight segments of one virus. These silent mutations serve as genetic tags which allow for differentiation of WT (untagged) vs VAR (tagged) segments in IAV progeny using high-resolution melt (HRM) analysis. Co-infections were performed as follows: i) unpassaged P99wt HA_NLPS + unpassaged P99var15 HA_P99PS, ii) P10 P99wt HA_P99PS + unpassaged P99var15 HA_P99PS, and iii) P10 P99wt HA_NLPS + unpassaged P99var15 HA_P99PS, the final of which was performed twice using two independent VAR virus stocks. At 12 hr post-infection (p.i.), cell culture supernatants from each of the triplicate co-infections were harvested. Plaque isolates derived from two of the three supernatant samples were then genotyped to determine reassortment outcomes.

Results from the unpassaged heterologous co-infection (P99wt HA_NLPS + P99var15 HA_P99PS) showed the same phenotype we have previously described (12). HA segments carrying heterologous H1 packaging signals are significantly disfavored for incorporation into a H3N2 background, as a majority of the HA segments packaged carried homologous, VAR, packaging signals (**Fig. 2a**). In the P10 P99wt HA_P99PS + unpassaged P99var15 HA_P99PS co-infection, both HA segments carried homologous P99 packaging signals, so we expected a roughly equal distribution of WT vs VAR HA segments in the reassortant progeny. We observed this predicted phenotype in our data set (**Fig. 2b**), confirming that serial passage of the homologous HA segment does not alter its preference for packaging compared to an unpassaged HA segment. In the final co-infection, the WT HA segment carried heterologous NL packaging signals and had been passaged ten times, while the VAR HA segment carried homologous P99 packaging signals

and had not been passaged. If serial passage and the accompanying T1864C mutation eased the packaging constraint demonstrated in **Fig. 2a**, then an increase in packaging of the WT HA segment would be observed. However, increased packaging of the WT heterologous HA segment was not observed in our data set (**Fig. 2c-d**), as the packaging defect for the WT HA segment was still present. We performed this co-infection two times using different VAR virus stocks, with the same result (**Fig. 2c-d**). Taken together, these data suggest that serial passage of a virus carrying heterologous packaging signals on HA does not increase the packaging efficiency of the mismatched segment under the conditions tested.

Generation of an unpassaged recombinant virus containing the T1864C mutation failed to increase HA packaging efficiency. We observed that serial passage of an HA segment carrying heterologous packaging signals did not increase its packaging efficiency. However, considering that the T1864C mutation arose three independent times during serial passage, we wondered if this single nucleotide change would alter the HA packaging phenotype in the context of an unpassaged virus. To this end, we generated an unpassaged recombinant P99-based virus containing the HA_NLPS T1864C mutation by site-directed mutagenesis and reverse genetics. The presence of the T1864C mutation in the resulting virus stock was confirmed via Sanger sequencing. We then performed co-infections in MDCK cells as follows: P99wt HA_NLPS + P99var15 HA_P99PS (same conditions as in **Fig. 2a**, as a control) and P99wt HA_NLPS T1864C + P99var15 HA_P99PS (with the WT HA segment containing the introduced T1864C mutation). All viruses used in these co-infections were not passaged. Cell culture supernatants from each of the triplicate co-infections were harvested, and plaque isolates derived from these supernatants were then genotyped to determine reassortment outcomes. As shown in **Fig. 3**, the presence of the T1864C mutation in the HA segment did not increase the packaging efficiency of an unpassaged heterologous HA segment,

as the % WT HA incorporation for both co-infections were similar. These data show that the substitution of a C for T at position 1864 does not allow for better packaging of an HA segment carrying H1 packaging signals into H3N2 viruses.

T1864C did not alter IAV growth kinetics. Although the T1864C mutation did not increase HA packaging efficiency, it could potentially increase the efficiency of another aspect of the viral life cycle, such as replication. In order to assess whether the T1864C mutation increases virus growth, we performed multicycle growth analyses. The P99 wild-type virus (A/Panama/2007/99; P99wt) was included as a control in parallel with the test viruses. MDCK cells were infected in triplicate with either P99wt, P99var15 HA_P99PS, unpassaged P99wt HA_NLPS, or P99wt HA_NLPS T1864C, and output titers over time were determined by plaque assay. Although the three viruses with modified HA packaging signals were slightly attenuated compared to the P99wt control virus, the presence of the T1864C mutation did not confer a growth advantage relative to the parental HA_NLPS virus (**Fig. 4**). Notably, however, the T1864C mutation was also not detrimental to virus growth, as titers of the virus containing the T1864C mutation were always equal to or higher than the corresponding titers of the parental HA_NLPS virus (**Fig. 4**).

Discussion

The purpose of this study was to identify nucleotides that are important for mediating packaging of the HA segment. To date, it is currently unknown which nucleotides of each IAV segment are essential for mediating packaging. By serially passaging a H3N2 virus containing heterologous H1N1 packaging signals on HA, we aimed to uncover compensatory mutations in the HA packaging signal regions which eased the H1N1:H3N2 packaging constraint. Although we did

uncover a single mutation, T1864C, in all three independently passaged virus lineages, this mutation did not appear to enable better packaging of the HA segment.

We have previously demonstrated that HA segments carrying heterologous H1N1 packaging signals do not efficiently enter human seasonal H3N2 viruses (12). In the current study, we serially passaged these heterologous HA segments contained within H3N2 viruses and hypothesized that, over time, the HA segment would accumulate mutations that enabled better packaging of the mismatched segment. The location of the mutations would suggest specific HA nucleotides that play a role in packaging. It was previously reported that nucleotides 1659-1671 of the H1N1 HA segment were critical for efficient packaging (21). The mutation identified in this study, T1864C (T1668C in wild-type NL/09 HA), falls within this previously identified critical region. However, subsequent experiments failed to show any improvement in HA segment packaging or virus growth when this mutation was present, and several possible explanations for this lack of phenotype exist.

First, it is possible that this mutation only allows for better HA segment packaging in the context of a single infection. The serial passages were conducted as single infections, while the subsequent analyses of packaging efficiency were conducted under co-infection conditions. Perhaps when competing with a better matched segment (as in the co-infection experiments), the T1864C mutation cannot overcome the incorporation barrier. In contrast, when the P99 HA_NLPS segment is the only HA segment available for packaging into H3N2 viruses (as in the serial passage experiment), the T1864C mutation eases the packaging constraint and allows for more efficient HA segment incorporation. The titers obtained throughout serial passage for the P99 HA_NLPS virus were comparable to the titers obtained for the control P99 HA_P99PS virus, suggesting no growth defects of the P99 HA_NLPS virus (data not shown). Further experiments such as RNA

gels and northern blotting utilizing purified P99 HA_NLPS virus could help to clarify if any increase in packaging efficiency is conferred to the heterologous HA segment in the context of a single infection.

Second, it is possible that the T1864C mutation acts in concert with another mutation elsewhere in the IAV genome. We only sequenced a portion of the HA segment, and therefore were unable to identify other mutations that might have occurred during passage in the remaining segments. The explanation that T1864C enables better HA segment packaging along with another mutation on a different IAV segment is satisfactory to explain the lack of better packaging in the co-infection using the recombinant unpassaged P99 HA_NLPS T1864C virus, but unsatisfactory for the co-infection using the passaged P99 HA_NLPS virus, as any other segment mutations would have also been present in the passaged virus. It is possible that the T's at position 1864 were almost completely converted to C's after ten passages (lineages 1 and 2 showed full conversion, while lineage 3 showed majority but not full conversion; **Table 1**), but that the position it was acting in combination with had not yet mutated to a level that could be detected by our sequencing assay after ten passages. We chose ten passages for practical reasons and from previous studies suggesting that this yields enough replication cycles for IAV adaptive mutations to reach high frequency in cell culture (22, 23). Nevertheless, carrying out the serial passage to twenty or more passages could provide additional information.

We aligned the region of the T1864C mutation to a wide array of IAV strains, including seasonal H1N1 viruses, pandemic H1N1 viruses, avian H1N1 viruses, swine H1N1 viruses, and H3N2 viruses, encompassing a collection date spanning the last 100 years. We found that the T at position 1668 (1864 in the current study) was 100% conserved across these various IAV lineages over time (data not shown). In nature, position 1668 falls within the terminal coding region of the H1 HA

segment. In the design of our heterologous P99 HA_NLPS segment, the H1N1 packaging signals are not translated; they contain coding sequence, but have no impact on HA protein because they are introduced upstream of the start codon and downstream of the stop codon. T1668C results in a coding change of serine to proline. This change could be disfavored in nature, as the introduction of a proline residue would likely alter the structure of the protein being made (24-26). The lack of packaging signal translation in our system could allow for a mutation to arise that would otherwise be unsuitable in nature, since the substitution in our system would not affect protein structure. Perhaps position 1668 of the NL/09 HA has the potential to ease RNA mismatch, but is prevented from occurring in nature due to the coding change that would result.

Of final note, the sequencing results obtained herein point towards the stability of grafted and silently mutated regions of IAV segments. The control virus passaged alongside the P99 HA_NLPS virus contained a considerable number of modifications to the HA segment prior to the onset of passage. This control HA segment consisted of the P99 HA ORF with 136 nucleotides introduced onto both the 3' and 5' ends. These 136 nucleotides encompassed the P99 HA untranslated region plus packaging signal coding region. The ATG's in the introduced 3' end were mutated so that translation would not begin prematurely. In addition, the first 60 and last 60 nucleotides of the P99 HA ORF were modified by silently mutating every codon (with the exception of start, stop, Met and Trp codons) in order to disrupt the packaging function inherent to those regions. After ten passages in MDCK cells, 100% of these introduced mutations were maintained, suggesting that these alterations are stable over time and have minimal negative impact on viral fitness.

In conclusion, serial passage of a H3N2 virus carrying H1N1 packaging signals on the HA segment revealed a single HA mutation, T1864C, arising in three independently-passaged virus lineages.

This mutation failed to confer more efficient packaging to the HA segment when competing with a better matched HA segment, and also failed to enable better virus growth. However, further experiments are needed to elucidate the role that this mutation may have on viral fitness, as the selection for this mutation three independent times seems beyond chance. It is possible that in the context of a single infection, T1864C eases RNA mismatch between H3N2 and H1N1 viruses, but additional experiments must be performed to directly test this hypothesis.

Materials and Methods

Cells and viruses. Madin-Darby canine kidney (MDCK) cells were maintained in minimum essential medium (Gibco) supplemented with penicillin-streptomycin and 10% fetal bovine serum (FBS). Human embryonic kidney cells (293T) were maintained in Dulbecco's Modified Eagle Medium (Gibco) supplemented with 10% FBS. Reverse genetics-derived influenza A/Panama/2007/99 (H3N2; P99) virus was used, and HA packaging signal regions were taken from P99 as well as from influenza A/Netherlands/602/2009 (H1N1; NL) virus as described previously (12). Virus stocks were generated in 9-11 day old embryonated hens' eggs (Hy-Line) and passaged through eggs once.

Serial passage of viruses with modified HA packaging signals. WT P99 HA_P99PS and P99 HA_NLPS viruses were serially passaged ten times in triplicate in MDCK cells (**Figure 1**). Each passage was performed at a low multiplicity of infection (MOI) in the presence of *tosyl phenylalanyl chloromethyl ketone* (TPCK)-treated trypsin for 48 hr at 33° C. After 48 hr, the supernatants were harvested, frozen at -80° C, titered via plaque assay on MDCK cells, and used for subsequent inoculation. Prior to each infection, the cells were washed 3x with PBS. Passage 1 – passage 4 were performed in 6 well dishes at a MOI of 0.01. Due to the abundance of defective

interfering (DI) segments in the stocks lowering each subsequent titer (data not shown), passage 5 was performed in 6 well dishes at a MOI of 0.001. Changing the MOI from 0.01 to 0.001 significantly lowered the prevalence of DI segments in the stocks and improved stock titers (data not shown). However, due to the concern of potentially selecting against viral variants using the lower MOI in such a small vessel, passage 6 – passage 10 were performed in T75 flasks at a MOI of 0.001 in order to increase the number of cells in the assay while maintaining a low MOI to decrease DI segments. The final result was three passage 10 P99 HA_P99PS virus stocks and three passage 10 P99 HA_NLPS virus stocks. Passage 10 stock titers were determined via plaque assay on MDCK cells and used for subsequent experiments.

Sequencing HA segments of passage 10 viruses. RNA was extracted from the six passage 10 virus stocks using 280 µL of virus stock and the QIAamp Viral RNA Mini Kit (QIAGEN) following the manufacturer's instructions with the following modifications: carrier RNA was not added to the AVL lysis buffer and the RNA was eluted in 30 µL RNase-free water. Twelve microliters of RNA was then reverse-transcribed using Maxima reverse transcriptase (Fermentas) following the manufacturer's instructions, and the cDNA was used in standard PCR to amplify the 3' and 5' packaging signal ends of each HA segment (~400 bp amplicons). The PCR products were purified using the QIAquick PCR Purification Kit (QIAGEN) following the manufacturer's instructions with the following modifications: 2 µL of 3M sodium acetate (pH 5) was added to each sample contained in Buffer PB, the dry spin time was extended to 2 min, and the purified DNA was eluted in 30 µL MilliQ water after allowing the water to incubate on the column membranes for 2 min at room temperature. The purified PCR products were then sequenced via Sanger sequencing (Genewiz). The resulting reads were aligned to the reference sequences (unpassaged P99 HA_P99PS and P99 HA_NLPS plasmid sequences) and analyzed for differences.

Generation of recombinant T1864C virus. The P99 HA_NLPS plasmid used to generate the P99 HA_NLPS virus was obtained, and the T1864C point mutation was introduced into the HA plasmid using QuikChange site-directed mutagenesis (Agilent). The T1864C virus was then rescued via transfection of 293T cells with the T1864C HA plasmid and the pPOL1 P99 reverse genetics system, which would allow for virus rescue in a P99 background (27, 28). Briefly, a 15 plasmid rescue system based on pPOL1 and pCAGGS helper plasmids (PB2, PB1, PA, HA, NP, NA, and NS) was used. At 22 hr post-transfection, the transfected 293T cells were injected into 9-11 day old embryonated hens' eggs and incubated for 50 hr at 33° C to generate the initial virus stock. Success of the rescue was determined via plaque assay on MDCK cells. A single plaque was then used to infect eggs at a concentration of 100 PFU/egg and incubated for 48 hr at 33° C to generate the final virus stock. The titer of the stock was determined via plaque assay on MDCK cells and used for subsequent experiments. The presence of the T1864C mutation in the final virus stock was confirmed via Sanger sequencing (Genewiz).

Co-infection of MDCK cells with modified viruses. Triplicate wells of MDCK cells were co-infected at a MOI of 5 PFU/cell for each virus, giving a final MOI of 10 PFU/cell to ensure high levels of co-infection (29). The control co-infections used WT (untagged) and VAR (tagged) viruses with matched HA packaging signals (P99 for both), and the heterologous co-infections used WT viruses carrying mismatched H1N1 packaging signals on HA and VAR viruses carrying matched P99 packaging signals on HA. Inoculations were performed on ice using the WT-VAR virus pairs. After a 45 min incubation period at 4° C to allow for virus attachment, the virus inoculum was removed and the cells were washed 3x with cold PBS to remove unattached virus. Warm media was then added to allow for synchronized virus entry and the cells were incubated at 33° C for 3 hr. After 3 hr, the media was removed from the cells and replaced with media

supplemented with 1M ammonium chloride and HEPES buffer. The absence of TPCK-treated trypsin and the presence of ammonium chloride ensures a single cycle of viral replication. Cells were then incubated at 33° C for an additional 9 hr. Twelve hours p.i., supernatants were harvested, aliquoted, and frozen at -80° C for use in reassortment analyses.

Genotyping virus isolates from co-infected cells. Viruses present in the co-infection supernatants were sampled randomly via plaque-purification on MDCK cells. Well-separated and distinct plaque isolates were sampled into 150 μL PBS, one isolate per PBS aliquot. Twenty-one plaque isolates were picked for each supernatant sample. Depending on the experiment, either two of the three or all three of the triplicate assays were used for genotyping. RNA was extracted from the plaque isolates using the Zymo Research ZR-96 Viral RNA kit following the manufacturer's instructions with the following modification: 40 μL water was used for the elution step. Twelve point eight microliters of RNA was reverse-transcribed using Maxima reverse transcriptase (Fermentas) following the manufacturer's instructions. The synthesized cDNA was then diluted 1:4 in water and used in quantitative PCR (qPCR) with Precision Melt Supermix (Bio-Rad) and primers specific for each of the eight segments of P99 virus, as described previously (12). Briefly, these primers bind to sequences that are identical to both WT and VAR viruses, but the short amplicons produced contain the tagged region of the VAR gene segments (20). qPCR was performed in white, thin-walled, 384-well plates (Bio-Rad) in a CFX384 Real-Time PCR detection system (Bio-Rad). PCR amplification was immediately followed with a melt curve analysis. The conditions of PCR amplification and melt analysis followed the protocol provided with the Precision Melt Supermix. Data were analyzed using Precision Melt Analysis software (Bio-Rad), and WT and VAR cDNA controls were used for data comparison. Thus, the genotype of each segment in each plaque isolate was determined to be either WT or VAR depending on which

control the melt curves clustered with in the software. Genotype data were then analyzed by calculating the percentage of genomes that carried the WT version of each of the eight gene segments. Only reassortant virus isolates were included in the analyses, as parental genotypes could have been produced by singly, rather than co-infected, cells. The means of the resulting data ± 1 standard deviation (S.D.) were then graphed.

Virus growth kinetics. The multi-cycle growth properties of each unpassaged virus were assessed as follows. Triplicate wells of MDCK cells were infected at a MOI of 0.01 PFU/cell alongside the P99 wild-type virus as a control. After incubating for 1 hr at 33° C, virus inoculum was removed and media containing TPCK-treated trypsin was added. Plates were re-incubated at 33° C for the remainder of the experiment. A sample of medium from each well was collected at 1 hr, 12 hr, 24 hr, 48 hr, and 72 hr p.i., stored at -80° C, and subsequently titered via plaque assay on MDCK cells. Mean titers of the three replicates ± 1 S.D. were plotted against time. The limit of detection was 50 PFU/mL.

Acknowledgments

This work was funded in part by the NIAID Centers of Excellence in Influenza Research and Surveillance (CEIRS), contract number HHSN272201400004C to A.C.L. and J.S., and by R01 grants AI125268 and AI099000 to A.C.L.

Figures

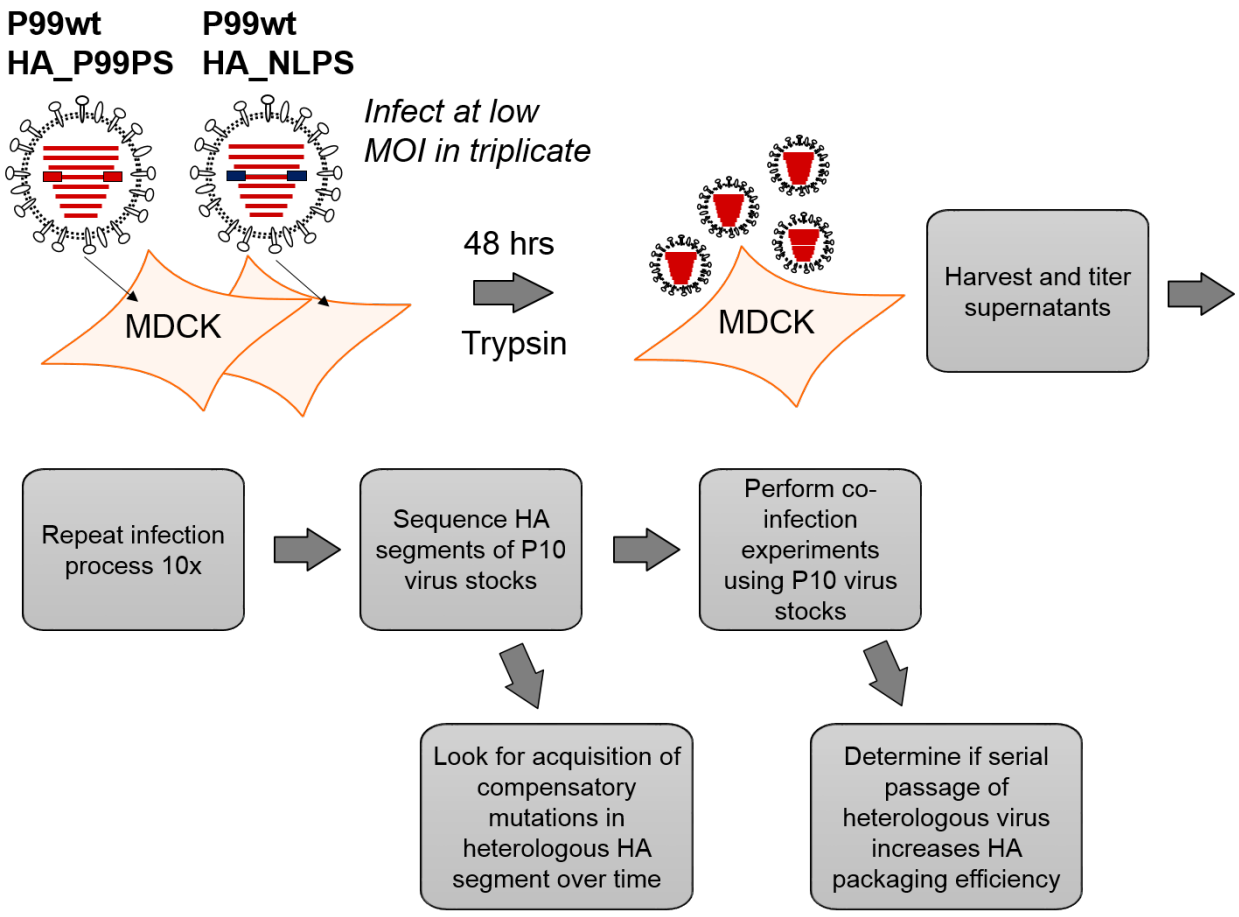

Fig. 1. Schematic of serial passage of viruses with modified HA packaging signals. WT P99 HA_P99PS and P99 HA_NLPS viruses were serially passaged ten times in triplicate in MDCK cells at low MOI in the presence of TPCK-treated trypsin for 48 hr at 33° C. Cells were infected either with P99 HA_P99PS or P99 HA_NLPS. Passage 10 (P10) virus stocks were then sequenced and analyzed for compensatory mutations in the HA segment. P10 virus stocks were also used in co-infection experiments in order to determine if serial passage of an HA segment carrying heterologous packaging signals increases HA packaging efficiency.

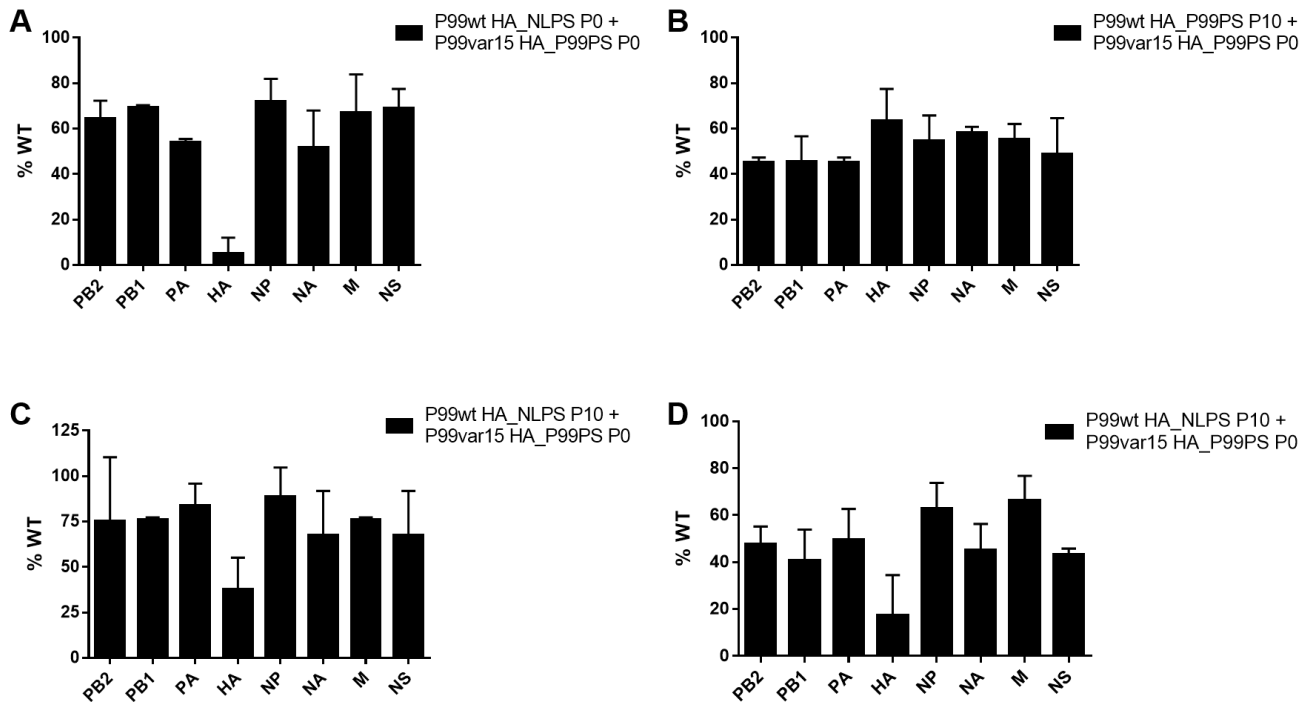

Fig. 2. Serial passage of viruses carrying heterologous H1 packaging signals on HA did not increase HA packaging efficiency into H3N2 viruses. P99wt HA_P99PS and P99wt HA_NLPS viruses were serially passaged ten times in MDCK cells (P10). The P99var15 HA_P99PS virus was not passaged (P0). MDCK cells were then co-infected with these WT-VAR virus pairs and co-infection supernatants were harvested at 12 hr p.i. Virus isolates were subsequently genotyped using HRM analysis. The percentage of virus isolates that contained a WT segment for each of the eight IAV segments is plotted on the Y-axis. (A) Unpassaged (P0) P99wt HA_NLPS + unpassaged (P0) P99var15 HA_P99PS viruses, N = 2; (B) Passage 10 (P10) P99wt HA_P99PS + unpassaged (P0) P99var15 HA_P99PS viruses, N = 2; (C and D) Passage 10 (P10) P99wt HA_NLPS + unpassaged (P0) P99var15 HA_P99PS viruses, N = 2. For (C and D), two different unpassaged (P0) P99var15 HA_P99PS virus stocks were used. All data are shown as mean with SD.

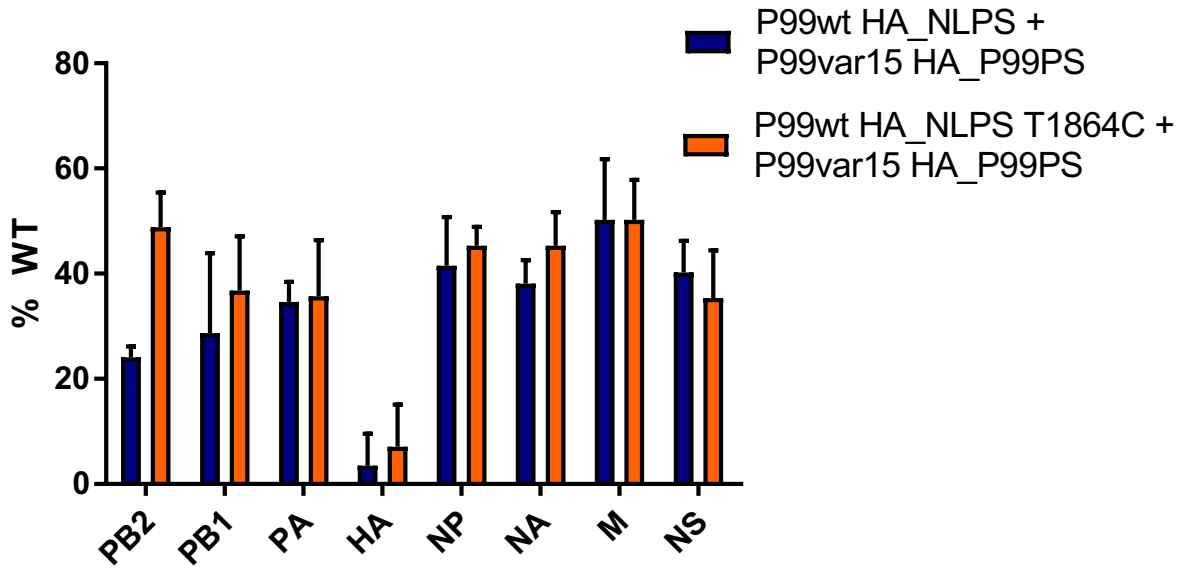

Fig. 3. An unpassaged recombinant virus containing the T1864C mutation did not demonstrate an increase in HA packaging efficiency. MDCK cells were co-infected in triplicate with either P99wt HA_NLPS + P99var15 HA_P99PS viruses as a control (navy bars; same conditions as in **Fig. 2a**) or P99wt HA_NLPS T1864C + P99var15 HA_P99PS viruses (orange bars; the WT HA segment contained the introduced T1864C mutation). Co-infection supernatants harvested at 12 hr p.i. were then plaque-purified on MDCK cells and virus isolates were genotyped via HRM analysis. The percentage of virus isolates that contained a WT segment for each of the eight IAV segments is plotted on the Y-axis. Data are shown as mean with SD; N = 3.

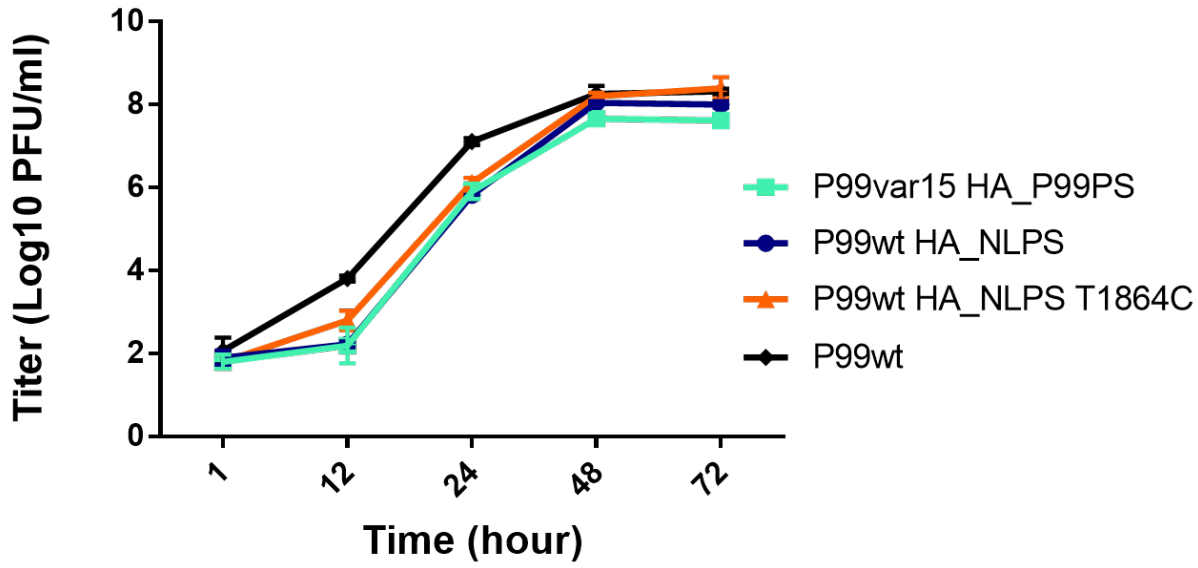

Fig. 4. The presence of the T1864C mutation did not alter IAV growth kinetics. Multi-cycle growth of each unpassaged virus was assessed by infecting triplicate wells of MDCK cells at a MOI of 0.01 PFU/cell alongside the P99 wild-type control virus (P99wt). Samples were taken at 1 hr, 12 hr, 24 hr, 48 hr, and 72 hr p.i. and titered via plaque assay on MDCK cells. Mean titers of the three replicates ± 1 S.D. were plotted against time. The limit of detection was 50 PFU/mL.

Tables

Table 1. Mutations acquired in the HA_NLPS segment after 10 passages in MDCK cells[1]

Lineage	*3' or 5' PS*	*Mutation*[2]	*Partial or Full*[3]
1	5'	T1864C	Full
2	5'	T1864C	Full
3	5'	T1864C	Partial
1	3'	C54T	Partial
2	3'	C54T	Partial
3	3'	C54T	Partial
3	5'	A1848C	Partial

[1]Compared to the unpassaged HA_NLPS segment

[2]Numbering includes grafted 3' and 5' PS regions on NL/09 HA ORF

[3]As determined by Sanger sequencing

Table 2. Alignment of identified T1864C mutation region with other H1 influenza A viruses

Virus name	*Sequence*
A/PR8/34	CTT TTG GTC TCC CTG GGG GCA
A/WSN/33	CTT TTG GTC TCC CTG GGG GCA
A/Netherlands/602/2009	CTG GTA GTC TCC CTG GGG GCA
A/Panama/2007/99 carrying NL/09 PS[1] on HA	CTG GTA GTC CCC CTG GGG GCA

[1]PS = packaging signals

References

1. **Shaw ML, Palese P.** 2013. Orthomyxoviridae, p 1151–1185. *In* Knipe D, Howley P (ed), Fields Virology, vol 1. Lippincott Williams & Wilkins, Philadelphia, PA.
2. **Steinhauer DA, Wharton SA, Skehel JJ, Wiley DC.** 1995. Studies of the membrane fusion activities of fusion peptide mutants of influenza virus hemagglutinin. J Virol **69:**6643-6651.
3. **Holmes EC, Ghedin E, Miller N, Taylor J, Bao Y, St George K, Grenfell BT, Salzberg SL, Fraser CM, Lipman DJ, Taubenberger JK.** 2005. Whole-Genome Analysis of Human Influenza A Virus Reveals Multiple Persistent Lineages and Reassortment among Recent H3N2 Viruses. PLoS Biol **3:**e300.
4. **Westgeest KB, Russell CA, Lin X, Spronken MI, Bestebroer TM, Bahl J, van Beek R, Skepner E, Halpin RA, de Jong JC, Rimmelzwaan GF, Osterhaus AD, Smith DJ, Wentworth DE, Fouchier RA, de Graaf M.** 2014. Genomewide analysis of reassortment and evolution of human influenza A(H3N2) viruses circulating between 1968 and 2011. J Virol **88:**2844-2857.
5. **Kawaoka Y, Krauss S, Webster RG.** 1989. Avian-to-human transmission of the PB1 gene of influenza A viruses in the 1957 and 1968 pandemics. J Virol **63:**4603-4608.
6. **Garten RJ, Davis CT, Russell CA, Shu B, Lindstrom S, Balish A, Sessions WM, Xu X, Skepner E, Deyde V, Okomo-Adhiambo M, Gubareva L, Barnes J, Smith CB, Emery SL, Hillman MJ, Rivailler P, Smagala J, de Graaf M, Burke DF, Fouchier RAM, Pappas C, Alpuche-Aranda CM, López-Gatell H, Olivera H, López I, Myers CA, Faix D, Blair PJ, Yu C, Keene KM, Dotson PD, Boxrud D, Sambol AR, Abid SH, St. George K, Bannerman T, Moore AL, Stringer DJ, Blevins P, Demmler-Harrison GJ, Ginsberg M, Kriner P, Waterman S, Smole S, Guevara HF, Belongia EA, Clark**

PA, Beatrice ST, Donis R, et al. 2009. Antigenic and Genetic Characteristics of Swine-Origin 2009 A(H1N1) Influenza Viruses Circulating in Humans. Science **325:**197-201.

7. **Smith GJD, Vijaykrishna D, Bahl J, Lycett SJ, Worobey M, Pybus OG, Ma SK, Cheung CL, Raghwani J, Bhatt S, Peiris JSM, Guan Y, Rambaut A.** 2009. Origins and evolutionary genomics of the 2009 swine-origin H1N1 influenza A epidemic. Nature **459:**1122-1125.
8. **Lubeck MD, Palese P, Schulman JL.** 1979. Nonrandom association of parental genes in influenza A virus recombinants. Virology **95:**269-274.
9. **Greenbaum BD, Li OT, Poon LL, Levine AJ, Rabadan R.** 2012. Viral reassortment as an information exchange between viral segments. Proc Natl Acad Sci U S A **109:**3341-3346.
10. **Essere B, Yver M, Gavazzi C, Terrier O, Isel C, Fournier E, Giroux F, Textoris J, Julien T, Socratous C, Rosa-Calatrava M, Lina B, Marquet R, Moules V.** 2013. Critical role of segment-specific packaging signals in genetic reassortment of influenza A viruses. Proc Natl Acad Sci U S A **110:**E3840-E3848.
11. **Baker SF, Nogales A, Finch C, Tuffy KM, Domm W, Perez DR, Topham DJ, Martinez-Sobrido L.** 2014. Influenza A and B Virus Intertypic Reassortment through Compatible Viral Packaging Signals. J Virol **88:**10778-10791.
12. **White MC, Steel J, Lowen AC.** 2017. Heterologous Packaging Signals on Segment 4, but Not Segment 6 or Segment 8, Limit Influenza A Virus Reassortment. J Virol **91**.
13. **Li C, Hatta M, Watanabe S, Neumann G, Kawaoka Y.** 2008. Compatibility among polymerase subunit proteins is a restricting factor in reassortment between equine H7N7 and human H3N2 influenza viruses. J Virol **82:**11880-11888.

14. **Hatta M, Halfmann P, Wells K, Kawaoka Y.** 2002. Human influenza a viral genes responsible for the restriction of its replication in duck intestine. Virology **295:**250-255.

15. **Shelton H, Smith M, Hartgroves L, Stilwell P, Roberts K, Johnson B, Barclay W.** 2012. An influenza reassortant with polymerase of pH1N1 and NS gene of H3N2 influenza A virus is attenuated in vivo. J Gen Virol **93:**998-1006.

16. **Goto H, Muramoto Y, Noda T, Kawaoka Y.** 2013. The Genome-Packaging Signal of the Influenza A Virus Genome Comprises a Genome Incorporation Signal and a Genome-Bundling Signal. J Virol **87:**11316-11322.

17. **Noda T, Sugita Y, Aoyama K, Hirase A, Kawakami E, Miyazawa A, Sagara H, Kawaoka Y.** 2012. Three-dimensional analysis of ribonucleoprotein complexes in influenza A virus. Nat Commun **3:**639.

18. **Fournier E, Moules V, Essere B, Paillart JC, Sirbat JD, Cavalier A, Rolland JP, Thomas D, Lina B, Isel C, Marquet R.** 2012. Interaction network linking the human H3N2 influenza A virus genomic RNA segments. Vaccine **30:**7359-7367.

19. **Watanabe T, Watanabe S, Noda T, Fujii Y, Kawaoka Y.** 2003. Exploitation of nucleic acid packaging signals to generate a novel influenza virus-based vector stably expressing two foreign genes. J Virol **77:**10575-10583.

20. **Marshall N, Priyamvada L, Ende Z, Steel J, Lowen AC.** 2013. Influenza virus reassortment occurs with high frequency in the absence of segment mismatch. PLoS Pathog **9:**e1003421.

21. **Marsh GA, Hatami R, Palese P.** 2007. Specific residues of the influenza A virus hemagglutinin viral RNA are important for efficient packaging into budding virions. J Virol **81:**9727-9736.

22. **McKimm-Breschkin JL, Rootes C, Mohr PG, Barrett S, Streltsov VA.** 2012. In vitro passaging of a pandemic H1N1/09 virus selects for viruses with neuraminidase mutations conferring high-level resistance to oseltamivir and peramivir, but not to zanamivir. J Antimicrob Chemother **67:**1874-1883.

23. **Wormann X, Lesch M, Welke RW, Okonechnikov K, Abdurishid M, Sieben C, Geissner A, Brinkmann V, Kastner M, Karner A, Zhu R, Hinterdorfer P, Anish C, Seeberger PH, Herrmann A, Meyer TF, Karlas A.** 2016. Genetic characterization of an adapted pandemic 2009 H1N1 influenza virus that reveals improved replication rates in human lung epithelial cells. Virology **492:**118-129.

24. **Schimmel PR, Flory PJ.** 1968. Conformational energies and configurational statistics of copolypeptides containing L-proline. J Mol Biol **34:**105-120.

25. **Cordes FS, Bright JN, Sansom MS.** 2002. Proline-induced distortions of transmembrane helices. J Mol Biol **323:**951-960.

26. **Li SC, Goto NK, Williams KA, Deber CM.** 1996. Alpha-helical, but not beta-sheet, propensity of proline is determined by peptide environment. Proc Natl Acad Sci U S A **93:**6676-6681.

27. **Fodor E, Devenish L, Engelhardt OG, Palese P, Brownlee GG, García-Sastre A.** 1999. Rescue of Influenza A Virus from Recombinant DNA. J Virol **73:**9679-9682.

28. **Steel J, Lowen AC, Mubareka S, Palese P.** 2009. Transmission of influenza virus in a mammalian host is increased by PB2 amino acids 627K or 627E/701N. PLoS Pathog **5:**e1000252.

29. **Fonville JM, Marshall N, Tao H, Steel J, Lowen AC.** 2015. Influenza Virus Reassortment Is Enhanced by Semi-infectious Particles but Can Be Suppressed by Defective Interfering Particles. PLoS Pathog **11:**e1005204.

Chapter IV: H5N8 and H7N9 Packaging Signals Constrain HA Reassortment with a Seasonal H3N2 Influenza A Virus

Maria C. White[1], Hui Tao[1], John Steel[1], and Anice C. Lowen[1]

[1]Department of Microbiology and Immunology, Emory University School of Medicine, Atlanta, GA, USA

Published in *PNAS*, 2019, 116(10):4611-4618, PMID: 30760600

All figures were generated by MCW with input from ACL, with the exceptions of Figure 2, Figure 3, and Figure S6, in which sample processing was performed by HT

Abstract

Influenza A virus (IAV) has a segmented genome, which i) allows for exchange of gene segments in co-infected cells, termed reassortment, and ii) necessitates a selective packaging mechanism to ensure incorporation of a complete set of segments into virus particles. Packaging signals serve as segment identifiers and enable segment-specific packaging. We have previously shown that packaging signals limit reassortment between heterologous IAV strains in a segment-dependent manner. Here, we evaluated the extent to which packaging signals prevent reassortment events that would raise concern for pandemic emergence. Specifically, we tested the compatibility of hemagglutinin (HA) packaging signals from H5N8 and H7N9 avian IAVs with a human seasonal H3N2 IAV. By evaluating reassortment outcomes, we demonstrate that HA segments carrying H5 or H7 packaging signals are significantly disfavored for incorporation into a human H3N2 virus in both cell culture and a guinea pig model. However, incorporation of the heterologous HAs was not excluded fully, and variants with heterologous HA packaging signals were detected at low levels in vivo, including in naïve contact animals. This work indicates that the likelihood of reassortment between human seasonal IAV and avian IAV is reduced by divergence in the RNA packaging signals of the HA segment. These findings offer important insight into the molecular mechanisms governing IAV emergence and inform efforts to estimate the risks posed by H7N9 and H5N8 subtype avian IAVs.

Significance

Influenza A viruses (IAV) can exchange genetic material in co-infected cells in a process termed reassortment. The last three IAV pandemic strains arose from reassortment events involving human and non-human IAVs. Because introduction of the hemagglutinin (HA) gene from a non-

human virus is required for a pandemic, we addressed the compatibility of human and avian IAV. We show that sequence differences between human and avian HA genes limit the potential for reassortment. However, human IAV still incorporated heterologous HA genes at a low level in co-infected animals. This observed low level of incorporation could become significant if reassortant viruses had a fitness advantage within the host, such as resistance to pre-existing immunity, and highlights the continued need for IAV surveillance.

Introduction

Influenza A virus (IAV) exhibits a broad host range, including wild birds, poultry, and humans (1). The segmented nature of the IAV genome allows for gene segments to be exchanged through reassortment in co-infected cells (2). This process contributes to both pandemic and epidemic influenza; notably, reassortment involving IAVs adapted to differing host species played a critical role in the formation of the last three IAV pandemic strains (3-5). Antigenic novelty is a key feature of IAV pandemics and is achieved through the introduction of a novel HA, which can be facilitated by reassortment. As such, reassortment of human IAV with avian IAV presents a pandemic risk. Zoonotic transmission of avian IAVs of the H5N1 and H7N9 subtypes has caused multiple outbreaks of severe disease in humans over the last two decades (6-8). H5N8 subtype viruses, while yet to cause disease in humans, derive the HA segment from the influenza A/goose/Guangdong/1/96 (H5N1) lineage associated with zoonosis (9). Since emergence and global expansion of the H5Nx lineage in 2014, this poultry-adapted H5 HA has reassorted extensively with IAVs circulating in wild waterfowl and the resultant viruses have caused major outbreaks in poultry (10-12). The exposure of humans at the animal-human interface to H5Nx

and H7N9 viruses engenders a risk of avian-human IAV reassortment. Importantly, however, the genetic compatibility of these avian viruses with human seasonal IAVs remains poorly understood.

Here we sought to address this knowledge gap by evaluating the compatibility of H5N8 and H7N9 genetic components with those of a seasonal H3N2 virus, focusing on the RNA packaging signal regions of the HA segment. IAV packaging signals direct the incorporation of the eight gene segments into virus particles, and have previously been shown by us and others to influence reassortment outcomes between different IAV strains (13-15). In this study, we assessed the compatibility of HA packaging signals originating from H5N8 and H7N9 subtype IAVs with a seasonal H3N2 strain background. We isolated the effects of the RNA packaging signals by generating chimeric viruses that retained the coding capacity of the seasonal H3N2 strain but included the terminal packaging signal regions derived from H5 or H7 HA segments. We then determined the frequency with which HA segments carrying homologous vs heterologous packaging signals were taken up during reassortment. Our data show that H5N8 and H7N9 HA packaging signals (HA_H5PS and HA_H7PS, respectively) are disfavored for reassortment into the H3N2 strain background to varying degrees in both MDCK cells and a guinea pig model. In guinea pigs co-infected with HA_H3PS plus HA_H5PS, HA segments carrying H5N8 packaging signals were transmitted to a subset of naïve contacts, while in animals co-inoculated with HA_H3PS plus HA_H7PS viruses, HA segments with the H7N9 packaging signals showed very limited transfer to contacts. These data indicate that the packaging signals of H5 and H7 HA segments constrain reassortment with a seasonal H3N2 virus. Importantly, however, exclusion of heterologous packaging signals was not complete, suggesting that reassortment of H5 or H7 HA segments into seasonal H3N2 backgrounds is likely to proceed at an appreciable level in co-

infected hosts. Incompatibilities at the RNA level were also not sufficiently strong to fully prevent propagation of these reassortants to contacts.

Results

Chimeric HA segments for quantifying mismatch among packaging signals. To measure constraints on reassortment imposed at the level of packaging, we generated a panel of HA segments that differed only in the packaging signals. Each segment encoded the influenza A/Panama/2007/99 (H3N2; Pan/99) HA protein but carried terminal packaging signals from influenza A/mute_swan/Croatia/70/2016 (H5N8), influenza A/Anhui/1/2013 (H7N9), or Pan/99 viruses (*SI Appendix*, Fig. S1 A-D). These packaging signals were introduced upstream and downstream of the ORF, effectively lengthening the untranslated regions (UTRs) of the HA segments. To disrupt native packaging function in the Pan/99 ORF, we silently mutated the terminal 20 codons at the 5' and 3' ends, as in (16). As a control to verify disruption of native packaging function, we also produced a Pan/99 HA segment with these silent mutations in the ORF and no introduced packaging signals, termed PSmut_HA (*SI Appendix*, Fig. S1 E).

We generated virus pairs using our Pan/99 WT-VAR system, designed to track the origins of segments in reassortant progeny (15, 17) (*SI Appendix*, Fig. S2 A). The VAR virus contains silent genetic tags, while the WT virus is untagged. We allowed the PSmut_HA virus to co-infect MDCK cells with a Pan/99 VAR virus containing intact packaging signals on HA and measured the frequency with which each HA segment was incorporated into reassortant progeny by screening plaque isolates. Results showed that packaging of the PSmut_HA segment was significantly disfavored, confirming disruption of ORF packaging function (*SI Appendix*, Fig. S2

B and C). We also confirmed that the PSmut_HA segments were replicated efficiently by the viral polymerase (*SI Appendix*, Fig. S2 D and E).

Viruses with modified packaging signals did not differ in growth. To determine if the introduced packaging signals altered viral growth, we first analyzed single cycle replication in MDCK cells with our HA segment-modified viruses (*SI Appendix*, Fig. S1 A-D) and Pan/99 virus as a control. Over the course of 24 h, all viruses displayed similar growth kinetics, indicating that the packaging signal modifications did not suppress virus growth (*SI Appendix*, Fig. S3 A). We next analyzed multicycle growth of a subset of these viruses in guinea pigs. Growth of all viruses was similar in vivo, further substantiating that the introduced packaging signal modifications had minimal impact on virus growth (*SI Appendix*, Fig. S3 B).

Chimeric Pan/99 HA segments were replicated efficiently. To assess replication of the modified HA segments within co-infected cells, we used a RT droplet digital PCR (ddPCR) assay to enumerate total copies of each of the HA segments present in co-infected cells and matched supernatants. Replication of the HA segments carrying Pan/99 packaging signals (HA_H3PS) and H7N9 packaging signals (HA_H7PS) were equal over time except at the 10 h time point, where more of the HA_H7PS segment was detected (*SI Appendix*, Fig. S4). Replication of the HA_H3PS segment was slightly more efficient than replication of the HA segment carrying H5N8 packaging signals (HA_H5PS) (*SI Appendix*, Fig. S4).

HA segments carrying H5N8 or H7N9 packaging signals were disfavored for incorporation into a H3N2 background. To determine if heterologous H5 or H7 HA packaging signals limited reassortment, we co-infected MDCK cells with WT:VAR virus pairs that differed only in the packaging signal regions on the HA segment (Fig. 1 A-C). After a single cycle of replication, we harvested the supernatants and genotyped reassortant progeny. We performed co-infections

under two different conditions for the HA_H3PS plus HA_H5PS virus pairing to account for the differences in HA segment replication observed in Fig. S4. Under all conditions tested, the heterologous HA_H5PS and HA_H7PS segments were significantly underrepresented in reassortant progeny (Fig. 1 D-F). However, in co-infections performed in parallel under 1:1 WT:VAR input conditions, the HA_H7PS segment was packaged more frequently than the HA_H5PS segment (Fig. 1 D and F). Taken together, these data suggest that HA segments carrying H5N8 or H7N9 packaging signals are not efficiently incorporated into a human seasonal H3N2 background, but that H7N9 HA packaging signals exhibit a lower incorporation barrier.

HA segments carrying H5N8 or H7N9 packaging signals were not incorporated as efficiently as homologous segments in co-infected guinea pigs. To determine if the phenotypes observed in cell culture were also observed in vivo, we co-infected female guinea pigs with our modified viruses as shown in Fig. 1 B and C. At 16 h post-inoculation (p.i.), a naïve guinea pig was co-caged with each inoculated animal. Nasal lavage was performed daily over a 7 d time course to determine virus titers. Viruses grew in all inoculated animals and all contacts contracted infection (*SI Appendix*, Fig. S5). Nasal washes from each inoculated animal at 2 d and 4 d p.i. were processed for reassortment analysis. Parental VAR genotypes were more abundant than parental WT genotypes in the inoculated animals despite slight overrepresentation of WT virus in the inocula (Fig. 2 and *SI Appendix*, Fig. S6). This observation suggests that the heterologous packaging signals on the HA of both WT viruses hindered virus propagation in vivo when in competition with a better-matched (VAR) virus. Analysis of the reassortant progeny revealed that, at both time points, the HA_H5PS segment was packaged significantly less frequently than the HA_H3PS segment (Fig. 3 A-D), confirming the results obtained in cell culture. Results for the HA_H3PS plus HA_H7PS co-infection showed there was no preference

for either HA segment at 2 d p.i., but 4 d p.i. revealed a significant preference for HA_H3PS (Fig. 3 E-H). Thus, reassortment analyses again supported the results obtained in cell culture. In contrast to examination of viral growth during single infections in cell culture and in vivo, however, the predominance of parental VAR genotypes in vivo under co-infection conditions suggested that the presence of heterologous packaging signals on HA is detrimental to propagation when in competition with a virus that carries homologous packaging signals on HA.

HA segments carrying H5N8, but not H7N9, packaging signals were transmitted. Next, we evaluated which HA segments were transmitted to the naïve cage mates and how long these HA segments persisted in the host over time. We used primers specific for the 3' HA packaging signal region in a RT ddPCR assay to determine copy numbers of each modified HA segment over time in the nasal washings of contact animals. We found that, in all eight contact animals, the HA_H3PS segment was abundant and copy numbers correlated with infectious titers (Fig. 4 A and C). We were able to robustly detect HA_H5PS in two of the four exposed guinea pigs at multiple time points and, in one animal, total copies of HA_H5PS exceeded the total copies of HA_H3PS at 5 d p.i. (Fig. 4B). In contrast, robust detection of the HA_H7PS segment was not observed in any of the exposed guinea pigs (Fig. 4D), suggesting that neither the Pan/99 HA_H7PS parental virus nor reassortant viruses carrying the HA_H7PS segment were shed at sufficient levels to transmit in the context of a contact transmission model. We validated these findings by repeating the transmission experiment a second time. In this second experiment, fresh aliquots of the same WT:VAR mixtures analyzed in Fig. 2 and Fig. S6 were used for inoculation. In all eight inoculated animals, both WT and VAR HA segments were detected at 2 d p.i. but, as before, the VAR HA_H3PS predominated (*SI Appendix*, Fig. S7 A-D). In all eight contact animals the HA_H3PS segment was abundant over time, with kinetics similar to the first

experiment (*SI Appendix*, Fig. S7 E and G). We were again able to robustly detect HA_H5PS in two of the four exposed guinea pigs at multiple time points (*SI Appendix*, Fig. S7 F) and observed minimal HA_H7PS transfer to contacts with no robust replication (*SI Appendix*, Fig. S7 H). Thus, results of this second transmission experiment closely matched the results of the first experiment. The data suggest that HA segments carrying H5N8 or H7N9 packaging signals are not efficiently transmitted within a human seasonal H3N2 background, but that H5N8 HA packaging signals functioned slightly better than the H7N9 packaging signals in this regard.

HA segments carrying H5N8 or H7N9 packaging signals were present less frequently than Pan/99 HA segments in virus particles. Our reassortment data obtained from co-infected cells clearly indicated that, when in direct competition, HA_H3PS was more efficiently incorporated into the H3N2 background than HA segments carrying either H5 or H7 packaging signals. To test the extent to which competition during genome assembly contributes to this phenotype, we evaluated the efficiency with which each HA segment was packaged into particles during standard propagation of the individual viruses. Thus, we concentrated HA_H3PS, HA_H5PS, HA_H7PS, and control Pan/99 viruses grown in eggs through a sucrose cushion and used RT ddPCR to measure HA segment copy numbers in the resultant virus preparations. We saw no significant difference between HA segment copy number in the HA_H3PS virus preparation compared to the control Pan/99 virus with no packaging signal modifications (Fig. 5 A-B). In contrast, the HA segment in the HA_H5PS virus was present significantly less frequently. The HA of the HA_H7PS virus was also low compared to the Pan/99 control, but significance varied with the primer set used (Fig. 5 A-B). These data suggest that, even in the absence of competition between HA segments within a co-infected cell, the presence of H5 or H7 packaging signals on HA lowers packaging efficiency into a Pan/99 virus. We then extended these analyses

to include all eight IAV segments and noted modest packaging defects for a handful of non-HA segments (Fig. 5C).

Discussion

This study aimed to determine HA packaging signal compatibility between a human H3N2 virus and zoonotic H5N8 and H7N9 viruses. We previously showed that HA segments carrying homologous H3N2 packaging signals were significantly preferred for packaging into H3N2 viruses over HA segments carrying heterologous H1N1 packaging signals (15). We sought to test this concept for other IAV strain pairings, particularly those which carry pandemic potential. We isolated the effects of packaging signals on reassortment by designing virus pairs that retained H3N2 protein coding capacity but differed in the packaging signals on the HA segment. Our results showed that HA segments carrying homologous H3N2 packaging signals were taken up into reassortant viruses significantly more frequently than HA segments carrying H5N8 or H7N9 packaging signals, extending previous observations of packaging signal constraint on reassortment to viruses that present a pandemic risk (13, 14). This phenotype was observed in both MDCK cells and guinea pigs. Importantly, onward transmission of HA segments carrying heterologous packaging signals occurred with low efficiency from co-infected guinea pigs, underlining the fitness implications of packaging signal mismatch. It is noteworthy, however, that HA segments carrying H5 packaging signals were consistently detected in a subset of the naïve contacts of co-infected animals, while minimal transfer of HA_H7PS segments to contacts was detected. These findings suggest that H5 packaging signals are sufficiently compatible with H3N2 viruses to allow a low level of transmission.

Reassortment can facilitate host species transfer of IAVs, and reassortment between human and avian IAV is of particular concern for the emergence of novel pandemic strains (18). Areas such as backyard poultry farms and live bird markets, where humans are in close contact with poultry, provide an environment where human and avian IAVs could co-infect and undergo reassortment (19). We previously showed that reassortment occurs readily when co-infecting IAVs are highly homologous (17). Constraints on reassortment can arise, however, due to incompatibilities between heterologous viruses at both the RNA and protein levels (reviewed in (20)). This phenomenon of segment mismatch is complex, owing to negative epistasis involving multiple components simultaneously. Our data show that HA packaging signal mismatch disfavors, but does not completely prevent, the formation of genotypes containing HA H5N8 or H7N9 packaging signals. The production of these heterologous genotypes at low levels could be significant in contexts where HA reassortant viruses possess a fitness advantage over other variants, such as in hosts with pre-existing immunity. The extent of HA protein mismatch between human and avian IAV would offer additional insights into the potential for reassortants to be propagated once formed.

Notably, we observed a higher incorporation barrier for HA segments carrying H5 compared to H7 packaging signals. A possible explanation for this observation is the increased phylogenetic relatedness of H3 and H7 subtypes. IAV HA genes are divided phylogenetically into two major groups (21). Group 1 includes H1 and H5, while group 2 includes H3 and H7. Given our current and past findings using H1, H3, H5, and H7 packaging signals, it is tempting to speculate that an H3N2 virus such as Pan/99 would more readily incorporate H7 packaging signals than H1 or H5 packaging signals due to higher HA sequence conservation. However, more HA subtype pairings would be needed to robustly test this hypothesis. The nucleotide identity between the H3N2 vs

H5N8 and H3N2 vs H7N9 IAV strains used in this study are 52.9% and 56.6%, respectively, in the HA packaging signal regions as defined herein. While H3 and H7 share slightly higher identity than H3 and H5 in these regions, the significance of this difference is difficult to predict given the lack of knowledge surrounding which nucleotides are important for mediating HA segment packaging.

In our animal study, despite there being more WT (heterologous HA_PS) than VAR (homologous HA_PS) virus in both of the co-infection inocula, the VAR virus strongly predominated over WT in nasal lavage samples. This phenotype was most striking in the HA_H3PS plus HA_H7PS inoculated animals, where the parental VAR isolates also outnumbered reassortants at 2 d p.i. The relative levels of WT, VAR, and reassortant genotypes detected suggest linkage among the eight segments is maintained early during infection by a relative lack of reassortment. In this situation, the VAR virus would be expected to maintain a fitness advantage because the HA segment in the VAR system carries homologous packaging signals. This outgrowth of VAR virus in the HA_H3PS plus HA_H7PS inoculated animals may have contributed to the lack of a packaging phenotype at 2 d p.i. because a reduced number of reassortant isolates were available for analysis of HA packaging preference.

Our reassortment data demonstrate that, when in competition within co-infected cells, the HA segment carrying heterologous packaging signals was usually excluded in favor of the HA segment carrying the better-matched, homologous, packaging signals. Corresponding packaging defects were observed when the heterologous HA segment was the only HA segment available for packaging, and in both cases the defect was more pronounced for HA_H5PS compared to HA_H7PS. Notably, however, the frequency of incorporation of the heterologous segments was lower in reassortant progeny viruses compared to clonal virus preparations, suggesting that

competition between HA segments within co-infected cells exacerbated the packaging defects of HA_H5PS and HA_H7PS segments. Of note, we did not observe a difference in HA segment frequency in the concentrated HA_H3PS virus preparation compared to the control Pan/99 virus preparation, suggesting that the artificial lengthening of the HA_PS segments and the accompanying silent mutations did not disrupt HA packaging efficiency.

Given the relatively low incorporation of HA segments into virions, we were somewhat surprised by the lack of a growth defect of the HA_H5PS and HA_H7PS viruses compared to the HA_H3PS virus. The lack of detectable growth deficits may be attributable to the relatively small effect of the introduced sequences on packaging efficiency. In virions, the reduction in packaging of HA was approximately 2-fold for the HA_H5PS segment and 1.3-fold for the HA_H7PS segment. During growth under single cycle conditions in cell culture or from a relatively high dose in vivo these reductions in packaging efficiency may not be strong enough to markedly affect viral growth.

Limitations of our study include the absence of protein mismatch and the lack of pre-existing immunity in our animal model. In order to isolate the effects of packaging signal mismatch on reassortment, we kept all proteins identical. In a natural setting, both the packaging signals and the proteins of the co-infecting viruses would differ and could constrain reassortment. Additionally, pre-existing immunity to IAV is widespread in the human population, from natural infection and/or vaccination (22, 23). Our animal model does not recapitulate the immunological environment that co-infecting viruses would encounter in a natural host and pre-existing immunity can play a major role driving the emergence of novel IAV reassortants (24, 25).

To date, the locations of the packaging signals on the eight IAV segments have been mapped largely within an H1N1 (WSN) virus (reviewed in (26)). We used a conservative estimate of the

packaging signals determined for the H1 HA when designing our chimeric HA segments (27). Results obtained with the PSmut_HA segment suggest that the mutation strategy employed to disrupt native packaging function of the Pan/99 HA ORF did indeed target the H3 packaging signals. The residual level of incorporation of the PSmut_HA (~14%) is likely attributable to the presence of wild type Pan/99 UTRs, which were left intact and have been shown to be involved in packaging in conjunction with the terminal coding regions (28, 29). It is also possible that sequences internal to the introduced mutations contribute to packaging.

A current gap in our knowledge of IAV genome incorporation relates to the network of interactions formed among the segments during the assembly process. During virus assembly, the eight segments are arranged into a "7+1" pattern, with one central segment surrounded by seven outer segments (30, 31). However, the identity of the segments in this pattern, which specific segments interact, and at what point during the viral life cycle the segments are bundled together, remain unclear. Further investigation of these points will help clarify not only the packaging process but also the role that packaging signal divergence plays in this process.

In summary, this work indicates that the likelihood of reassortment between human seasonal IAV and avian IAV is reduced by divergence in the RNA packaging signals of the HA segment. Nevertheless, HA segments carrying H5N8 or H7N9 packaging signals were incorporated into H3N2 viruses at a low level and, in the case of H5N8 packaging signals, propagated sufficiently in co-infected hosts to allow transmission to contact animals. These data will help to inform the reassortment potential of human and zoonotic IAV.

Materials and Methods

Design of chimeric HA segments and virus generation. Chimeric HA segments were designed as described previously (15, 16). Briefly, the introduced 3' and 5' packaging signal regions consisted of 136 nt derived from influenza A/mute_swan/Croatia/70/2016 (H5N8), influenza A/Anhui/1/2013 (H7N9), or Pan/99 (H3N2) HA segments. All chimeric segments and the PSmut_HA carried synonymous changes throughout 60 nucleotide regions adjacent to the start and stop codons. The PSmut_HA segment lacked introduced packaging signals. Viruses containing these modified HA segments were rescued in either a WT or VAR Pan/99 background as described previously (15). Our WT-VAR system outlined in (17) consists of Pan/99 virus pairs that are either tagged with 1-6 silent mutations in each of the eight IAV segments (VAR) or untagged (WT). Genotyping can then be achieved by detecting the presence or absence of these mutations using high resolution melt (HRM) analysis (32). HRM primers used can be found in *SI Appendix*, Table S1.

Virus growth. MDCK cells were inoculated at a multiplicity of infection (MOI) of 5 PFU/cell in triplicate. Single cycle replication conditions were achieved with ammonium chloride addition at 3 h p.i. Supernatants were sampled at 1, 4, 8, 12, 16, and 24 h p.i. and titered via plaque assay on MDCK cells. Guinea pigs were inoculated with 5×10^5 PFU of virus, 4 animals per virus. Nasal lavage was performed daily on day 1 through day 5 p.i. and samples were titered via plaque assay on MDCK cells.

Co-infection of MDCK cells and reassortment analysis. MDCK cells were co-infected with WT-VAR virus pairs in triplicate (unless otherwise stated) as described previously (15). Briefly, an MOI of 10 PFU/cell for 1:1 WT:VAR infections was used to ensure high levels of co-infection (33), and virus replication was limited to a single cycle with ammonium chloride. Supernatants were harvested at 12 h p.i. and virus isolates were obtained by plaque-purification

on MDCK cells. For each sample, 21 plaques were picked randomly and genotyped as described previously (15). Briefly, quantitative PCR targeting each of the eight segments was performed and HRM analysis of amplicons was used to determine the parental origin of each segment in a given viral isolate.

Droplet digital PCR (ddPCR) to evaluate vRNA replication. To measure replication of the various modified HA segments over time, triplicate wells of MDCK cells were co-infected with 5 PFU/cell of each virus under single cycle replication conditions. At 1, 4, 7, and 10 h p.i., co-infected cells and supernatants were harvested together as a single sample. RNA was extracted, converted to cDNA, and used in ddPCR (34) as described in (15). Primers used were specific for the 3' packaging signal region of each HA segment and showed no cross-priming. QuantaSoft software (Bio-Rad) was used to calculate HA copy numbers. ddPCR primers used can be found in *SI Appendix*, Table S2.

Reassortment and virus transmission in guinea pigs. All animal work was performed following the *Guide for the Care and Use of Laboratory Animals* and was approved by the Emory Institutional Animal Care and Use Committee under protocol number DAR-2002738-ELMNTS-A. Intranasal inoculation and nasal lavage was performed as described previously (35). A 5 x 10^5 PFU mixture of WT and VAR virus diluted in PBS was used for the inoculation. Nasal wash samples of inoculated animals were processed for reassortment analysis in the same manner as the co-infection supernatants above. To evaluate transmission, RNA was extracted from contact animal nasal wash samples, converted into cDNA, and ddPCR was performed with 3' HA packaging signal-specific primers to enumerate total HA copies as described above.

Quantification of vRNA in concentrated virus preparations. Viruses were grown in embryonated eggs and pelleted through a 25% sucrose cushion. Resulting virus pellets were

lysed, RNA was extracted, converted to cDNA, and used in ddPCR as described above with IAV segment-specific primers. The HA primers used were specific for a region of the HA segment conserved across all modified HA segments. IAV segment copy number was normalized to the corresponding PB2 copy number and then to the control Pan/99 values (also normalized to PB2). For quantification of the HA segment, two independent primer sets for both the HA and PB2 segments were used and generated data were graphed separately.

Statistical and sequence analyses. Statistical analyses were performed in GraphPad Prism. Alignment of packaging signal sequences derived from IAV HA was performed using Clustal W.

Acknowledgments

We thank Daniel Perez for the pDP2002 plasmid, Ketaki Ganti for assistance with animal experiments, and Nathan Jacobs for helpful discussion. This work was funded in part by the NIH/NIAID Centers of Excellence in Influenza Research and Surveillance (CEIRS), contract number HHSN272201400004C (to A.C.L. and J.S.) and by NIH/NIAID grant R01 AI125268 (to A.C.L.).

Figures

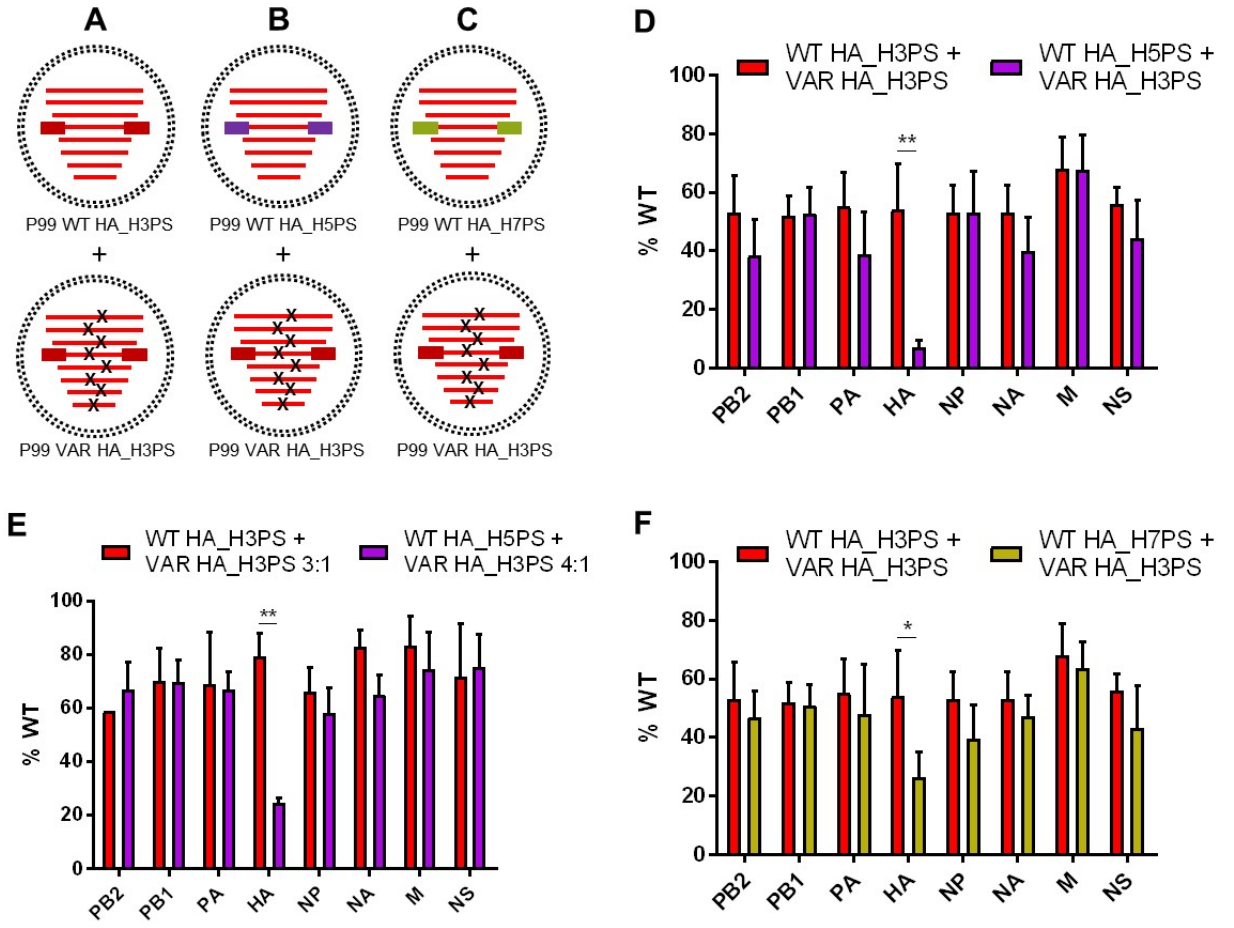

Fig. 1. HA segments carrying H5 or H7 packaging signals constrained reassortment with H3N2 viruses in cell culture. (A-C) Co-infections were performed using virus pairs that contained modified HA segments in a Pan/99 background. Within each pairing, one virus, designated as VAR, contained silent genetic tags (x's) while the other virus was untagged (WT). The control virus pairing in (A) carried homologous H3N2 packaging signals on the HA of both viruses (red boxes). For the heterologous co-infections, the WT virus carried either H5N8 (purple boxes) or H7N9 (gold boxes) packaging signals on HA, while the VAR virus carried homologous H3N2 packaging signals (B and C, respectively). (D-F) MDCK cells were co-infected with the indicated viruses at a high MOI. Supernatants were harvested 12 h p.i. and

virus isolates were genotyped via HRM analysis. The percentage of virus isolates that carried a WT segment for each of the eight IAV segments is shown. Only reassortant virus isolates were included in the analysis. (D and F) Input ratios of 1:1 WT:VAR were used and N = 6 for each co-infection (two biological replicates performed in triplicate). The control dataset shown in both panels is the same and all three co-infections were performed in parallel. (E) Input ratio of 3:1 WT:VAR for the control co-infection and 4:1 WT:VAR for the heterologous co-infection were used and N = 3 (one biological replicate performed in triplicate). Data are plotted as mean with SD. **$p < 0.0001$, *$p = 0.0032$ using two-way ANOVA with Tukey's multiple comparisons.

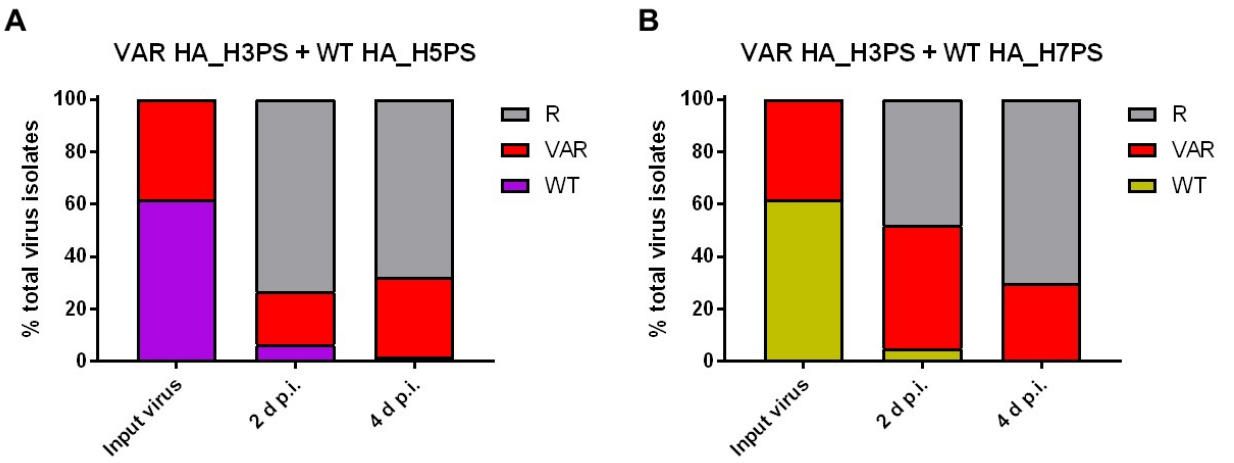

Fig. 2. Heterologous packaging signals on the HA segment of both WT viruses hindered virus propagation in co-infected guinea pigs. Guinea pigs were inoculated with a 1:1 WT:VAR virus mixture consisting of HA_H3PS plus HA_H5PS (A) or HA_H3PS plus HA_H7PS viruses (B). Genotyping was performed on the input virus and virus isolates sampled from the inoculated animals at 2 and 4 d p.i. Data from all four guinea pigs in each group are pooled. (A) N = 21 virus isolates for the input virus, N = 79 virus isolates for 2 d p.i., and N = 56 virus isolates for 4 d p.i. (B) N = 21 virus isolates for the input virus, N = 81 virus isolates for 2 d p.i., and N = 80 virus isolates for 4 d p.i. The reassortant isolates in (A and B) are the same isolates analyzed in Fig. 3. WT = parental WT genotype, VAR = parental VAR genotype, R = reassortant genotype.

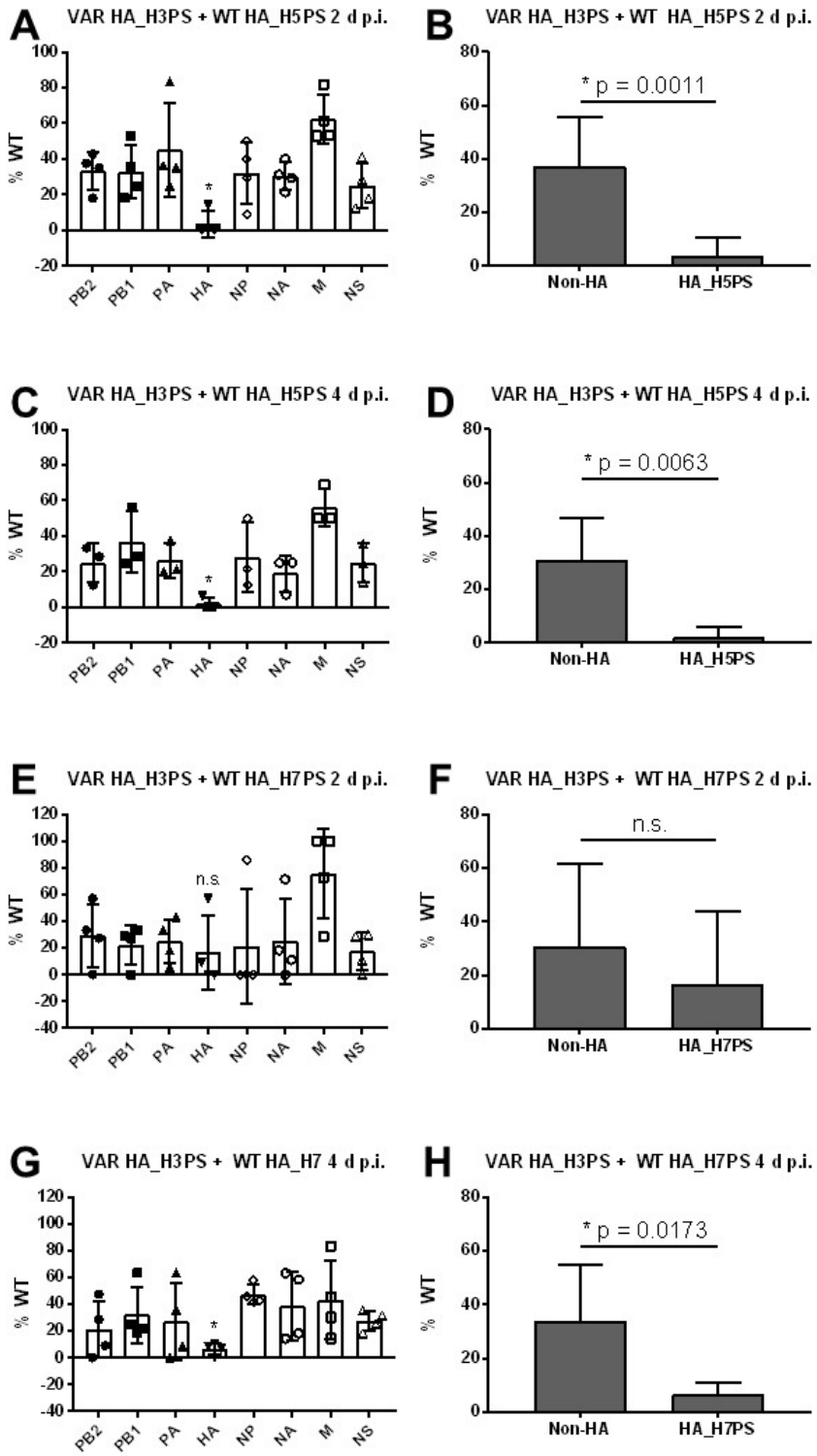

Fig. 3. H5 or H7 packaging signals limited HA reassortment with H3N2 viruses in co-infected animals. Guinea pigs were co-infected with either HA_H3PS plus HA_H5PS viruses

(A-D) or HA_H3PS plus HA_H7PS viruses (E-H) and viruses sampled by nasal lavage at 2 d p.i. (A, B, E, and F) and 4 d p.i. (C, D, G, and H) were genotyped via HRM analysis. The percentage of virus isolates that carried a WT gene segment for each of the eight IAV segments is plotted on the Y axis. The WT HA segment in each co-infection carried heterologous (H5 or H7) packaging signals. Only reassortant virus isolates were included in the analysis (same reassortant isolates reported in Fig. 2). Each data point represents one animal: N = 4 animals for (A); N = 3 animals for (C), N = 4 animals for (E); N = 4 animals for (G). (B, D, F, and H) Unpaired *t* test was used to analyze the difference between % WT for the modified HA segment vs unmodified (non-HA) segments for each reassortment data set. All data are plotted as mean with SD. Calculated p values are displayed on the graphs; n.s. = not significant.

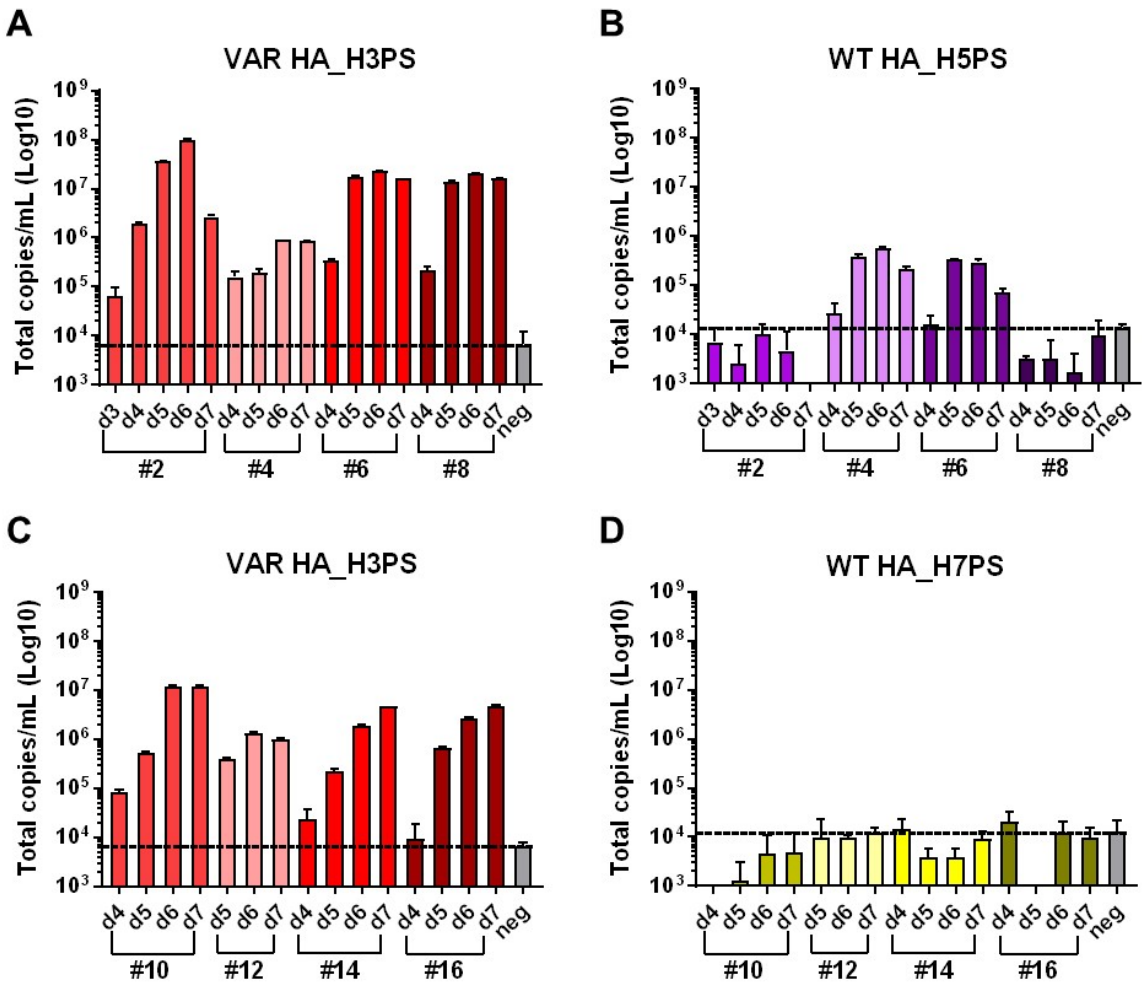

Fig. 4. HA segments carrying H5, but not H7, packaging signals were transmitted to naïve contact animals. Nasal wash fluid of animals exposed to co-infected guinea pigs was analyzed by RT ddPCR to detect HA segment transmission. Primers specific to the 3' packaging signal of each HA segment were used, and each reaction was performed in duplicate. The day of sampling is shown on the X axis and guinea pig ID numbers are indicated underneath. The background values of the assay (measured using primer + dH2O) were used to define the negative (neg), which is represented by a dotted black line. (A and B) Animals exposed to HA_H3PS plus HA_H5PS co-infected animals; (C and D) animals exposed to HA_H3PS plus HA_H7PS co-infected animals. Data are plotted as mean with SD.

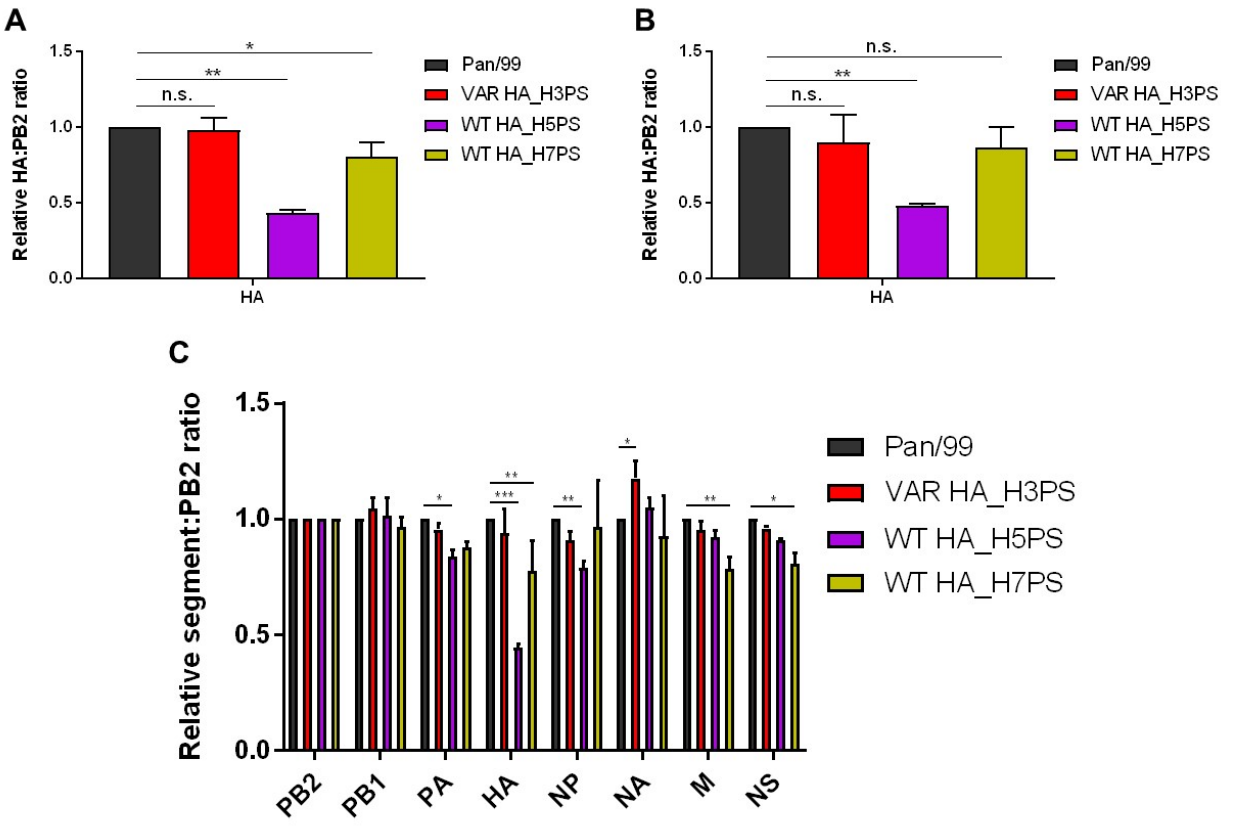

Fig. 5. HA segments carrying H5 or H7 packaging signals were present less frequently than control Pan/99 HA segments in virus particles. Triplicate stocks of HA_H3PS, HA_H5PS, HA_H7PS, and control Pan/99 viruses were grown in embryonated eggs. Each of the resultant twelve stocks was processed individually by concentration through a sucrose cushion. RT ddPCR was used to enumerate segment copy number in the resultant virus preparations. (A and B) HA copy numbers were normalized to PB2 copy numbers and then normalized to the control Pan/99 values. N = 3 for each virus (three technical replicates with ddPCR performed in duplicate for each). Independent sets of PB2 and HA primers were used to generate data shown in (A) and (B). Data are plotted as mean with SD and analyzed using one-way ANOVA with Dunnett's multiple comparisons. (A) **p < 0.0001, *p = 0.0119, n.s. = not significant; (B) **p = 0.0013, n.s. = not significant. (C) All segment copy numbers were normalized to PB2 copy

numbers and then normalized to the control Pan/99 values. N = 3 for each virus (three technical replicates with ddPCR performed in duplicate for each). HA data were acquired using the primer set in (A) and at a separate time from the remaining seven segments. Data are plotted as mean with SD and analyzed within segments using two-way ANOVA with Dunnett's multiple comparisons; ***$p < 0.0001$, **$p < 0.0005$, *$p < 0.01$.

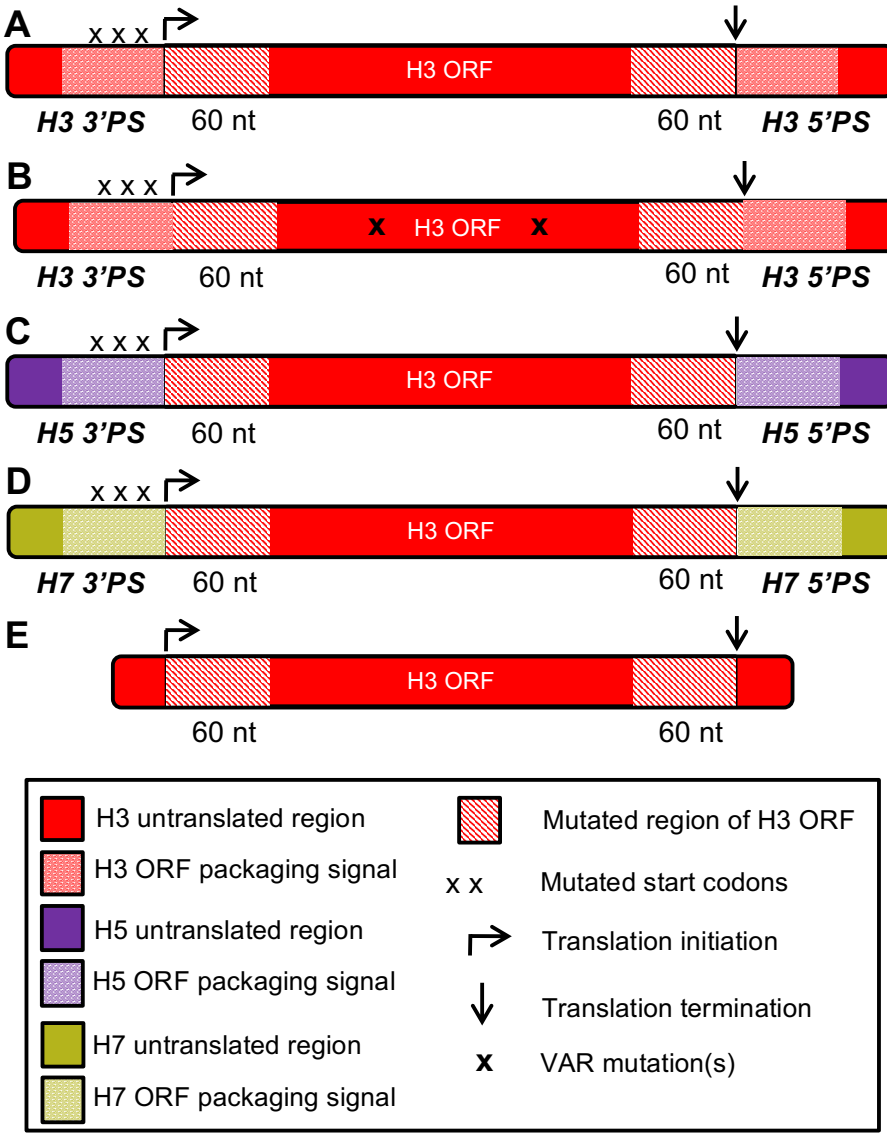

Fig. S1. Pan/99 HA segments constructed have identical ORFs but differing packaging signal regions. Chimeric HA segments were designed so that each segment encoded Pan/99 protein but carried packaging signals originating from H3N2 (Pan/99) (A and B), H5N8 (C), or H7N9 (D). The ORFs were silently mutated within 60 nt terminal regions (hatched boxes) so that packaging would be directed by the introduced 3' and 5' regions. The PSmut_HA segment (E) did not contain introduced packaging signals and was designed to test the disruption of packaging signal function in the ORF. Segments in (A, C, D, and E) are untagged (WT) while

the segment in (B) contains silent mutations in the ORF that serve as genetic identifiers (VAR). Segments are shown in the positive sense and not to scale.

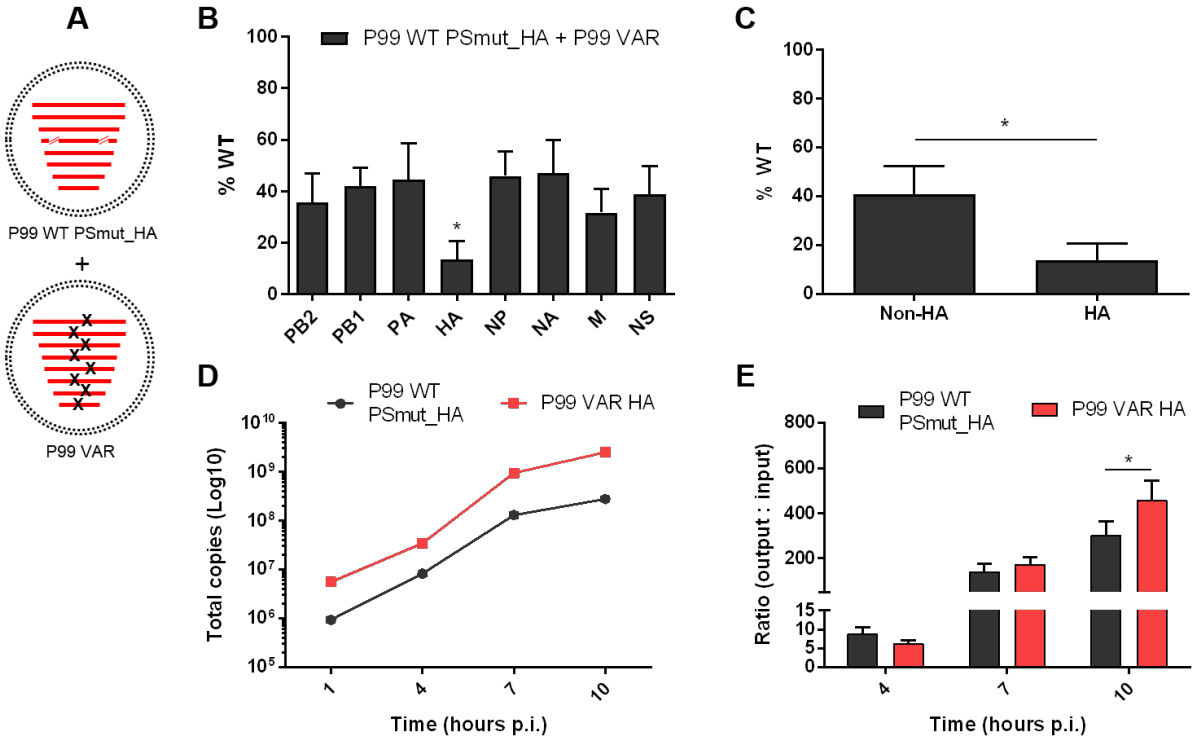

Fig. S2. The introduced HA ORF mutations disrupted packaging function but did not markedly affect segment replication efficiency. MDCK cells were co-infected at a high MOI with a WT virus carrying a full-length Pan/99 HA segment with silent mutations in the packaging signal regions of the ORF (red slash marks) and a VAR virus carrying a full-length Pan/99 HA segment with intact packaging signals in the ORF as shown in (A). Supernatants were harvested at 12 h p.i. and virus isolates were genotyped via HRM analysis. (B) The percentage of virus isolates that carried a WT segment for each of the eight IAV segments is plotted. Only reassortant virus isolates were included in the analysis. N = 8 (two biological replicates with four technical replicates each). Mean with SD is shown. (C) Statistical analysis of data presented in (B). Unpaired, two sided *t* test was used to analyze the difference between % WT for the PSmut_HA segment vs unmodified (non-HA) segments; *p < 0.0001. (D) To evaluate segment replication efficiency, MDCK cells were co-infected at a high MOI with the

viruses shown in (A). At 1, 4, 7, and 10 h p.i., cells and supernatants were harvested as a single sample and RT ddPCR was performed to enumerate total copies of each HA segment over time. Primers used were specific for the 3' HA packaging signal region of each segment, with the forward primer binding in the region of the silent ORF mutations (or lack thereof). N = 3 (three technical replicates with ddPCR performed in duplicate for each). Mean with SD is shown. (E) Because results plotted in (D) suggested a difference in the input amount of the two viruses, HA segment replication over time was normalized by dividing the 4, 7, and 10 h output values by the 1 h input values and resulting ratios were graphed. N = 3; *p = 0.0041 using two-way ANOVA with Sidak's multiple comparisons. Mean with SD is shown.

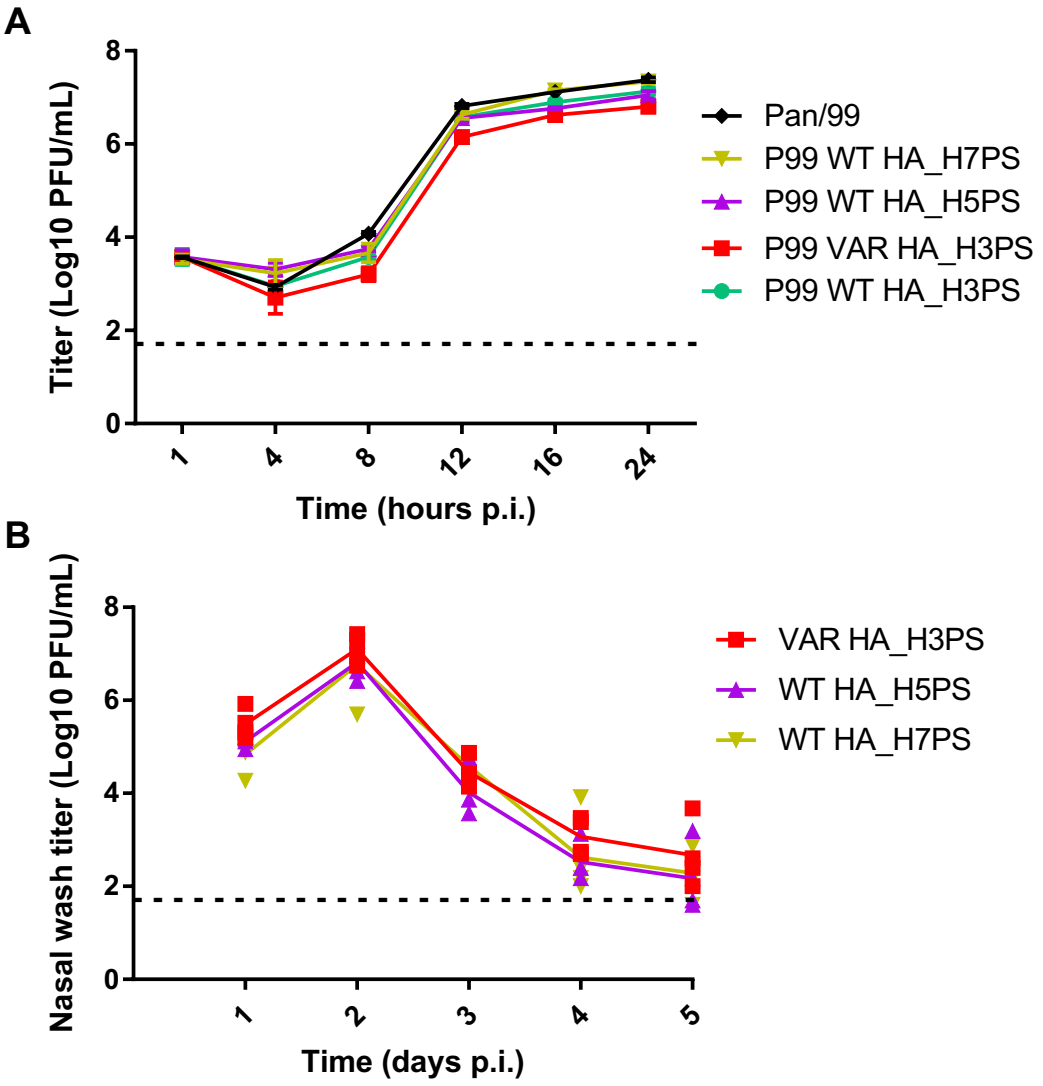

Fig. S3. The introduction of packaging signal regions to Pan/99 HA segments did not alter viral growth. (A) MDCK cells were infected at an MOI 5 PFU/cell and virus replication was allowed to proceed for a single cycle. Supernatants were sampled at 1, 4, 8, 12, 16, and 24 h p.i. and titered via plaque assay on MDCK cells. Colored lines represent Pan/99-based viruses with modified HA segments and the black line represents the control Pan/99 virus. N = 3 technical replicates per virus. Data are plotted as mean with SD. The limit of detection was 50 PFU/mL and is represented by a dotted black line. (B) Guinea pigs were inoculated intranasally with 5 x 10^5 PFU of virus and nasal lavage of each animal was performed daily on day 1 through day 5

p.i. Samples were titered via plaque assay on MDCK cells. N = 4 animals per virus. Individual data points are plotted and the means at each time point are connected. Analysis of the data using two-way ANOVA with Tukey's multiple comparisons revealed no significant differences across viruses. The limit of detection was 50 PFU/mL and is represented by a horizontal dotted black line. Values below the limit of detection were plotted as 25 PFU/mL.

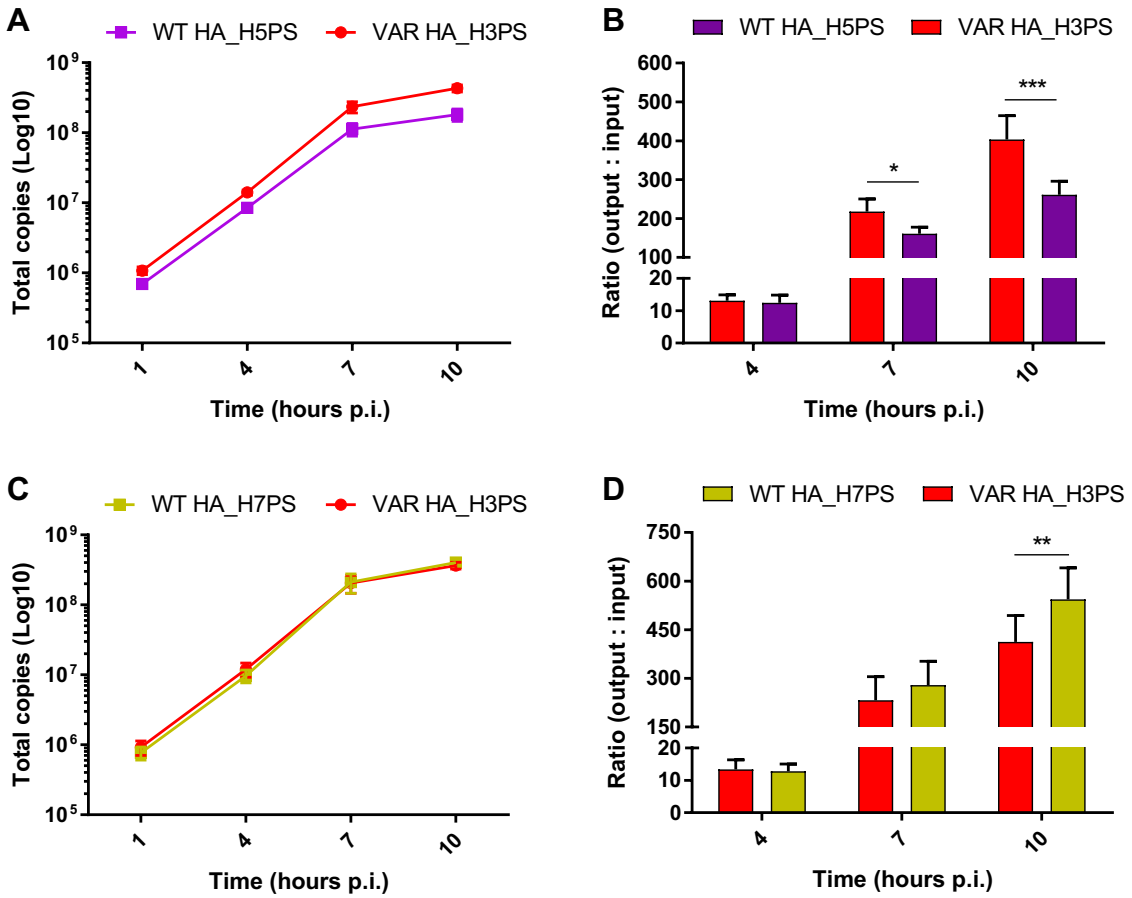

Fig. S4. Chimeric Pan/99 HA segments were replicated efficiently. MDCK cells were co-infected at a high MOI with HA_H3PS plus HA_H5PS viruses (A and B) or HA_H3PS plus HA_H7PS viruses (C and D). At 1, 4, 7, and 10 h p.i., cells and supernatants were harvested as a single sample and RT ddPCR was performed to enumerate total copies of each HA segment over time. Primers used were specific for the 3' HA packaging signal region of each segment. N = 6 (two biological replicates performed in triplicate with ddPCR performed in duplicate for all). (B and D) HA segment replication over time was normalized to input virus by dividing the 4, 7, and 10 h output values by the 1 h input values and resulting ratios were graphed; ***$p < 0.0001$, **$p = 0.0058$, *$p = 0.0158$ using two-way ANOVA with Sidak's multiple comparisons. All data are plotted as mean with SD.

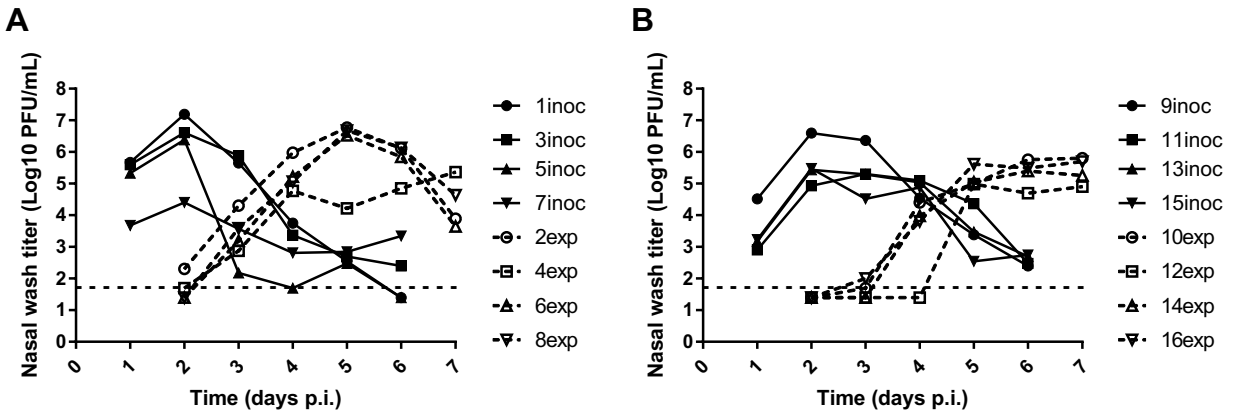

Fig. S5. Guinea pigs co-infected with modified HA viruses supported robust virus growth and transmission to naïve contacts. Guinea pigs were co-infected with either HA_H3PS plus HA_H5PS viruses (A) or HA_H3PS plus HA_H7PS viruses (B) and nasal lavage was performed daily up to day 6 p.i. and titered via plaque assay on MDCK cells (solid black curves). At day 1 p.i., a naïve contact animal was co-housed with each inoculated animal. Nasal lavage of exposed (exp) animals was performed daily day 2 - day 7 p.i. and titered via plaque assay on MDCK cells (dotted black curves). Each line represents one animal, N = 4 for each condition. The limit of detection was 50 PFU/mL and is represented by a horizontal dotted black line. Values below the limit of detection were plotted as 25 PFU/mL.

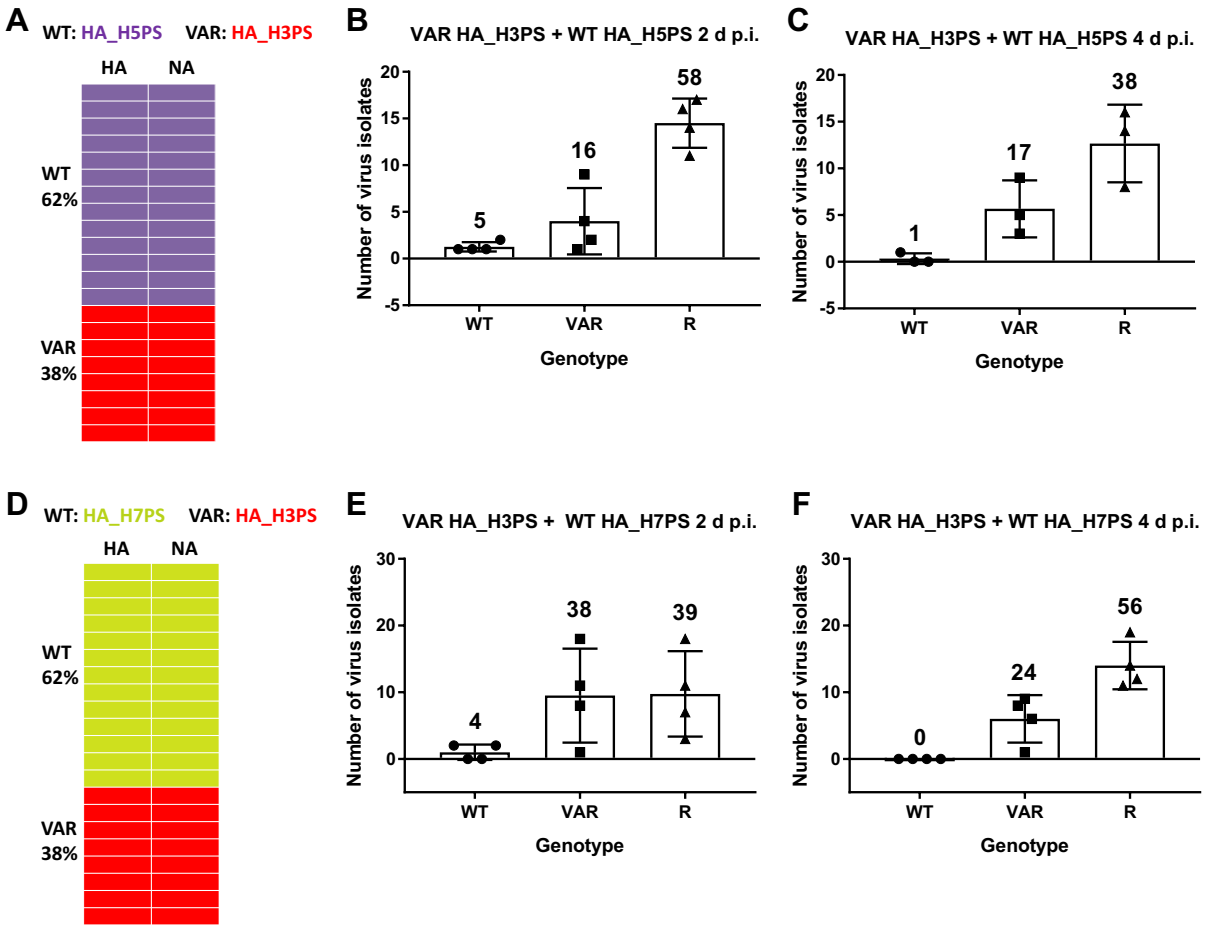

Fig. S6. The VAR virus strongly predominated over WT in nasal lavage samples despite slight overrepresentation of WT in the inocula. Guinea pigs were inoculated with a WT:VAR virus mixture consisting of HA_H3PS plus HA_H5PS (A-C) or HA_H3PS plus HA_H7PS viruses (D-F). The input virus was genotyped (A and D) as well as virus isolates from the inoculated animals taken at 2 d p.i. (B and E) and 4 d p.i. (C and F). Values are plotted as mean with SD, with total virus isolates identified as each genotype stated above the mean. Each data point represents one animal: N = 4 animals for (B); N = 3 animals for (C), N = 4 animals for (E); N = 4 animals for (F). N = 21 virus isolates for (A and D); N = 79 virus isolates for (B); N = 56 virus isolates for (C); N = 81 virus isolates for (E); N = 80 virus isolates for (F). The reassortant isolates in (B, C, E, and F) are the same isolates characterized in Fig. 3. All data originate from

Fig. 2. WT = parental WT genotype, VAR = parental VAR genotype, R = any reassortant genotype.

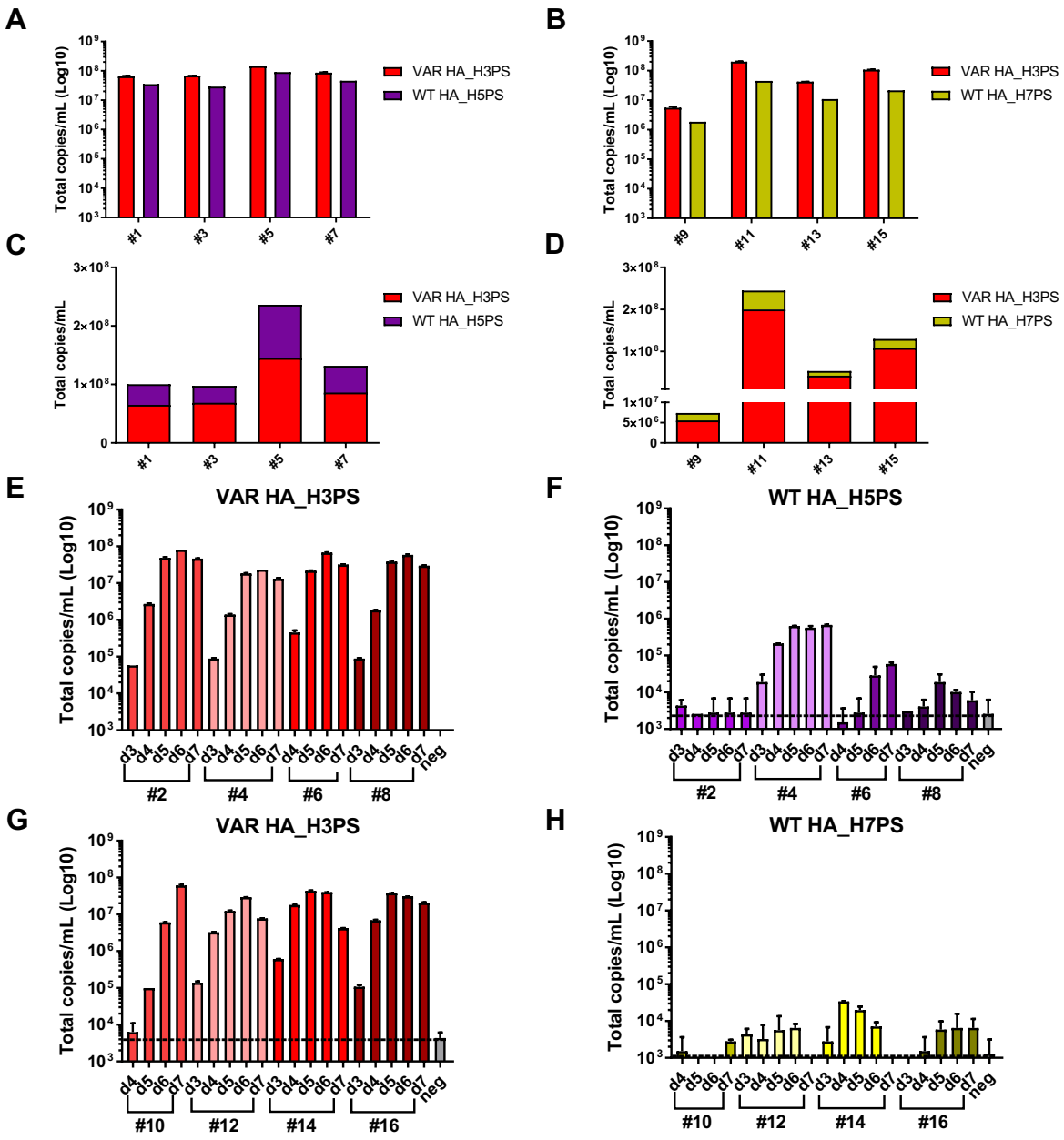

Fig. S7. HA segments carrying H5, but not H7, packaging signals were transferred robustly to a subset of naïve contact animals. Nasal wash fluid of co-infected (donor) animals on day 2 p.i (A-D) or contact animals exposed to co-infected guinea pigs (E-H) was analyzed by RT ddPCR to evaluate HA segment presence. Primers specific to the 3' packaging signal of each HA segment were used, and each reaction was performed in duplicate. (A-D) HA segment

expression on day 2 p.i. of guinea pigs inoculated with HA_H3PS plus HA_H5PS viruses (A and C) or HA_H3PS plus HA_H7PS viruses (B and D). N = 4 animals per condition. Data are plotted as mean with SD (A and B) or as grouped means for each segment (C and D). Guinea pig ID numbers are indicated on the X axis. (E-H) HA segment transmission to animals exposed to HA_H3PS plus HA_H5PS co-infected animals (E and F) or HA_H3PS plus HA_H7PS co-infected animals (G and H). The day of sampling is shown on the X axis and guinea pig ID numbers are indicated underneath. The background values of the assay (measured using primer + dH2O) were used to define the negative (neg), which is represented by a dotted black line. For (E), the background values were zero and therefore the dotted line does not appear on the graph. Data are plotted as mean with SD.

Tables

Table S1. Primers used for HRM analysis

Segment	*Forward Primer*	*Reverse Primer*
Pan/99 PB2	TGGAATAGAAATGGACCTGTGA	GGTTCCATGTTTTAACCTTTCG
Pan/99 PB1	AGGCTAATAGATTTCCTCAAGGATG	ACTCTCCTTTTTCTTTGAAAGTGTG
Pan/99 PA	TGCAACACTACTGGAGCTGAG	CTCCTTGTCACTCCAATTTCG
Pan/99 HA	CCTTGATGGAGAAAACTGCAC	CAACAAAAAGGTCCCATTCC
Pan/99 NP	CAACATACCAGAGGACAAGAGC	ACCTTCTAGGGAGGGTCGAG
Pan/99 NA	TCATGCGATCCTGACAAGTG	TGTCATTTGAATGCCTGTTG
Pan/99 M	GTTTTGGCCAGCACTACAGC	CCATTTGCCTGGCCTGACTA
Pan/99 NS	ACCTGCTTCGCGATACATAAC	AGGGGTCCTTCCACTTTTTG

Table S2. Primers used for ddPCR

Segment	*Forward Primer*	*Reverse Primer*	*Figure*
PB2 Terminal	GGAACCTGATGTCGCAGTCT	CTTTTCCTGTCTCCCTGATG	*Fig. 5*
Pan/99 HA	CCTTGATGGAGAAAACTGCAC	CAACAAAAAGGTCCCATTCC	*Fig. 5*
Pan/99 PB2	TGGAATAGAAATGGACCTGTGA	GGTTCCATGTTTTAACCTTTCG	*Fig. 5*
HA Internal	TAAGGGGTGTCTCCAGCAGA	CCAATGGGTGCATCTGACCT	*Fig. 5*
PB1 Terminal	CCTAAAGGTTCCAGCGCAAA	TGTGTCCATGGTGTACCCTG	*Fig. 5*
PA Terminal	CAACCCGATGATTGTCGAAC	CAAGTGAGTGCATATTGCTGC	*Fig. 5*
NP Terminal	GCGTCCCAAGGCACCAAAC	CCATCAATCATCTTCCCGAC	*Fig. 5*
NA Terminal	GGCTCTGTTTCTCTCACTATTG	GGGAGTTGCATTCATATTGCTTG	*Fig. 5*
M Terminal	CGTATGTTCTCTCTATCGTTCC	GAGAGCCTCAAGATCTGTG	*Fig. 5*
NS Terminal	CTTTGGCATATCCGGAAGCAAG	GCTTTGATGTCTAGACCGAG	*Fig. 5*
HA_PSmut	CACTTTCCTATATCCTTTGCCTC	CCGTTTGACACTGCATGG	*Fig. S2*
HA VAR	CTTTGAGCTACATTTTATGTCTGG	CCGTTTGACACTGCATGG	*Fig. S2*
HA_H3PS	AAGACTATCATTGCTTTGAGCTAC	GTTGCCGTGCTGTTGTAAT	*Fig. S4*
HA_H5PS	TAGTGCTTCTTCTTGCAATAGT	TGCTCTGTCGAGTTGTTTG	*Fig. S4*
HA_H7PS	TCAAATCCTGGTATTCGCT	CGTTTGACACGGAATGATG	*Fig. S4*

References

1. **Wright P, Neumann G, Kawaoka Y.** 2013. Orthomyxoviruses. *In* Knipe D, Howley P (ed), Fields Virology, 6th ed, vol 1. Lippincott Williams & Wilkins.
2. **Desselberger U, Nakajima K, Alfino P, Pedersen FS, Haseltine WA, Hannoun C, Palese P.** 1978. Biochemical evidence that "new" influenza virus strains in nature may arise by recombination (reassortment). Proc Natl Acad Sci U S A **75:**3341-3345.
3. **Kawaoka Y, Krauss S, Webster RG.** 1989. Avian-to-human transmission of the PB1 gene of influenza A viruses in the 1957 and 1968 pandemics. J Virol **63:**4603-4608.
4. **Smith GJD, Vijaykrishna D, Bahl J, Lycett SJ, Worobey M, Pybus OG, Ma SK, Cheung CL, Raghwani J, Bhatt S, Peiris JSM, Guan Y, Rambaut A.** 2009. Origins and evolutionary genomics of the 2009 swine-origin H1N1 influenza A epidemic. Nature **459:**1122-1125.
5. **Kilbourne ED.** 2006. Influenza pandemics of the 20th century. Emerg Infect Dis **12:**9-14.
6. **Chan PK.** 2002. Outbreak of avian influenza A(H5N1) virus infection in Hong Kong in 1997. Clin Infect Dis **34 Suppl 2:**S58-64.
7. **Gao R, Cao B, Hu Y, Feng Z, Wang D, Hu W, Chen J, Jie Z, Qiu H, Xu K, Xu X, Lu H, Zhu W, Gao Z, Xiang N, Shen Y, He Z, Gu Y, Zhang Z, Yang Y, Zhao X, Zhou L, Li X, Zou S, Zhang Y, Li X, Yang L, Guo J, Dong J, Li Q, Dong L, Zhu Y, Bai T, Wang S, Hao P, Yang W, Zhang Y, Han J, Yu H, Li D, Gao GF, Wu G, Wang Y, Yuan Z, Shu Y.** 2013. Human Infection with a Novel Avian-Origin Influenza A (H7N9) Virus. N Engl J Med **368:**1888-1897.

8. **Claas EC, Osterhaus AD, van Beek R, De Jong JC, Rimmelzwaan GF, Senne DA, Krauss S, Shortridge KF, Webster RG.** 1998. Human influenza A H5N1 virus related to a highly pathogenic avian influenza virus. Lancet **351:**472-477.

9. **GlobalConsortiumforH5N8andRelatedInfluenzaViruses.** 2016. Role for migratory wild birds in the global spread of avian influenza H5N8. Science **354:**213-217.

10. **de Vries E, Guo H, Dai M, Rottier PJ, van Kuppeveld FJ, de Haan CA.** 2015. Rapid Emergence of Highly Pathogenic Avian Influenza Subtypes from a Subtype H5N1 Hemagglutinin Variant. Emerg Infect Dis **21:**842-846.

11. **Pohlmann A, Starick E, Harder T, Grund C, Hoper D, Globig A, Staubach C, Dietze K, Strebelow G, Ulrich RG, Schinkothe J, Teifke JP, Conraths FJ, Mettenleiter TC, Beer M.** 2017. Outbreaks among Wild Birds and Domestic Poultry Caused by Reassorted Influenza A(H5N8) Clade 2.3.4.4 Viruses, Germany, 2016. Emerg Infect Dis **23:**633-636.

12. **Lee DH, Bertran K, Kwon JH, Swayne DE.** 2017. Evolution, global spread, and pathogenicity of highly pathogenic avian influenza H5Nx clade 2.3.4.4. J Vet Sci **18:**269-280.

13. **Essere B, Yver M, Gavazzi C, Terrier O, Isel C, Fournier E, Giroux F, Textoris J, Julien T, Socratous C, Rosa-Calatrava M, Lina B, Marquet R, Moules V.** 2013. Critical role of segment-specific packaging signals in genetic reassortment of influenza A viruses. Proc Natl Acad Sci U S A **110:**E3840-E3848.

14. **Baker SF, Nogales A, Finch C, Tuffy KM, Domm W, Perez DR, Topham DJ, Martinez-Sobrido L.** 2014. Influenza A and B Virus Intertypic Reassortment through Compatible Viral Packaging Signals. J Virol **88:**10778-10791.

15. **White MC, Steel J, Lowen AC.** 2017. Heterologous Packaging Signals on Segment 4, but Not Segment 6 or Segment 8, Limit Influenza A Virus Reassortment. J Virol **91**.

16. **Gao Q, Chou Y-Y, Doğanay S, Vafabakhsh R, Ha T, Palese P.** 2012. The Influenza A Virus PB2, PA, NP, and M Segments Play a Pivotal Role during Genome Packaging. J Virol **86:**7043-7051.

17. **Marshall N, Priyamvada L, Ende Z, Steel J, Lowen AC.** 2013. Influenza virus reassortment occurs with high frequency in the absence of segment mismatch. PLoS Pathog **9:**e1003421.

18. **Ma EJ, Hill NJ, Zabilansky J, Yuan K, Runstadler JA.** 2016. Reticulate evolution is favored in influenza niche switching. Proc Natl Acad Sci U S A **113:**5335-5339.

19. **Reperant LA, Kuiken T, Osterhaus AD.** 2012. Adaptive pathways of zoonotic influenza viruses: from exposure to establishment in humans. Vaccine **30:**4419-4434.

20. **White MC, Lowen AC.** 2018. Implications of segment mismatch for influenza A virus evolution. J Gen Virol **99:**3-16.

21. **Gamblin SJ, Skehel JJ.** 2010. Influenza hemagglutinin and neuraminidase membrane glycoproteins. J Biol Chem **285:**28403-28409.

22. **Gostic KM, Ambrose M, Worobey M, Lloyd-Smith JO.** 2016. Potent protection against H5N1 and H7N9 influenza via childhood hemagglutinin imprinting. Science **354:**722-726.

23. **Hensley SE.** 2014. Challenges of selecting seasonal influenza vaccine strains for humans with diverse pre-exposure histories. Curr Opin Virol **8:**85-89.

24. **Ince WL, Gueye-Mbaye A, Bennink JR, Yewdell JW.** 2013. Reassortment complements spontaneous mutation in influenza A virus NP and M1 genes to accelerate adaptation to a new host. J Virol **87:**4330-4338.

25. **Mathews JD, McBryde ES, McVernon J, Pallaghy PK, McCaw JM.** 2010. Prior immunity helps to explain wave-like behaviour of pandemic influenza in 1918-9. BMC Infect Dis **10:**128.

26. **Hutchinson EC, von Kirchbach JC, Gog JR, Digard P.** 2010. Genome packaging in influenza A virus. J Gen Virol **91:**313-328.

27. **Watanabe T, Watanabe S, Noda T, Fujii Y, Kawaoka Y.** 2003. Exploitation of nucleic acid packaging signals to generate a novel influenza virus-based vector stably expressing two foreign genes. J Virol **77:**10575-10583.

28. **Fujii K, Fujii Y, Noda T, Muramoto Y, Watanabe T, Takada A, Goto H, Horimoto T, Kawaoka Y.** 2005. Importance of both the coding and the segment-specific noncoding regions of the influenza A virus NS segment for its efficient incorporation into virions. J Virol **79:**3766-3774.

29. **Goto H, Muramoto Y, Noda T, Kawaoka Y.** 2013. The Genome-Packaging Signal of the Influenza A Virus Genome Comprises a Genome Incorporation Signal and a Genome-Bundling Signal. J Virol **87:**11316-11322.

30. **Noda T, Sagara H, Yen A, Takada A, Kida H, Cheng RH, Kawaoka Y.** 2006. Architecture of ribonucleoprotein complexes in influenza A virus particles. Nature **439:**490-492.

31. **Nakatsu S, Sagara H, Sakai-Tagawa Y, Sugaya N, Noda T, Kawaoka Y.** 2016. Complete and Incomplete Genome Packaging of Influenza A and B Viruses. MBio **7**.

32. **Wittwer CT, Reed GH, Gundry CN, Vandersteen JG, Pryor RJ.** 2003. High-resolution genotyping by amplicon melting analysis using LCGreen. Clin Chem **49:**853-860.

33. **Fonville JM, Marshall N, Tao H, Steel J, Lowen AC.** 2015. Influenza Virus Reassortment Is Enhanced by Semi-infectious Particles but Can Be Suppressed by Defective Interfering Particles. PLoS Pathog **11:**e1005204.

34. **Schwartz SL, Lowen AC.** 2016. Droplet digital PCR: A novel method for detection of influenza virus defective interfering particles. J Virol Methods **237:**159-165.

35. **Lowen AC, Mubareka S, Tumpey TM, Garcia-Sastre A, Palese P.** 2006. The guinea pig as a transmission model for human influenza viruses. Proc Natl Acad Sci U S A **103:**9988-9992.

Chapter V: Discussion

Influenza A virus (IAV) has a segmented genome, which allows for the exchange of gene segments in co-infected cells by a process called reassortment (1, 2). The segmented nature of the virus also requires a mechanism by which the virus can differentiate the eight different gene segments and package them together to make a fully infectious virus. This segment differentiation is achieved through packaging signals, which are found on both termini of each IAV segment and comprise both non-coding and coding regions (3-8). Each packaging signal is unique to each segment, and can differ across IAV strains.

During reassortment, two different IAVs co-infect the same cell within the same host, and mixing of the viral genomes occurs. Incompatibilities between the two co-infecting viruses can arise during reassortment at both the RNA level (packaging signals) and the protein level. These incompatibilities, termed segment mismatch, are an important factor in the outcome of mixed IAV infections (9). Previous studies have shown that mismatch at the protein level affects the reassortant genotypes that form after a co-infection event (10-15). Similarly, two additional studies have demonstrated that mismatch at the RNA level limits reassortment efficiency (16, 17). However, the knowledge regarding the quantitative effects of this RNA mismatch, as well as which IAV segments are subject to RNA mismatch, is lacking. This dissertation sought to address these knowledge gaps and to provide new insights to the molecular mechanisms that control the emergence of new IAV strains.

Chapter II conclusions and implications

Chapter II of this dissertation quantifies the impact of RNA mismatch on IAV reassortment. We show that the presence of heterologous packaging signals from an H1N1 virus on the NS segment

does not affect IAV reassortment outcomes with a seasonal H3N2 virus, as roughly half of the reassortant progeny viruses genotyped incorporated the heterologous NS segment. Similarly, having heterologous H1N1 packaging signals on the NA segment does not significantly affect IAV reassortment outcomes with a H3N2 virus, although preference for matched packaging signals was trending. Conversely, we observed a significant preference for matched packaging signals on the HA segment, as only 15% of the reassortant progeny viruses genotyped incorporated a HA segment carrying heterologous H1N1 packaging signals. From these data, we conclude that the NA and NS segments from a H1N1 virus strain would move freely into a H3N2 virus background, while movement of the H1N1 HA segment into a H3N2 virus background would be constrained. These data also suggest that the importance of RNA mismatch in IAV reassortment is dependent on segment identity. Overall, this chapter indicates that the HA segment may be an important factor in determining whether two IAV strains of public health interest will undergo reassortment.

Chapter III conclusions and implications

Chapter III of this dissertation sought to identify nucleotides in the HA segment important for mediating packaging. We serially passaged the heterologous HA segment from Chapter II ten times in a cell line alongside a homologous HA segment as a control. We then sequenced the passaged HA segments and looked for compensatory mutations that might have formed to alleviate the packaging signal mismatch. Unfortunately, our approach was unable to identify nucleotides that mediate HA segment packaging. However, we did identify a single point mutation in the passaged heterologous HA segment which arose three independent times. This mutation, T1864C, did not allow for better packaging of the mismatched HA segment, nor did it allow for better virus growth. However, this mutation may have a yet-unidentified role in easing RNA mismatch during

IAV reassortment. Further studies would be needed to address this possibility, and are discussed below at the end of this discussion chapter.

Chapter IV conclusions and implications

Chapter IV of this dissertation examines how RNA mismatch might prevent IAV reassortment events that could lead to the formation of pandemic strains. We show that having H5N8 or H7N9 packaging signals (two pandemic potential avian subtype IAVs) on the HA segment restricts reassortment with a seasonal human H3N2 virus in both cell culture and an animal model. However, viruses with H5 or H7 packaging signals were still detected at low levels in both systems. This low level of reassortment could be significant in nature if the reassortment virus had a fitness advantage, such as antigenic novelty. Additionally, we show that viruses with H5, but not H7, packaging signals were transmitted to naïve hosts, suggesting that H5 packaging signals are sufficiently compatible with H3N2 viruses to allow contact transmission. Overall, these data show that avian-human IAV reassortment is restricted by RNA mismatch on the HA segment, and help to inform efforts to estimate the risks to human health presented by avian subtype IAVs.

Future Directions

This dissertation focuses on how RNA mismatch on three of the eight IAV segments (HA, NA, and NS) affects IAV reassortment. Future studies could be performed to address how heterologous packaging signals affect IAV reassortment efficiency of the PB2, PB1, PA, NP, and M segments using the above H1N1 and H3N2 virus strains. A previous study showed that there is a hierarchy in packaging; the PB2, PA, NP, and M segments are more critical to IAV packaging compared to the remaining four segments (18). We focused on the HA, NA, and NS segments because these

three segments are the most divergent in terms of the packaging signal regions across IAV strains. However, it is still unknown which nucleotides mediate segment packaging for each of the eight segments, and further insights could be gained by repeating the above studies for all IAV segments. In Chapter II, we chose to focus on H1N1 and H3N2 virus strains to generate data that were relevant for the two subtypes of IAV currently circulating in the human population. It would be interesting to repeat the above studies using different IAV strains and to compare the reassortment phenotypes observed. It is possible that the importance of RNA mismatch is not only segment dependent, but also IAV strain dependent. These experiments would be of particular interest given the results obtained in Chapter IV. These data suggest that HA groupings might influence IAV reassortment outcomes. IAV HA's are divided into two different groups based on phylogeny (19). Group 1 HA's include H1 and H5, while group 2 HA's include H3 and H7. Our data show that H3N2 viruses incorporate H7 HA's more easily than H5 HA's based on packaging signals. Our data also show that H3N2 viruses do not readily incorporate H1 HA's. The phylogenetic relatedness of the above HA subtypes could be a factor in determining reassortment outcomes, but additional experiments with more HA groupings would be needed to test this hypothesis.

For all reassortment experiments performed in this dissertation, MDCK cells were used. MDCK cells are routinely used for growing and characterizing IAV (20-23). However, it would be interesting to see if the reassortment phenotypes observed herein would also be replicated in different cell types. For example, HTBE (human tracheobronchial epithelial) cells would be of interest, since they are primary human respiratory cell cultures and reflect the differentiated nature of the human airway, where IAV would infect a human host (24). Differing substrates could be one explanation for the conflicting transmission data obtained in Chapter IV. Our data show that HA segments carrying H7 packaging signals encounter a lower incorporation barrier into H3N2

viruses than HA segments carrying H5 packaging signals. However, and somewhat surprisingly, our data also show that HA segments carrying H5, but not H7, packaging signals are transmitted to naïve contact animals. Even though we observed similar reassortment phenotypes for H3, H5 and H7 HA's in cell culture and *in vivo*, the apparent discordance in transmission compared to reassortment could be influenced by a difference in the cellular environment. To this end, more experiments are needed to help inform our transmission data.

All experiments in this dissertation were performed in a H3N2 virus background. The H3N2 virus used, influenza A/Panama/2007/99, grows well in eggs and can therefore can be grown to the high titers necessary to perform high MOI co-infections. Additionally, the WT-VAR system our lab employs to study reassortment has been optimized for this virus strain. However, as mentioned above, two IAV subtypes co-circulate in humans each year, the H3N2 and H1N1 subtypes. It would be of interest to perform the same experiments in a H1N1 virus background. Indeed, this project was attempted in the lab, but several complications arose. First, H1N1-based viruses do not grow to high titers, and therefore the high MOI co-infections performed with H3N2 viruses would not be feasible. This shortcoming can be compensated for by performing low MOI co-infections and screening more plaques. Second, the control H1N1 HA construct generated to carry homologous H1N1 packaging signals was shown to have a significant packaging defect. Perhaps secondary structure was introduced during the HA construct engineering, or NP binding was altered. Regardless of the cause of decreased packaging, the control H1N1 HA construct was unusable, since a control construct should have no impact on packaging in order for the resulting data to be interpretable. Due to the lack of an appropriate control, the project was put on hold. Future efforts at performing experiments in a H1N1 virus background would nonetheless be

informative to capture the complete picture of RNA mismatch in both IAV subtypes currently circulating in humans.

Segment mismatch encompasses the genetic incompatibilities between co-infecting viruses at both the RNA level and the protein level. This dissertation focuses solely on segment mismatch at the RNA level (packaging signals). Future studies are needed to determine the effects that protein divergence has on reassortment outcomes using the IAV strain pairings outlined in this dissertation. Once we have isolated the effects that RNA mismatch and protein mismatch independently have on reassortment outcomes, we can use these segment mismatch data to help inform pandemic preparedness efforts on not only the level of virus formation (RNA) but also the level of virus fitness and propagation (protein).

The aim of Chapter III was to identify nucleotides that are important for mediating HA segment packaging. Although the experiments performed in Chapter III were unable to answer this question, the samples obtained in Chapter IV may help to address this outstanding inquiry. Our transmission data in Chapter IV show that HA segments carrying H5, but not H7, packaging signals were transmitted to naïve contact animals, suggesting that H5 was sufficiently compatible with H3N2 viruses to allow transmission. Currently in collaboration with the Centers for Disease Control and Prevention (CDC), we are deep sequencing the nasal wash samples obtained from these animals that contracted infection with an H5 HA-carrying virus. We will compare the sequences obtained from these animals with reference sequences and look for compensatory mutations in either the HA segment or other segments in the IAV genome that might have allowed for better transmission and/or packaging of the heterologous H5 HA segment *in vivo*. Once potential compensatory mutations have been identified, we will generate recombinant viruses that carry these mutation(s) of interest and test whether they enable better packaging of the

heterologous HA segment into a H3N2 virus. Using this strategy, we hope to be able to identify critical regions and/or nucleotides of the HA segment important for mediating segment packaging, which will help to further inform the reassortment potential of different IAVs.

References

1. **Shaw ML, Palese P.** 2013. Orthomyxoviridae, p 1151–1185. *In* Knipe D, Howley P (ed), Fields Virology, vol 1. Lippincott Williams & Wilkins, Philadelphia, PA.
2. **Desselberger U, Nakajima K, Alfino P, Pedersen FS, Haseltine WA, Hannoun C, Palese P.** 1978. Biochemical evidence that "new" influenza virus strains in nature may arise by recombination (reassortment). Proc Natl Acad Sci U S A **75:**3341-3345.
3. **Liang Y, Hong Y, Parslow TG.** 2005. cis-Acting packaging signals in the influenza virus PB1, PB2, and PA genomic RNA segments. J Virol **79:**10348-10355.
4. **Fujii K, Fujii Y, Noda T, Muramoto Y, Watanabe T, Takada A, Goto H, Horimoto T, Kawaoka Y.** 2005. Importance of both the coding and the segment-specific noncoding regions of the influenza A virus NS segment for its efficient incorporation into virions. J Virol **79:**3766-3774.
5. **Fujii Y, Goto H, Watanabe T, Yoshida T, Kawaoka Y.** 2003. Selective incorporation of influenza virus RNA segments into virions. Proc Natl Acad Sci U S A **100:**2002-2007.
6. **Ozawa M, Fujii K, Muramoto Y, Yamada S, Yamayoshi S, Takada A, Goto H, Horimoto T, Kawaoka Y.** 2007. Contributions of two nuclear localization signals of influenza A virus nucleoprotein to viral replication. J Virol **81:**30-41.
7. **Ozawa M, Maeda J, Iwatsuki-Horimoto K, Watanabe S, Goto H, Horimoto T, Kawaoka Y.** 2009. Nucleotide sequence requirements at the 5' end of the influenza A virus M RNA segment for efficient virus replication. J Virol **83:**3384-3388.
8. **Watanabe T, Watanabe S, Noda T, Fujii Y, Kawaoka Y.** 2003. Exploitation of nucleic acid packaging signals to generate a novel influenza virus-based vector stably expressing two foreign genes. J Virol **77:**10575-10583.

9. **White MC, Lowen AC.** 2018. Implications of segment mismatch for influenza A virus evolution. J Gen Virol **99:**3-16.

10. **Li C, Hatta M, Watanabe S, Neumann G, Kawaoka Y.** 2008. Compatibility among polymerase subunit proteins is a restricting factor in reassortment between equine H7N7 and human H3N2 influenza viruses. J Virol **82:**11880-11888.

11. **Hatta M, Halfmann P, Wells K, Kawaoka Y.** 2002. Human influenza a viral genes responsible for the restriction of its replication in duck intestine. Virology **295:**250-255.

12. **Phipps KL, Marshall N, Tao H, Danzy S, Onuoha N, Steel J, Lowen AC.** 2017. Seasonal H3N2 and 2009 Pandemic H1N1 Influenza A Viruses Reassort Efficiently but Produce Attenuated Progeny. J Virol **91**.

13. **Hara K, Nakazono Y, Kashiwagi T, Hamada N, Watanabe H.** 2013. Co-incorporation of the PB2 and PA polymerase subunits from human H3N2 influenza virus is a critical determinant of the replication of reassortant ribonucleoprotein complexes. J Gen Virol **94:**2406-2416.

14. **Kuo RL, Krug RM.** 2009. Influenza a virus polymerase is an integral component of the CPSF30-NS1A protein complex in infected cells. J Virol **83:**1611-1616.

15. **Twu KY, Kuo RL, Marklund J, Krug RM.** 2007. The H5N1 influenza virus NS genes selected after 1998 enhance virus replication in mammalian cells. J Virol **81:**8112-8121.

16. **Essere B, Yver M, Gavazzi C, Terrier O, Isel C, Fournier E, Giroux F, Textoris J, Julien T, Socratous C, Rosa-Calatrava M, Lina B, Marquet R, Moules V.** 2013. Critical role of segment-specific packaging signals in genetic reassortment of influenza A viruses. Proc Natl Acad Sci U S A **110:**E3840-E3848.

17. **Baker SF, Nogales A, Finch C, Tuffy KM, Domm W, Perez DR, Topham DJ, Martinez-Sobrido L.** 2014. Influenza A and B Virus Intertypic Reassortment through Compatible Viral Packaging Signals. J Virol **88:**10778-10791.

18. **Gao Q, Chou Y-Y, Doğanay S, Vafabakhsh R, Ha T, Palese P.** 2012. The Influenza A Virus PB2, PA, NP, and M Segments Play a Pivotal Role during Genome Packaging. J Virol **86:**7043-7051.

19. **Gamblin SJ, Skehel JJ.** 2010. Influenza hemagglutinin and neuraminidase membrane glycoproteins. J Biol Chem **285:**28403-28409.

20. **Audsley JM, Tannock GA.** 2004. The role of cell culture vaccines in the control of the next influenza pandemic. Expert Opin Biol Ther **4:**709-717.

21. **Gaush CR, Smith TF.** 1968. Replication and plaque assay of influenza virus in an established line of canine kidney cells. Appl Microbiol **16:**588-594.

22. **Youil R, Su Q, Toner TJ, Szymkowiak C, Kwan WS, Rubin B, Petrukhin L, Kiseleva I, Shaw AR, DiStefano D.** 2004. Comparative study of influenza virus replication in Vero and MDCK cell lines. J Virol Methods **120:**23-31.

23. **Sidorenko Y, Reichl U.** 2004. Structured model of influenza virus replication in MDCK cells. Biotechnol Bioeng **88:**1-14.

24. **Danzy S, Studdard LR, Manicassamy B, Solorzano A, Marshall N, Garcia-Sastre A, Steel J, Lowen AC.** 2014. Mutations to PB2 and NP proteins of an avian influenza virus combine to confer efficient growth in primary human respiratory cells. J Virol **88:**13436-13446.